Seismic Data Acquisition
TA3600

G.G. Drijkoningen

Section Applied Geophysics & Petrophysics
Delft University of Technology
P.O. Box 5028
2600 GA Delft
The Netherlands

August 2003

Contents

Chapter 1

Seismic data acquisition

1.1 Introduction

Seismic data acquisition is the gathering / recording of seismic data in the field (be it on land or at sea) with the ultimate goal to make a seismic image of the subsurface.

Various supporting field activities are required for good seismic data acquisition. For example, seismic exploration for oil and gas is a complex interaction of activities requiring good management. Important aspects are:

- General administration/exploration concession and permit work ("land and legal"); topographic surveying and mapping, which is quite different for land- or marine work.
- More specific seismic aspects: placing and checking the seismic source, which on land is either an explosive (for example dynamite) or Vibroseis and at sea mostly an array of air-guns; positioning and checking the detectors, geophones on land, hydrophones at sea; operating the seismic recording system.

The organisation of a seismic land crew, often faced with difficult logistics, terrain- and access road conditions is quite different from that of marine seismic crew on board of an exploration vessel, where a compact streamlined combination of seismic and topo operations is concentrated on the decks of one boat; different circumstances require different strategies and different technological solutions.

1.2 Seismic instrumentation

The chapters 2, 3 and 4 deal with seismic instrumentation, i.e., all the necessary hardware to make seismic measurements in the field. First of all, we have to generate sound waves, with sufficient power and adequate frequency content in order to cause detectable reflections. This will be the discussed in the chapter 2 on sources. Then, when the waves have travelled through the subsurface, we want to detect the sound, and convert the motion to an electrical signal. This will be discussed in chapter 3 on geophones and hydrophones. Then, the electrical signal is transported via cables to the recording instrument where it

will be converted to a digital signal such that it can be stored, usually on tape, and can be read again at a later time. The recording part is discussed in chapter 4.

In the whole lecture notes, it assumed that we deal with linear time-invariant (LTI) systems, and thus the seismogram X(t) recorded on tape at the end of the data acquisition stream is seen as a convolution of the separate systems:

$$X(t) = S(t) * G(t) * R(t) * A(t) \tag{1.1}$$

in which

$S(t)$ = the source signal

$G(t)$ = the impulse response of the earth, or the Green's function

$R(t)$ = the detector (impulse) response

$A(t)$ = the seismograph impulse response

1.3 Seismic survey design

Before any measurements in the field are carried out, all the field parameters have to be set. For instance, if we decide to use dynamite, it is important to know how deep we must place it. A key parameter is the distances between shot and geophone positions. Another parameter is the setting of filters in the recording instrument in order to suppress unwanted signals. All these aspects can be caught under the caption of seismic survey design. This is important for the oil company who relies on the seismic contractor to carry out the measurements, as the quality of the data is often very much dependent on the parameter settings. In order to set these parameters, one has to understand certain characteristics of the seismic equipment, and therefore we will start the discussion with the hardware.

Chapter 2

Seismic sources

2.1 Introduction

This chapter deals with the seismic source. The source generates the (dynamical) mechanical disturbance that cause a seismic wave motion with a characteristic signal shape ("signature") to travel through the subsurface from source to receivers. The seismic source has a dominant influence on the signal response resulting from the total acquisition system, i.e. the response due to source, receiver(s) and seismic recording system. In this chapter the seismic sources as routinely used by the oil industry in the exploration for oil and gas will be treated: airguns as used in marine operations, dynamite and Vibroseis as used in land operations. For each type of source a general introduction will be given, then the most important aspects of the mechanical principles of operation will be treated and finally the characteristic seismic signal produced by the source (the source's "signature").

Along the way also, aspects of source geometry (array effects and directivity) and of the source locations combined with the near-source medium geometry, e.g., the effect of a free surface (the ghost effect) that may cause a complicated (compound) outgoing signal, will be treated as well.

2.2 The airgun and its mechanics

Many oil and gasfields are found in water-covered areas, such as the Gulf of Mexico and the North Sea. Ever since the 1960's companies were not allowed to use dynamite any more as seismic source because of fish dying massively due to the sharp and destructive strong shock-wave from the dynamite. Exploration companies had to look for alternatives. Many sources were developed since then, such as airguns, waterguns and even a marine equivalent of the Vibroseis. Airguns became the most popular marine source in the oil industry because of their renowned reliability and signature repeatability. The signature of one airgun has an inconveniently long and oscillatory character, the reason why airguns are used in specifically designed arrays, consisting of airguns with different volumes. The characteristics of the airgun, the array effects, i.e. directivity, and the effect of the free surface on the outgoing signal will be considered.

As is obvious from the name, the driving mechanism of the airgun is supplied by (compressed) air. In Figure (2.1) we have given a schematic view of an airgun. Air under

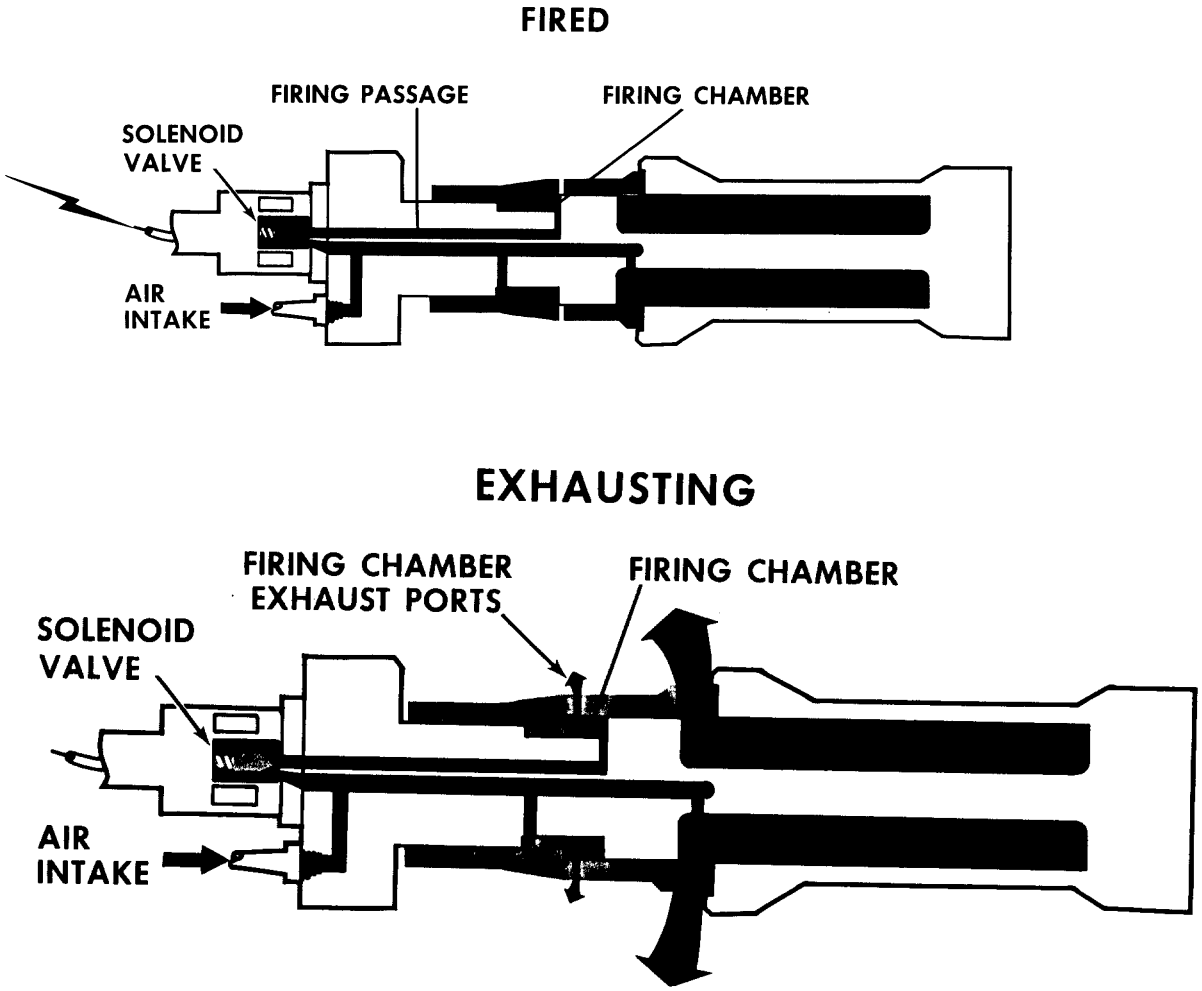

Figure 2.1: Cross-section of an airgun just when it is fired, and when the air is released.

pressure is pumped into a chamber. Using the piston, the air is suddenly released and the air leaves the chamber and starts to create a bubble in the surrounding water. Inside the bubble we have the air but there is a turbulent region which consists of many little bubbles, the non-linear zone. This is schematically given in figure (2.2) (a). The mechanism behind the behaviour of the airgun is depicted in figure (2.2) (b) and (c). The bubble increases in the beginning but after a while the pressure from outside, the hydrostatic pressure, is larger than the pressure from inside of the bubble and the expansion slows down. The expansion comes to an end and the bubble reaches its maximum radius when the kinetic energy of the outward moving water is fully converted into potential energy related to bubble radius, hydrostatic pressure and some heat losses. From there on, the bubble starts to collapse since the hydrostatic pressure from outside is larger than the pressure inside. The collapse slows down when we have again passed the equilibrium position (where the pressure inside the bubble is equal to the hydrostatic pressure) until we have reached a minimum radius where it will start to expand again, and so on. The collapses and expansions will not go on forever because of the heat dissipation into the water. The result from this behaviour is a damped oscillatory pressure signal, somewhat similar to a damped sine curve. The behaviour is depicted in the figure (2.2) (b) and (c), where both bubble radius and the pressure have been plotted as a function of time.

The modelling of an underwater explosion is given in Keller & Kolodner (1956), who derive a nonlinear equation for the bubble radius, derived from the Bernoulli equation. In the beginning of the explosion, a shock wave is generating the initial pressure pulse, and from then on the oscillations start and will be damped. In the beginning, the oscillations are not damped sinusoids; it can be shown analytically that this is only the case when the bubble radius is small compared to the equilibrium radius, thus at later times.

2.3 The signal from an airgun

The signal from a single airgun has typically a length of some 200 ms. Of course, this depends on the type of airgun and the pressure of the air supplied to the airgun. The larger the size, i.e. airgun airchamber volume, or the higher the pressure the longer the period in the oscillations (or, the lower the frequency content). Common pressures are 2000 and 3000 psi. The gun sizes are specified airchamber volume. Common values are 10, 20, 30 up to 100 cubic inches. The mostly used airgun today is the so-called sleeve gun, producing a more favourable individual signature. The conventional airguns had 4 port holes from which the air escaped the gun, but from the sleeve gun, as the name suggests, the air escapes via a complete ringed opening. The advantage of this type of gun is that, because there are less moving parts, it is more reliable. This is even more important in a routine production environment. A disadvantage is that they can only be made with smaller chamber volumes which has resulted in using subarrays of sleeve guns where each subarray releases the same power as the conventional airgun.

Extensive fluid mechanical research studies and experiments have been carried out over the last decades in order to describe the behaviour of the airgun. Assuming an incompressible fluid, it can be derived that the bubble period T amounts to:

$$T = K \frac{P_{\text{in}}^{1/3} V_{\text{in}}^{1/3}}{P_H^{5/6}} \tag{2.1}$$

in which P_{in} denotes the pressure inside the airgun before firing, V_{in} is the volume of the chamber, P_H is the hydrostatic pressure and K is some constant. This formula is known

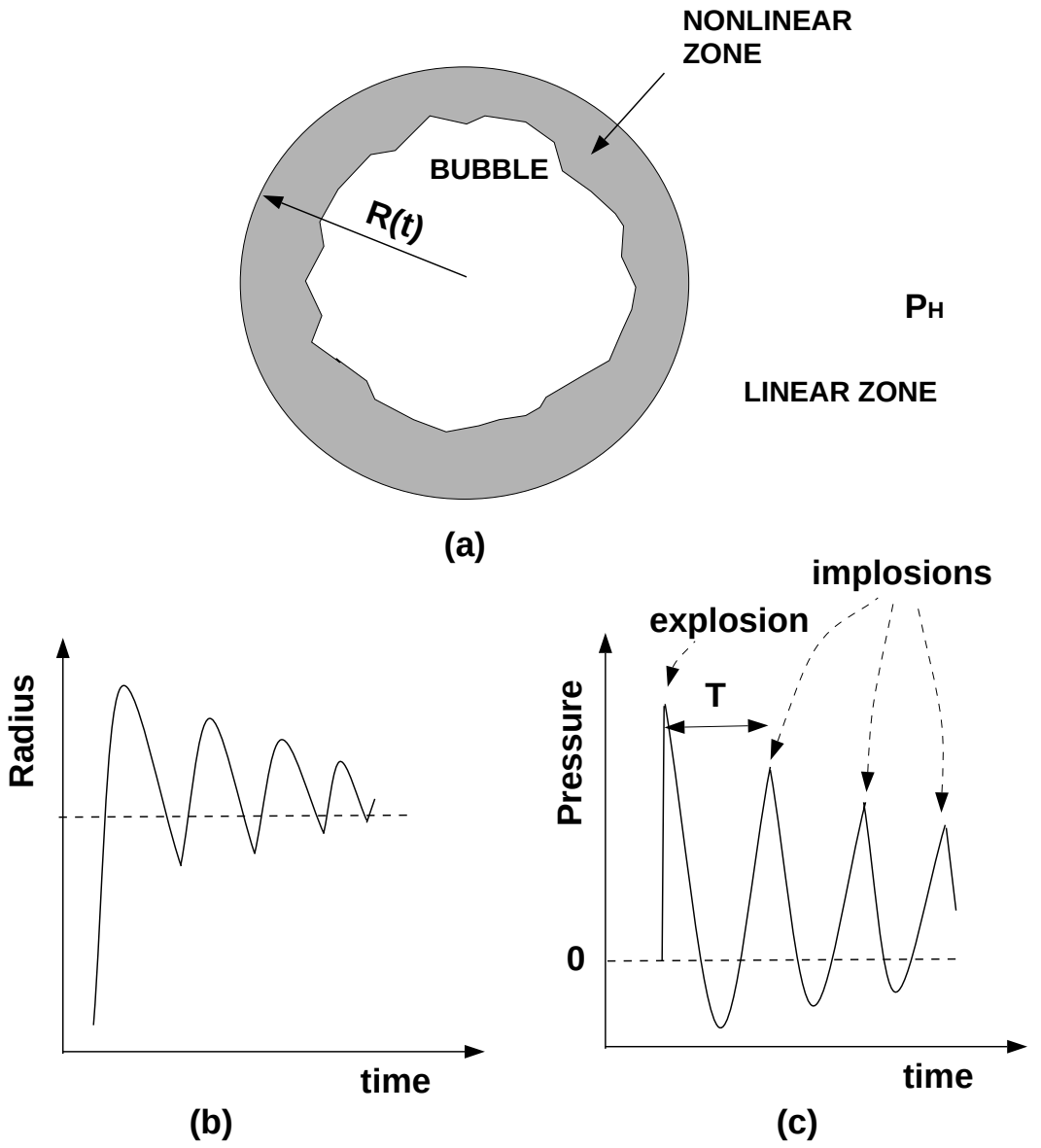

Figure 2.2: (a) Schematic section of the released air bubble; the radius (b) and the pressure (c) as a function of time for the air bubble of an airgun.

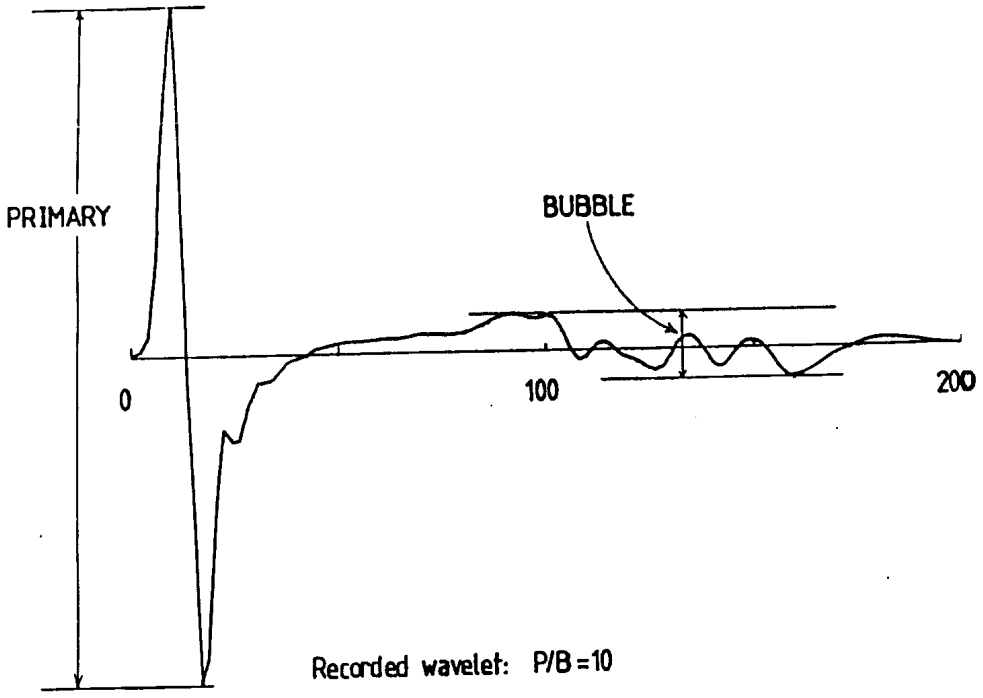

Figure 2.3: Far-field wavelet of tuned air-gun array

as the modified Rayleigh-Willis formula, which means that the airgun bubble period scales as the 1/3 power of the pressure or the volume, in general as the 1/3 power of the released energy.

2.4 Arrays and directivity

As mentioned in the previous section, the signature resulting from one airgun is an oscillatory signal which does not resemble the ultimate goal: creating a short seismic signature, preferably close to a band-limited delta pulse. This is the main reason why arrays are used. Airguns of different sizes and at different distances from each other are used such that the first pressure peaks coincide but the other peaks cancel, i.e., destructive interference for the other peaks. Usually with the design of airgun arrays, the largest gun is chosen to give the desired frequency content needed for a survey. Then smaller guns are used to cancel out the second, third, etc. peaks from this large gun. This is done in the frequency domain rather than in the time domain: a delta pulse in time corresponds to a flat amplitude spectrum in frequency. This has resulted in a few configurations of airgun arrays of which the so-called Shell array is a well-known one. This array has seven guns in one array. The quality of an array is measured via the so-called primary-to-bubble ratio, that means the ratio between the first peak and the second-largest peak. An example of such a signature is given in Figure (2.3). These days P/B ratios of 16 can be achieved.

The advantage of using an array is that a sharp signature can be produced, but has as a consequence that we introduce directivity, that means that the total signal shape is not constant in all directions but depends on the direction in which the wave is travelling. In order to illustrate the effect of directivity, consider two monopoles as depicted in figure

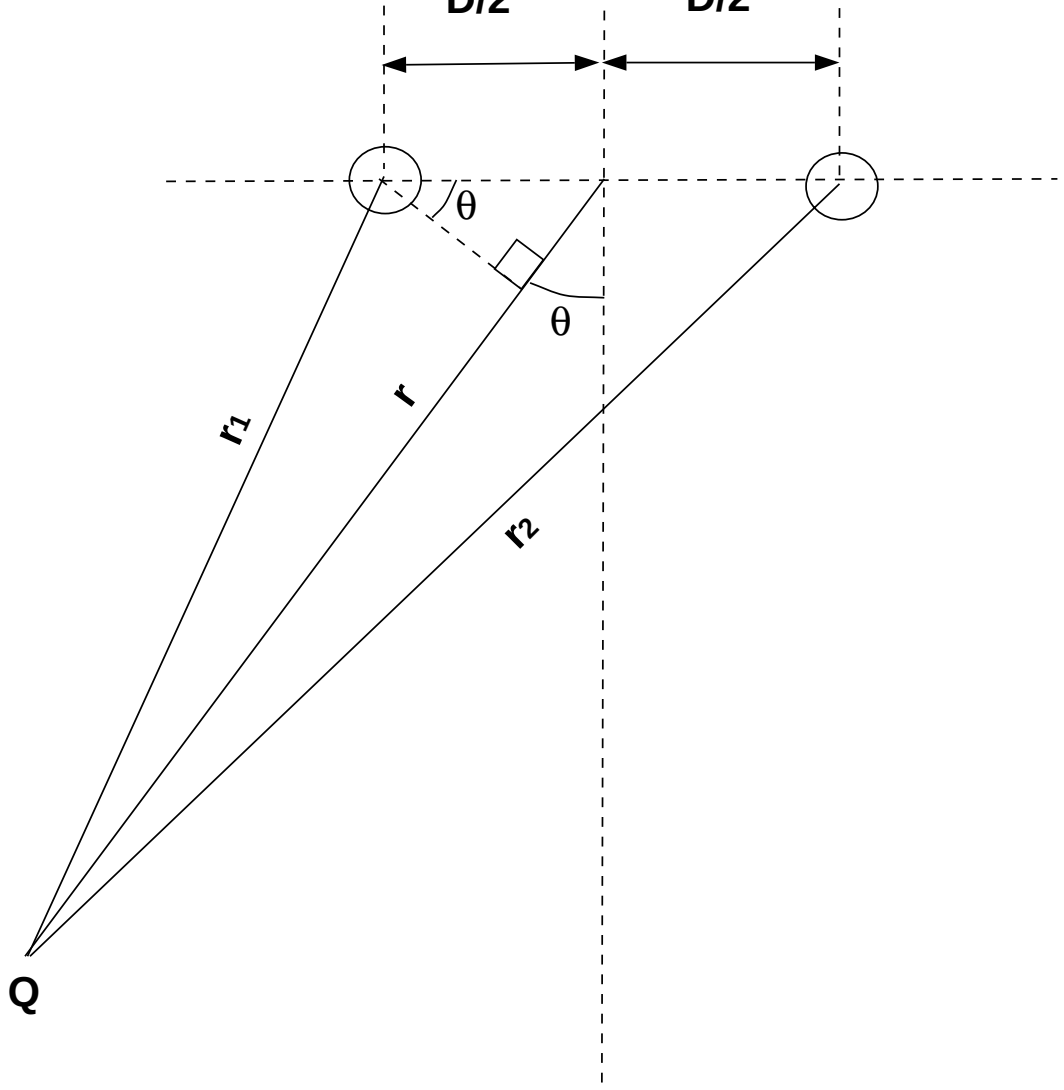

Figure 2.4: The configuration for determination of directivity effects of two monopoles

(2.4). Both have the same strength and are separated from each other by a distance D. We want to determine the signal at point Q which is at an angle θ with respect to the plane of symmetry going through the mid-point M on the connection line between the sources. The distance from Q to the one source is r_1 and to the other r_2; the distance to the mid-point between the two sources is r, and the wave speed in water is denoted by c. The pressure at Q is:

$$p_Q(t) = \frac{1}{r_1} s\left(t - \frac{r_1}{c}\right) + \frac{1}{r_2} s\left(t - \frac{r_2}{c}\right) \tag{2.2}$$

which is a solution of the wave equation for the pressure. The derivation of the wave equation is done in appendix B which is based on two fundamental laws: Newton's law and of mass Hooke's law, applied to an infinitessimal elementary volume of fluid.

Next, we define the Fourier Transform $S(\omega)$ of $s(t)$ as:

$$S(\omega) = \int_{-\infty}^{+\infty} s(t) \exp(-i\omega t)\, dt \tag{2.3}$$

When we transform equation (2.2) to the Fourier domain with respect to time, we obtain for the pressure:

$$P_Q(\omega) = \frac{1}{r_1} S(\omega) \exp(-i\omega \frac{r_1}{c}) + \frac{1}{r_2} S(\omega) \exp(-i\omega \frac{r_2}{c}) \tag{2.4}$$

Now let us assume that r is much larger than D such that $r_1 \approx r_2 \approx r$, then we approximate the pressure at Q by:

$$\begin{aligned} P_Q(\omega) &= \frac{1}{r} S(\omega) \left[\exp\left(-i\omega \frac{r - \frac{D}{2}\sin\theta}{c} \right) + \exp\left(-i\omega \frac{r + \frac{D}{2}\sin\theta}{c} \right) \right] \\ &= \frac{1}{r} S(\omega) \exp(-i\omega \frac{r}{c}) \left[\exp\left(i\omega \frac{\frac{D}{2}\sin\theta}{c} \right) + \exp\left(-i\omega \frac{\frac{D}{2}\sin\theta}{c} \right) \right] \\ &= \frac{1}{r} S(\omega) \exp(-i\omega \frac{r}{c}) 2\cos\left(\frac{\omega D \sin\theta}{2c} \right) \end{aligned} \tag{2.5}$$

For convenience we introduce the wavelength $\lambda = 2\pi c/\omega$ and we obtain:

$$P_Q(\omega) = \frac{1}{r} s(\omega) \exp(-i\omega \frac{r}{c}) 2\cos\left(\frac{\pi D \sin\theta}{\lambda} \right) \tag{2.6}$$

The total response is the response of a monopole with a term representing the directivity. We can observe certain features of the directivity. When D/λ is small then the directivity factor is nearly one and directivity is not important. Note then that the sine does not play an important role since it can be small but never be larger than 1. However, when D/λ is not small, then directivity is important when $\sin(\theta)$ is not small either. That $\sin\theta$ is not small means that we look at rather large angles from the vertical. At seismic frequencies in the range 10–100 Hz, the wavelengths are 150–15 m, respectively, when considering water with a wave speed of 1500 m/s. A typical airgun array is of a size of 20 m and this means that D/λ is not small compared with the 15 m wavelength. An example which shows the directivity is shown in Figure (2.5) where the array signature is given as a function of angle of observation.

It is obvious that when we are near to the array, we get complicated interferences of the signatures of the different guns, while far away we will not have these. Mathematically, this was established via approximating the distances $1/r_1$ and $1/r_2$ by $1/r$, and this approximation is the approximation of the far field, i.e., we are far enough away that we do get interference that is not a function of the distance any more. Nevertheless, at those distances, we still have a directivity, depending on the angle of observation!

Note that here there is also a difference between the single and the multiple-gun configuration; for the single gun the signature looks the same in the near as in the far field, for the array this is not the case. The far field of an array is there where the signature of the pressure wave becomes independent of distance. For instance, for an array of 20 m the far field starts at some 35 m (20 m + 15 m) for a bandwidth up to 100 Hz in water.

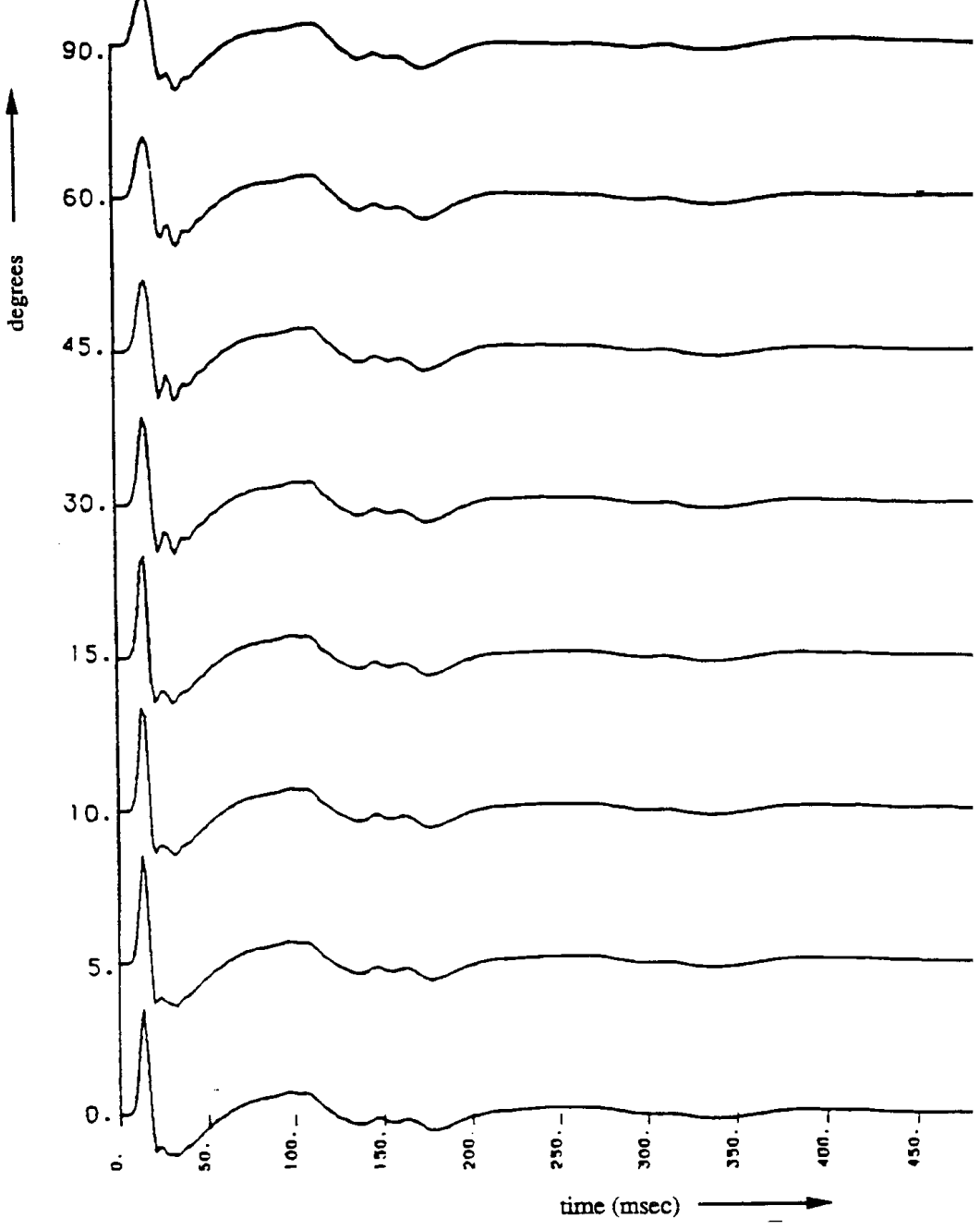

Figure 2.5: The airgun signature at different angles (directivity)

2.5 The effect of the free surface

In the marine situation, we always have the sea surface near to the source as well as near to the receivers. This has some effect on the outgoing signal in the far field. In the following this effect will be considered more closely. The derivation goes along similar lines as that for the directivity of an array. The configuration is depicted in figure (2.6). We have a direct signal arrival and an arrival which has been reflected against the sea surface with reflection coefficient -1. Let us denote the distance of the direct arrival r_+, and the distance for the arrival which reflected against the sea surface by r_-; the distance to the midpoint between the source and the image source is denoted by r, which lies on the sea surface. The distance between the source and the image source is denoted by D. The pressure at the observation point becomes:

$$p(t) = \frac{1}{r_+} s\left(t - \frac{r_+}{c}\right) + \frac{(-1)}{r_-} s\left(t - \frac{r_-}{c}\right) \tag{2.7}$$

Again transforming this equation to the Fourier domain, and letting r being much larger than D, we obtain:

$$\begin{aligned} P(\omega) &= \frac{1}{r_+} S(\omega) \exp\left(-i\omega \frac{r_+}{c}\right) - \frac{1}{r_-} S(\omega) \exp\left(-i\omega \frac{r_-}{c}\right) \\ &= \frac{1}{r} S(\omega) \left[\exp\left(-i\omega \frac{r - D\cos\theta}{c}\right) - \exp\left(-i\omega \frac{r + D\cos\theta}{c}\right)\right] \\ &= \frac{1}{r} S(\omega) \exp\left(-i\omega \frac{r}{c}\right) \left[\exp\left(\frac{i\omega D\cos\theta}{c}\right) - \exp\left(-\frac{i\omega D\cos\theta}{c}\right)\right] \\ &= \frac{1}{r} S(\omega) \exp\left(-i\omega \frac{r}{c}\right) \left[2i \sin\left(\frac{\omega D\cos\theta}{c}\right)\right] \end{aligned} \tag{2.8}$$

Again, we get the monopole response modified by a sort of directivity term, but now being a sine instead of a cosine. The amplitude of this latter function is plotted in figure (2.7).

In practice, this function determines at what depth the source and receiver will be placed. The amplitude will be maximum if the argument of the sine is $\pi/2$ plus an integer value of π. So take the first maximum, i.e.,:

$$\frac{\omega D\cos\theta}{c} = \frac{\pi}{2} \tag{2.9}$$

Assuming we are near vertical incidence, i.e. $\theta \approx 0$, and remember that $\omega = 2\pi f$, we get for D:

$$D = \frac{c}{4 f_{\text{peak}}} \tag{2.10}$$

Since $c = f\lambda$ in which λ is the wavelength, D will be:

$$D = \frac{\lambda_{\text{peak}}}{4}, \tag{2.11}$$

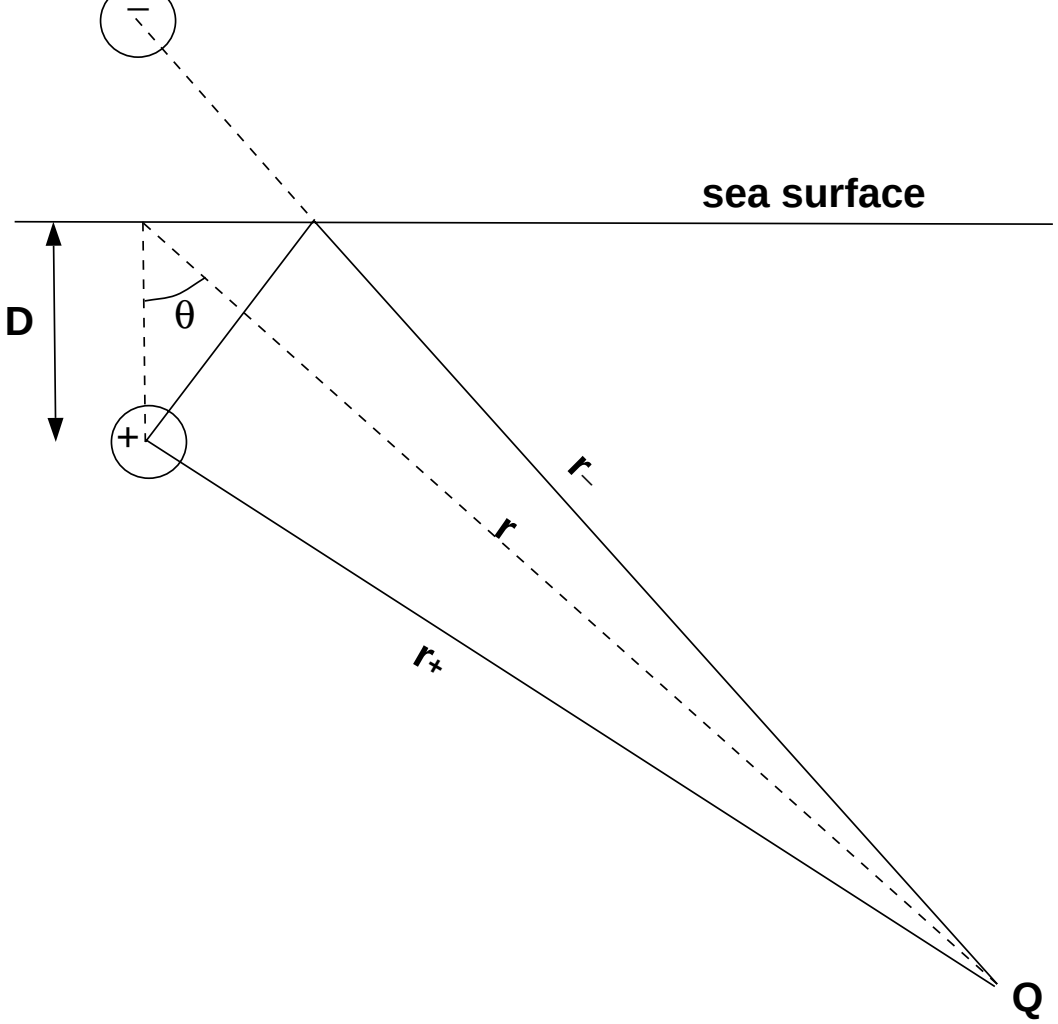

Figure 2.6: The configuration for determination of the effect of the sea surface

i.e., a quarter wavelength. Say, we want to have a peak frequency of 75 Hz which is the frequency content of a target at about 3 km depth. With the velocity of water being 1500 m/s we must have for a small angle of incidence:

$$D = \frac{c}{4f_{\text{peak}}} = \frac{1500}{4 \times 75} = 5 \text{ m} \tag{2.12}$$

This is pretty shallow. The problem here is that the noise from the sea waves is often too large so that the receivers will have to be put deeper. However, at a quiet sea, the receivers could even be put shallower with the advantage that the spectrum peak as well as the first notch shift to higher frequencies. Notice that this consideration is a consideration between resolution, Signal-to-Noise ratio and target depth!

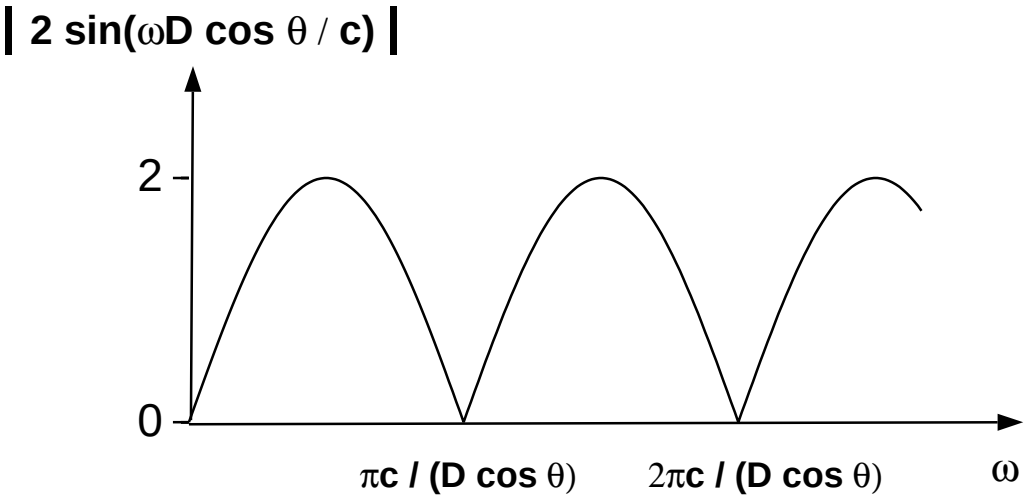

Figure 2.7: The spectral shaping due to the sea surface: $A(t) = 2|\sin(\omega D(\cos\theta)/c)|$.

2.6 Dynamite and its mechanics

Until the arrival of the Vibroseis technique, dynamite was the mostly used seismic source on land. Dynamite itself is very cheap, the costs involved are mainly the costs of drilling the shot-holes to place the dynamite. These costs may run up so high as to make the Vibroseis a good competitor of the dynamite source. Dynamite is usually used in non-urban areas for obvious reasons. A nice characteristic of dynamite is that it is resembling a (band-limited) form of the delta pulse, something we would ideally like to have, since we are interested in the impulse response of the earth. In this section some features of the dynamite source and the signature resulting from it will be discussed.

Dynamite is a chemical composition which burns extremely fast when detonating. Typically, 1 kilogram of dynamite burns in about 20 microseconds. In this very short time it vaporizes and generates very high pressures and temperatures. The dynamite is usually ignited with a detonator which is a small-size charge of dynamite as well, but enough to ignite the larger charge. The detonator must get a large current through it in order to be set off. For safety reasons, the detonator is designed such that a large current has to be applied. A typical current strength is some 5 Amp.

Explosives can be classified by their chemical composition. Dynamite itself consists of a combination of the explosives glyceroltrinitrate and glycoldinitrate. Since the combination of these two give a fluid, they are mixed with celluloid-nitrate and then give a gelatinous material. Additives of certain (secret) components result in different types of dynamite. Because all of these dynamites contain glyceroltrinitrate, contact with the skin or inhalation, causing head aches, must be avoided.

Since the burning of the dynamite takes place in a very short time generating sudden high pressures and temperatures, it is obvious that in the ground, immediately around the explosive a non-linear zone is created, that means the rock or soil will have undergone some permanent change by the explosion. Three processes are at work there: deformation

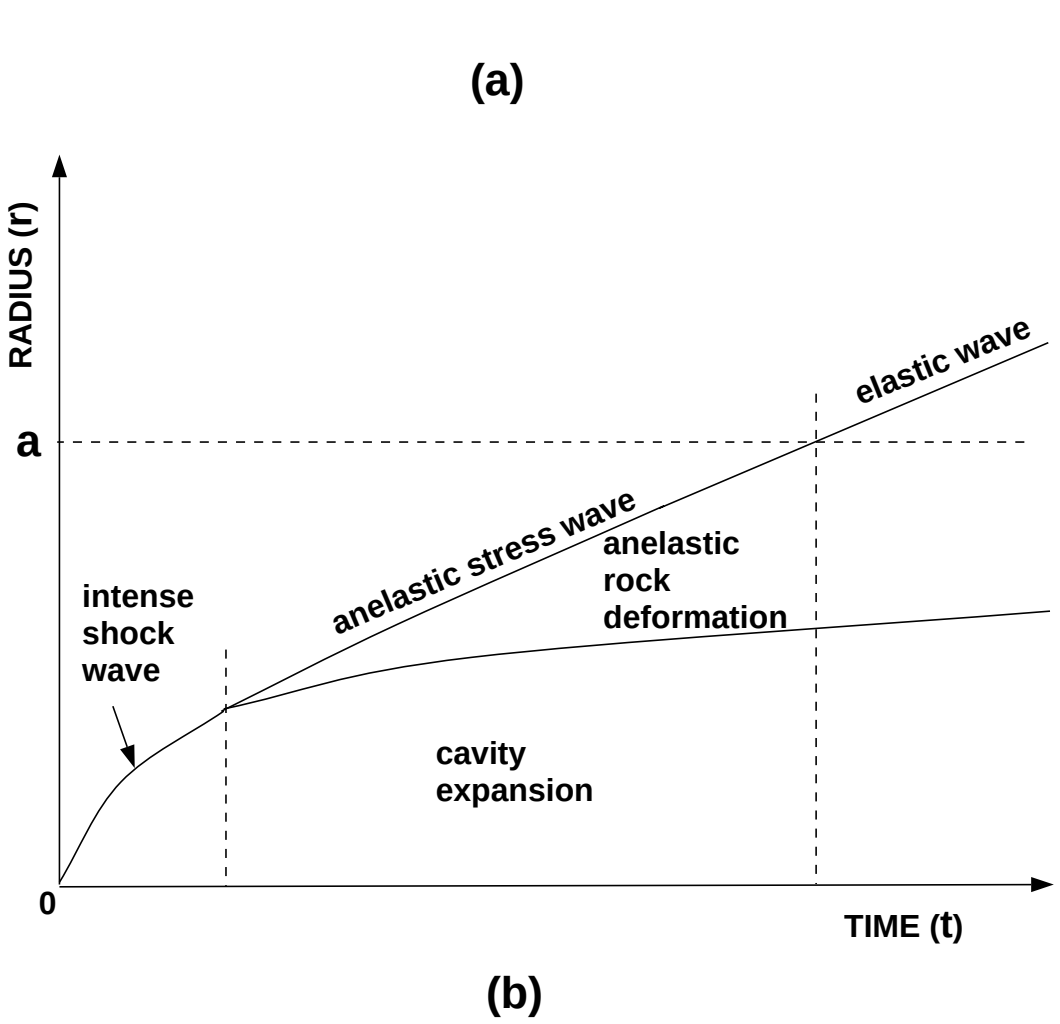

Figure 2.8: The behaviour of dynamite: (a) the characteristic zones in space, and (b) the radius as a function of time with its characteristic zones.

of the material, conversion of work into heat and geometrical spreading. There will be a distance from the source where there will be no deformation any more; this is given in Figure (2.8). The behaviour of the dynamite as a function of time is given in the lower of Figure (2.8). In time, we first have an intense shock wave with a complete shattering of the rock or soil. Then, at a certain time, we get two effects, namely a cavity expansion and anelastic rock deformation, until we reach finally a time where we left a cavity which stays there, and an elastic wave originating from this area. So there will always be a cavity left when using dynamite. This cavity is not the same as the radius where the anelastic wave becomes an elastic wave. There has actually been some people who have dug out these cavities in order to see how the cavity changed with a different charge of dynamite. It turned out that the cavity radius was proportional to the cube root of the charge mass.

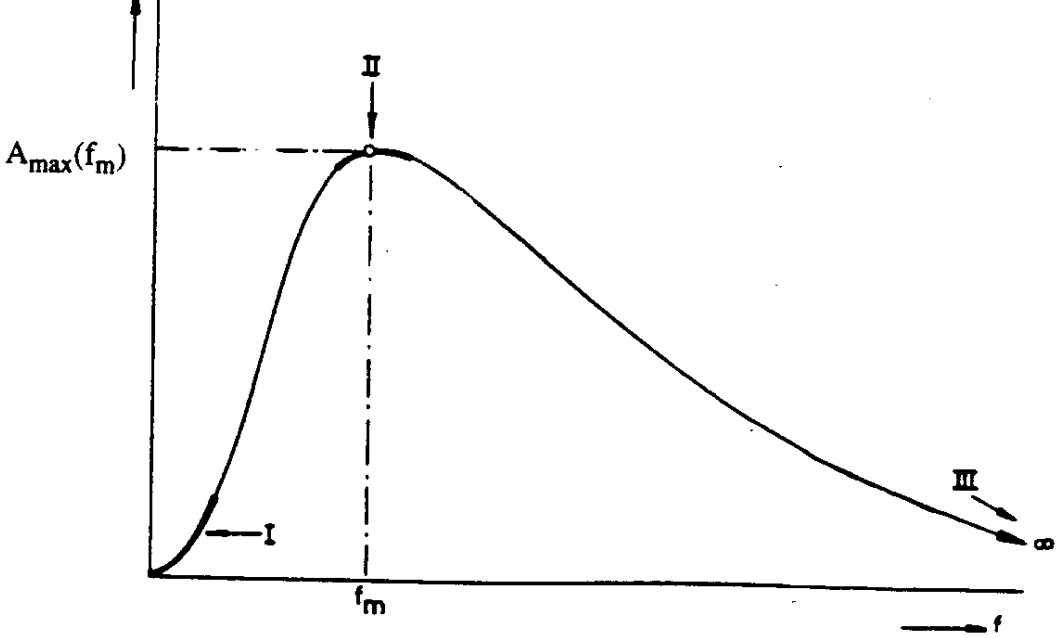

Figure 2.9: Amplitude as function of frequency of dynamite signature (from: Peet, 1960)

2.7 The dynamite signature

Let us now look at the pressure resulting from a dynamite explosion. It will not be shown how the following results are obtained; that is beyond the scope of these course notes. These results were derived from shock-wave theory, and are shown in Figure (2.9). Let's first concentrate on the upper figure. We see here three important regions: a low-frequency region, a central-frequency region around the maximum spectral amplitude and a high-frequency region. The low-frequency region (I) can be described by the function:

$$P(f) \propto f^2 M^{4/3} \tag{2.13}$$

The next region is there where the spectrum of the pressure peaks. In that region II the pressure is related to the mass of the dynamite via the equation:

$$P(f) \propto M^{2/3} \tag{2.14}$$

The last region is the high-frequency region III, where the pressure is related to the mass of the dynamite via:

$$P(f) \propto \frac{M^{1/3}}{f} \tag{2.15}$$

Figure (2.10) gives some interesting information, namely how a different charge affects the spectrum. It reflects the intuitive idea that if we use a larger charge, a lower frequency content will be the result. The ratios by which this happens is given on top of that figure. If we increase the mass by, say, a factor of 27, the frequency is reduced by a factor 3. This means that the frequency dependence is inversely proportional to the cube root of

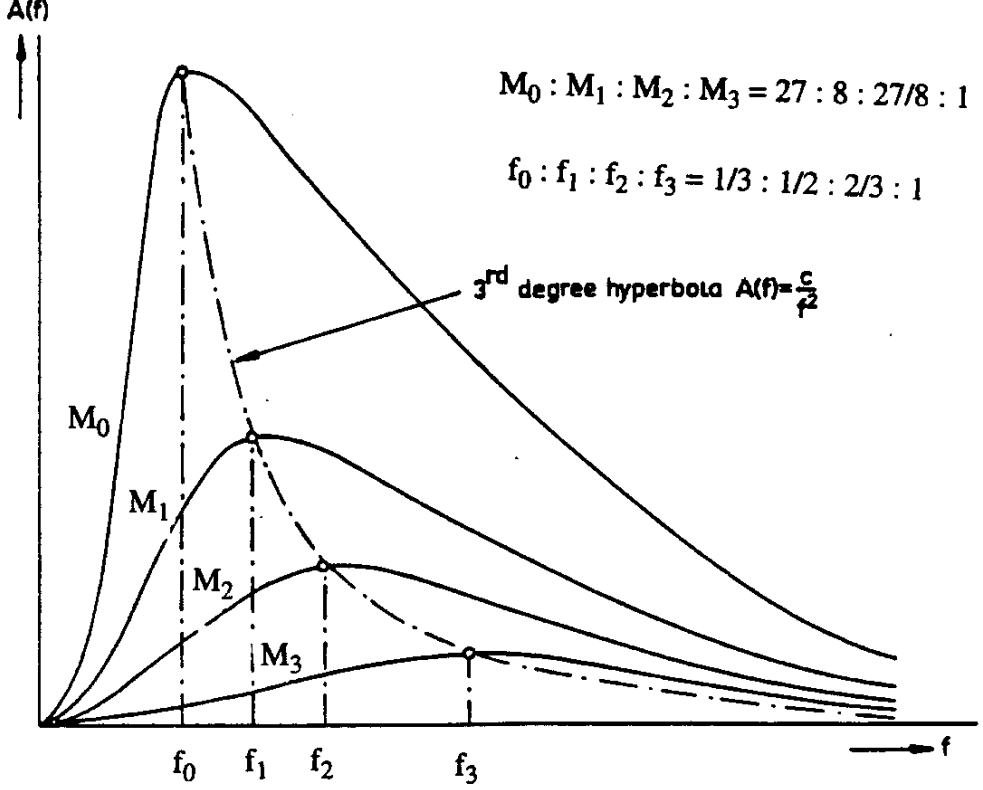

Figure 2.10: Scaling of amplitudes as function of frequency (from: Peet, 1960)

the mass, and if we include the result that the amplitude of the maximum is inversely proportional to the cube root of the mass, we arrive at:

$$P_3(f) = \frac{c}{M^{1/3}} P_0(fM^{1/3}) \tag{2.16}$$

In the marine case it is possible to measure the wavelet of an airgun because the water is such an homogeneous medium. The signal will not be distorted by inhomogeneities in the water. On land the situation is is different. There we have many inhomogeneities, especially in the shallow layers, which will change the signal so that it is not simple to measure an undistorted outgoing signal. There is no place in the world where the rocks are so homogeneous that we can measure the signature of the wavelet without distortions from the inhomogeneities. How can we determine then the signature? Recently, this has been done by using the behaviour as discussed in the previous section. We shall not go into detail how this is done. The only assumption the method had to make is that we are in the far field.

The result from this experiment is given in Figure (2.11), showing a pulse with a sharp peak at the beginning. The amplitude and phase spectrum are given in Figure (2.12) and Figure (2.13). An interesting result which can be seen is in the phase: it is minimum-phase.

This has always been assumed to be true although never shown. This can be seen by the fact that from the beginning to the end the phase spectrum comes back to zero again at the end; if it were not minimum-phase then the phase spectrum would have ended at $2\pi, 4\pi$ or n times 2π. The characteristic of minimum-phase is given in appendix C.

Dynamite is used on land and must be placed in a shothole at sufficient depth. This depth is determined by the effect of the consolidated and unconsolidated layer. One could

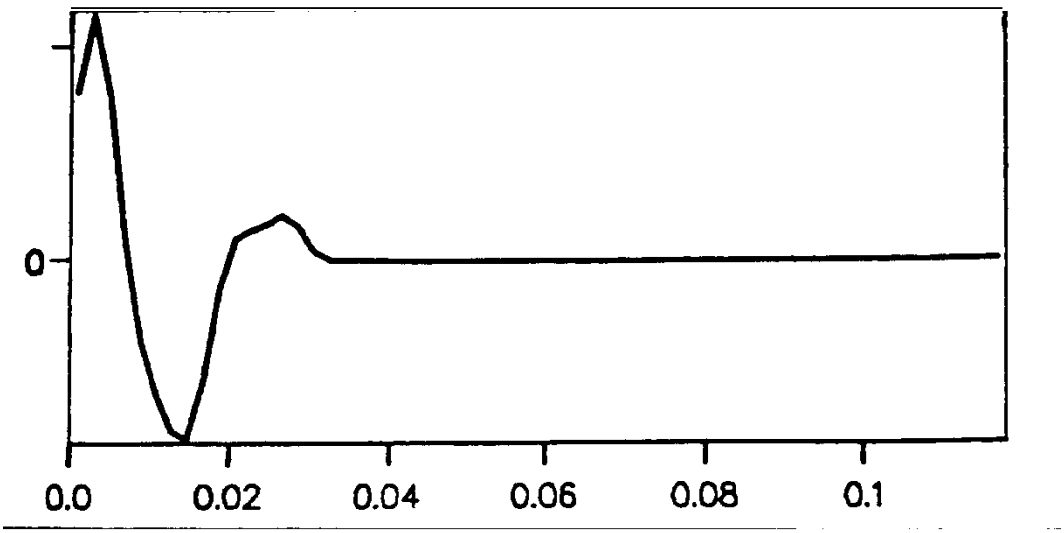

Figure 2.11: Time-domain signal of dynamite, obtained from measurements in the field.

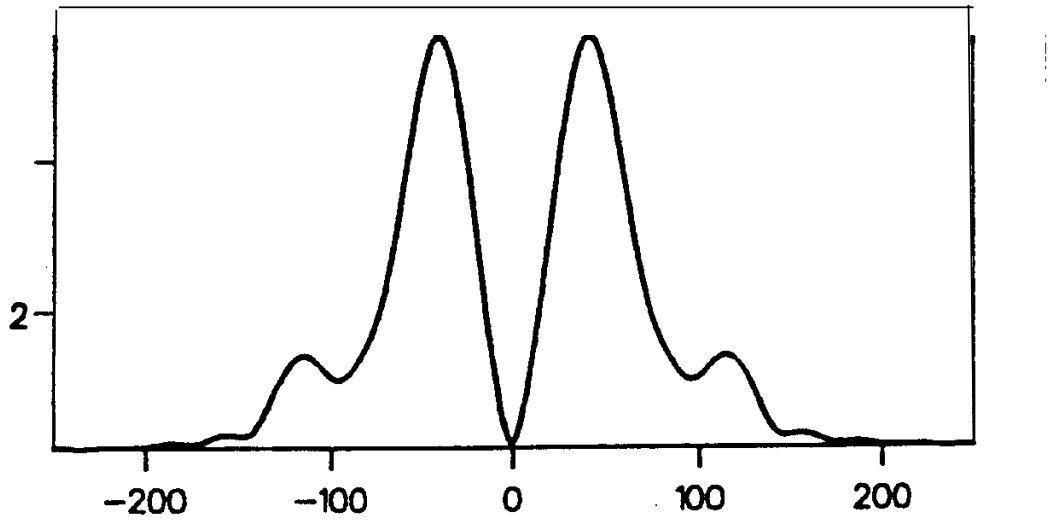

Figure 2.12: Amplitude spectrum of dynamite signature.

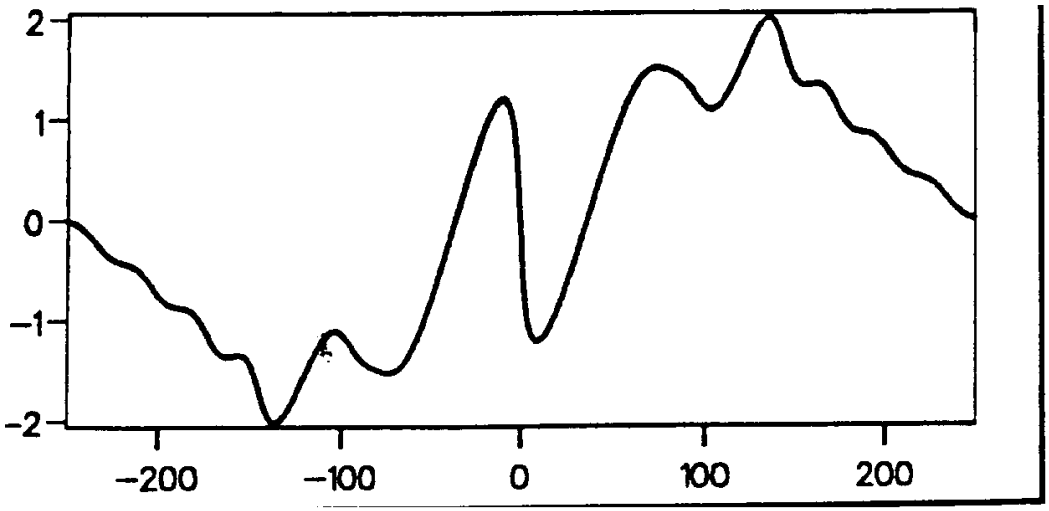

Figure 2.13: Phase spectrum of dynamite signature.

argue that the dynamite must placed at a depth below the free surface in the first layer but usually this layer is unconsolidated and thus a lot of energy will be dissipated in this layer. Therefore it is better to place the dynamite below the boundary between the consolidated and unconsolidated layer since the dynamite must be put in the consolidated layer anyway. We can investigate the spectral effect of the boundary on the total outgoing signal; this derivation runs in the same way as for the hydrophones and airguns beneath the sea surface, only the reflection coefficient would not be -1, however still large and negative. A similar kind of function will be obtained, and we can easily see that the optimum depth will again be a quarter wavelength of the dominant frequency below the weathered layer, i.e.,

$$D = \frac{\lambda_{\text{peak}}}{4} = \frac{c}{4f_{\text{peak}}} \tag{2.17}$$

On land, we usually do not know beforehand the velocity of the consolidated layer. This velocity c can be determined via shots at different depths so that an estimate can be made. Another way of determining these is via a small refraction experiment, from which the depth of the interface between the consolidated and unconsolidated layer can be determined rather accurately as well.

2.8 Vibroseis

In seismic exploration, the use of a vibrator as a seismic source has become widespread ever since its introduction as a commercial technique in 1961. In the following the principles of the Vibroseis$^{\text{TM}}$ (Registered trademark of Conoco Inc.) method are treated and the mechanism which allows the seismic vibrator to exert a pressure on the earth is explained. Two basic features of the force generated by the seismic vibrator are discussed: first, the non-impulsive signal generated by a seismic vibrator having a duration of several seconds; second, the monitoring system of the seismic vibrator allowing control over the outgoing vibrator signal. Finally, the advantages and disadvantages of Vibroseis over most impulsive sources are discussed.

The vibrator is a surface source, and emits seismic waves by forcing vibrations of the vibrator baseplate which is kept in tight contact with the earth through a pulldown weight. The driving force applied to the plate is supplied either by a hydraulic system, which is the most common system in use, or an electrodynamic system, or by magnetic levitation, the latter being a new development in the field of seismic vibrator technology. The direction in which the plate vibrates can also vary: P wave vibrators (where the motion of the plate is in the vertical direction) as well as S wave vibrators (vibrating in the horizontal direction) are used. Finally, a marine version of the seismic vibrator has been developed, however not in frequent use.

For all these vibrator types, the general principle which governs the generation of the driving force applied to the plate (usually referred to as the baseplate) can be described by the configuration shown in Figure (2.14). A force f is generated by a hydraulic, electrodynamic or magnetic-levitation system. A reaction mass supplies the system with the reaction force necessary to apply a force on the ground. In general, the peak force is such that the accelerations are in the order of several g's, so that an additional weight has to be applied to keep the baseplate in contact with the ground. For the hydraulic and electrodynamic vibrators, the weight of the truck is used for this purpose. This weight is commonly referred to as the holddown mass.

The means by which the force f is actually generated is illustrated in Figure (2.15), in which the principle of the hydraulic drive method is shown. By pumping oil alternately into the lower and upper chamber of the piston, the baseplate is moved up and down. The fluid flow is controlled by a servo valve. The driving force acting on the baseplate is equal and opposite to the force acting on the reaction mass, as can easily be inferred from Figure (2.15).

The holddown mass, as was given in Figure (2.14), is vibrationally isolated from the system shown in Figure (2.15) by an air spring system with a low spring stiffness (shown in figure (2.16)), and its influence on the actual output of the system is usually neglected. The resonance frequency of the holddown mass is in the order of 2 Hz, the lowest frequency of operation in Vibroseis seismic surveys for exploration purposes being usually not less than 5 Hz.

2.9 The force exerted on the baseplate

The mechanism by which the seismic vibrator applies a force to the baseplate is very complicated, and differs for different vibrators. In this section, the applied force is described using the mechanical model as introduced in the previous section, and was developed by Lerwill (1981).

Lerwill (1981) introduced a model of a compressional wave vibrator which describes the different components of the vibrator in terms of masses, springs and dashpots (i.e. shock absorbers). The model, shown in Figure (2.14), contains three masses. These are the holddown mass, which represents the weight of the truck and is used to keep the baseplate in contact with the ground; the reaction mass, which allows the vibrator to exert a force on the baseplate; and the baseplate, which is in contact with the earth's surface. The input force i, which is supplied by the vibrator's hydraulic system, is not the same as the force f exerted on baseplate and reaction mass due to the compressibility of the oil pumped in the cylinder. The suspension s_1 represents the means to support the reaction mass in its neutral position. The connection between truck and the baseplate by means of isolated air bags is represented by the dashpot K and suspension s_2. Gravity forces are not included in the analysis because they represent a static load, and do not affect the dynamic behaviour of the seismic vibrator. The holddown mass is vibrationally isolated

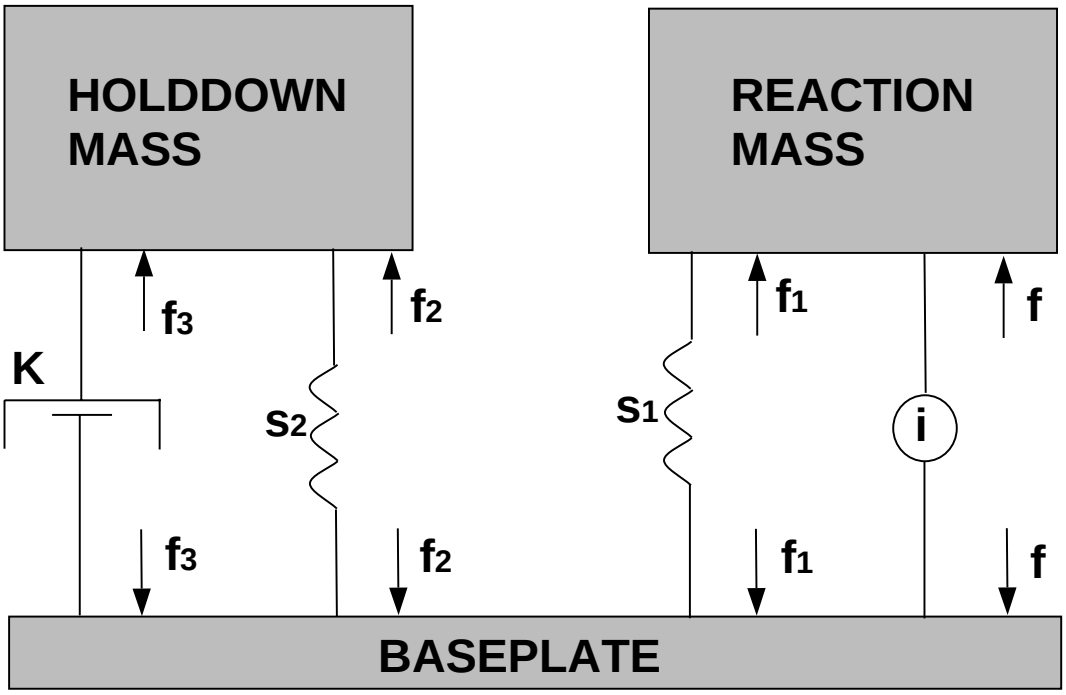

Figure 2.14: The mechanical model of the Vibroseis truck.

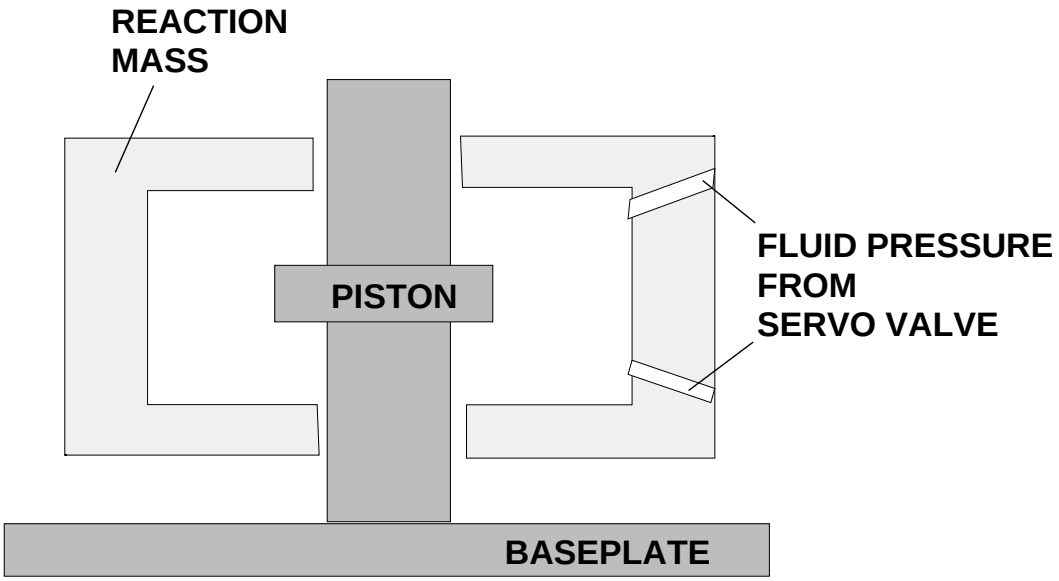

Figure 2.15: Schematic view of the generation of the driving force for a hydraulic vibrator.

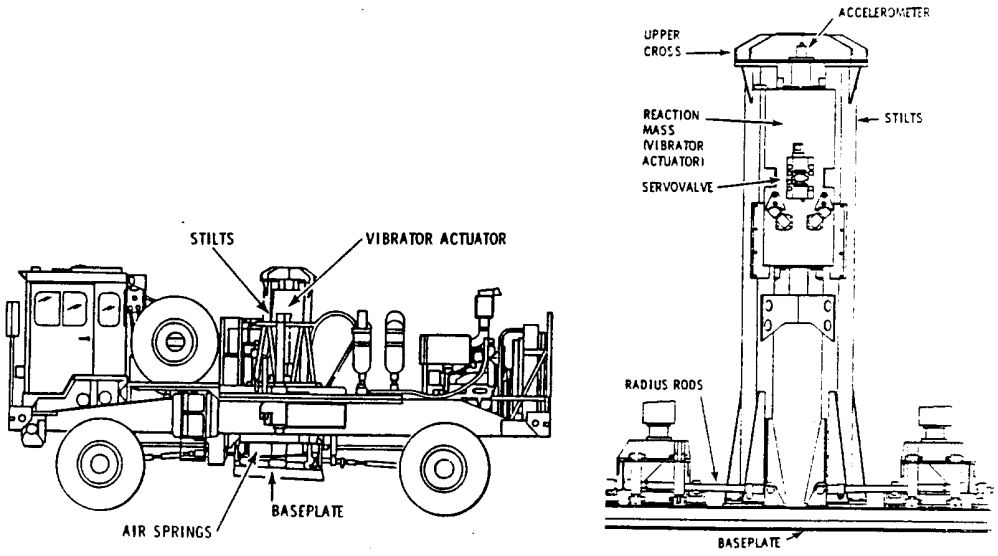

Figure 2.16: (a) schematic view of the Vibroseis truck with the air springs, the baseplate and the vibrator actuator (reaction mass), and (b) detailed view of the middle part of the truck.

from the baseplate by the system shown in Figure (2.14).

The displacement of the three masses is taken positive downwards. Using this convention, the forces due to the dashpot and suspensions are found to be:

$$f_1 = s_1(u_r - u_3) \tag{2.18}$$

$$f_2 = s_2(u_h - u_3) \tag{2.19}$$

$$f_3 = K\frac{d}{dt}(u_h - u_3) \tag{2.20}$$

in which u_h, u_r and u_3 denote the displacement of the holddown mass, the reaction mass and the baseplate, respectively. The displacement of the baseplate is not uniform over the plate, so that the baseplate displacement u_3 in the above equations should be interpreted as the displacement at the point on the baseplate where the relevant forces are applied.

The equations of motion of the holddown mass and the reaction mass are

$$-f_1 - f = M_r\frac{d^2u_r}{dt^2} \tag{2.21}$$

$$-f_2 - f_3 = M_h\frac{d^2u_h}{dt^2} \tag{2.22}$$

The total force applied on the top of the baseplate, f^{applied}, is now given by:

$$f^{\text{applied}} = f + f_1 + f_2 + f_3 = -M_r\frac{d^2u_r}{dt^2} - M_h\frac{d^2u_h}{dt^2} \tag{2.23}$$

In practice, this equation can be used when accelerometers are placed on the reaction mass and the holddown mass: by scaling each of these measurements by the mass, the total applied force can be determined.

Numerical values for the mechanical parameters of the mechanical model were given by Lerwill (1981).

2.10 The signal emitted by a seismic vibrator

The signal emitted by the seismic vibrator is not impulsive, but typically has a duration of some 10–15 sec. The use of such a relatively long signal seems to be in contradiction with the fact that seismic exploration methods aim at detecting the impulse response of the earth. This apparent contradiction can be clarified by taking a closer look at the properties of an impulse and the earth response to such an impulse.

A perfect impulse at time $t = 0$ contains all frequency components with equal amplitude and zero phase. This is illustrated in Figure (2.17). In practice, one cannot generate a perfect impulse because this would require an infinite amount of energy; the best one can achieve is to emit a bandlimited impulse, resulting in a finite-amplitude wavelet whose time duration is small compared with any dominant signal periods present in the earth's response.

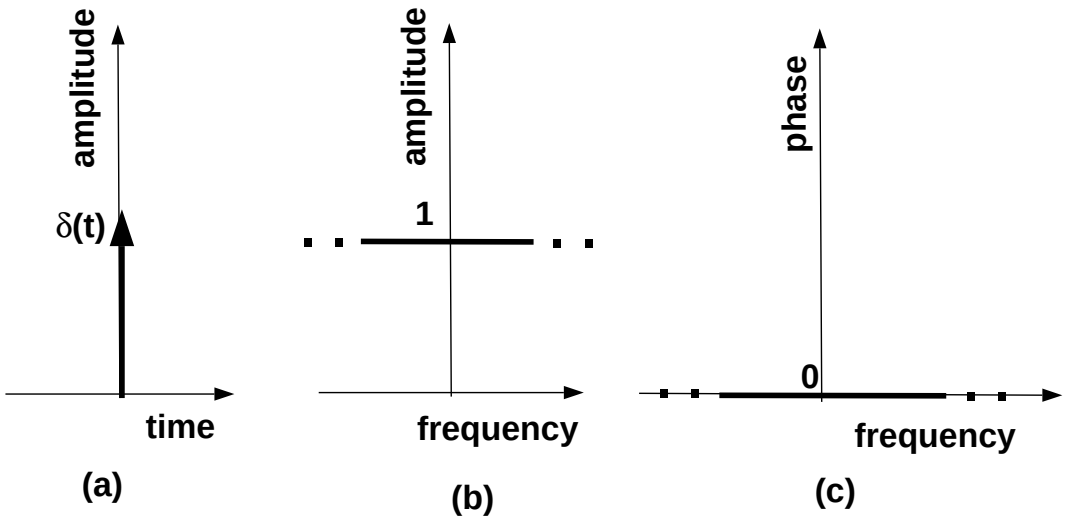

Figure 2.17: The notion of a perfect impulse, (a) in the time domain, and (b),(c) its corresponding frequency domain version.

The Vibroseis source emits a bandlimited, expanded impulse. The band limitation has two aspects: at the low frequency end, it is dictated by the mechanical limitations of the system and the size of the baseplate. The high frequency limit is determined by the mass and stiffness of the baseplate, the compliance of the trapped oil volume in the driving system for a hydraulic vibrator and mechanical limitations of the drive system.

The notion of an "expanded " impulse can be explained in terms of the amount of energy per unit time, known as energy density. In an impulsive signal, all energy is concentrated in a very short time period, leading to a very high energy density. In the Vibroseis method, a comparable amount of energy is transmitted over a longer time (i.e., smeared out over a longer time), so that the energy density of the signal is reduced considerably. This reduction in energy density is achieved by delaying each frequency component with a different time delay, while keeping the total energy contained in the signal constant. Thus, instead of emitting a signal with a flat amplitude spectrum and a zero phase spectrum, a signal is created which has the same flat amplitude spectrum in the frequency band of interest, however having a non-zero phase spectrum. The frequency-dependent phase shifts cause time delays which enlarge the duration of the signal. However, the total energy of the signal is determined only by its amplitude spectrum (Parseval's theorem!). The effect of the increased time duration of the emission on the recorded seismogram has to be eliminated. This is achieved by having full control of the phase function of the emitted signal. Then, the signal received at the geophone can be corrected for the non-zero phase spectrum of the source wavelet by performing a cross-correlation process of the received seismogram and the outgoing signal (source signal). To clarify this point, let the source wavelet be denoted by $s(t)$. If the convolutional model is adopted to describe the response at the geophone, x(t), the following expression is obtained in the absence of noise:

$$x(t) = s(t) * g(t) \tag{2.24}$$

where $g(t)$ denotes the impulse response of the earth, i.e., the layered geology, and "$*$"

denotes a convolution. Transforming equation (2.24) to the frequency domain yields

$$X(\omega) = S(\omega)G(\omega) \tag{2.25}$$

If the received signal $x(t)$ is cross-correlated with the source signal $s(t)$, the signal $c(t)$ is obtained which, in the frequency domain, is given by

$$C(\omega) = X(\omega)S^*(\omega) = |S(\omega)|^2 G(\omega) \tag{2.26}$$

since cross-correlation of $x(t)$ with $s(t)$ in the time domain corresponds to a multiplication in the frequency domain of $X(\omega)$ with the complex conjugate of $S(w)$. In this equation, the complex conjugate is denoted by the superscript "$*$". Since the amplitude spectrum of $S(\omega)$ is flat over the frequency band of interest , and zero outside this frequency band, it follows that by cross-correlating the measured seismogram $x(t)$ with the source function $s(t)$ the (scaled) bandlimited impulse response of the earth is obtained. The scaling factor is simply the (constant) amplitude spectrum of the source signal squared. In the time domain, the cross-correlated seismogram is a convolution of the earth's impulse response with the autocorrelation of the "sweep", i.e., the outgoing signal. In Vibroseis applications, the measured seismogram $x(t)$ is usually referred to as "vibrogram", whereas the seismogram after cross-correlation, $c(t)$, is denoted as "correlogram".

So, it is possible to emit a signal with a flat amplitude spectrum and an arbitrary phase spectrum, and still obtain the exact (bandlimited) impulse response of the earth, provided the phase spectrum of this source wavelet is known. It is important to note that this cross-correlation is merely a special deconvolution process, in which we exploit the fact that the amplitude spectrum is constant, thus avoiding the design of deconvolution filters.

This completes the general framework into which the vibrator's source signal is placed. The detailed shape chosen for the vibrator signal in practice is now described. A signal $q(t)$ (usually referred to as the "sweep") is generated by the sweep generator of the seismic vibrator. The signal $s(t)$ introduced in equation (2.24) is different from the sweep $q(t)$, for reasons that are explained later when the control of the vibrator source is discussed. The generated sweep $q(t)$ has the general form

$$q(t) = w(t)\sin[2\pi\theta(t)]. \tag{2.27}$$

$w(t)$ is a special "window" function of time which has at the beginning and at the end of the sweep a linear or cosine shaped roll-off ("taper") with a length of about 250 msec. The taper is applied at the beginning and at the end of the sweep to reduce artificially introduced oscillations due to the finite time window length, the so-called Gibbs' oscillations. The sweep typically has a duration T of some 10 s. The function $q(t)$ determines the frequency of the sine wave as a function of time; more specifically, the derivative of $q(t)$ is equal to the instantaneous frequency $f^{\text{inst}}(t)$ of the emitted sine wave:

$$\frac{d\theta(t)}{dt} = \theta'(t) = f^{\text{inst}}(t) \tag{2.28}$$

As an example, a sweep is considered where the instantaneous frequency varies linearly with time, as illustrated in Figure (2.18):

$$f^{\text{inst}}(t) = f_0 + \frac{f_1 - f_0}{T}t \tag{2.29}$$

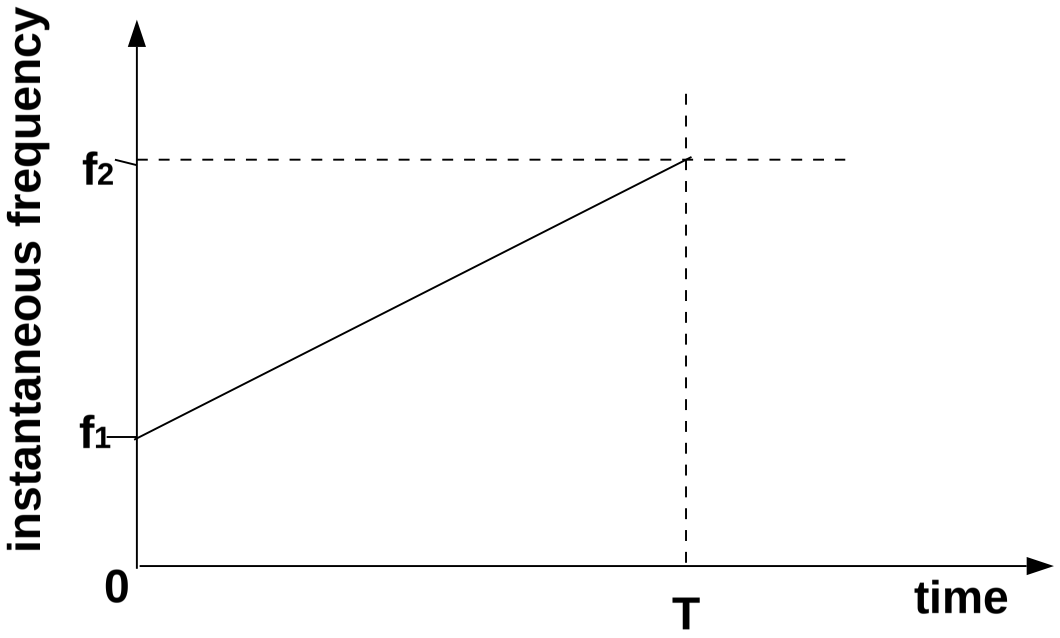

Figure 2.18: The instantaneous frequency of a linear sweep as a function of time.

in which f_0 is the starting frequency of the sweep, f_1 its end frequency and T sweep duration. This sweep with a linearly-varying instantaneous frequency is commonly referred to as a linear sweep, and is given by:

$$q(t) = w(t) \sin \left[2\pi \left(f_0 + \frac{1}{2}(f_1 - f_0)\frac{t}{T} \right) t \right] \tag{2.30}$$

If the first sweep frequency is smaller than the last frequency f_1, the sweep is called an upsweep; if f_0 is larger than f_1, it is called a downsweep.

Although the relation between the sweep and its instantaneous frequency as a function of time is readily established, the Fourier transform of the sweep cannot be expressed analytically. At this point, a clear distinction must be made between the concept of "instantaneous frequency", which is the single frequency contained in the signal at a single time instant, and the concept of a frequency component as used in conjunction with a Fourier-transformed time function.

In Figure (2.19) the concepts outlined above are illustrated for the example of a linear upsweep. An 8 sec, 10–100 Hz linear upsweep is used with a taper length of 250 msec. Figure (2.19) (a) shows the sweep $q(t)$. Because the oscillations in the sweep are too rapid to yield a clear picture, the frequency limits for this figure are 1–5 Hz. Figures (2.19) (b) and (2.19) (c) show the amplitude and phase, respectively, of $Q(f)$. It can be observed from these figures that the phase indeed is a quadratic function of frequency, and that the amplitude spectrum of the sweep is constant over the bandwidth, apart from some Gibbs' oscillations at the beginning and end frequencies. Finally, Figure (2.19) (d) shows the autocorrelation of the sweep.

The Vibroseis source is designed in such a way that the operator has, at least in principle, perfect control over the emitted wavelet. It follows from the previous discussion that knowledge of the source wavelet emitted by the vibrator is essential. The Vibroseis method presents the opportunity for this kind of signal control. This is achieved by the system shown in Figure (2.20).

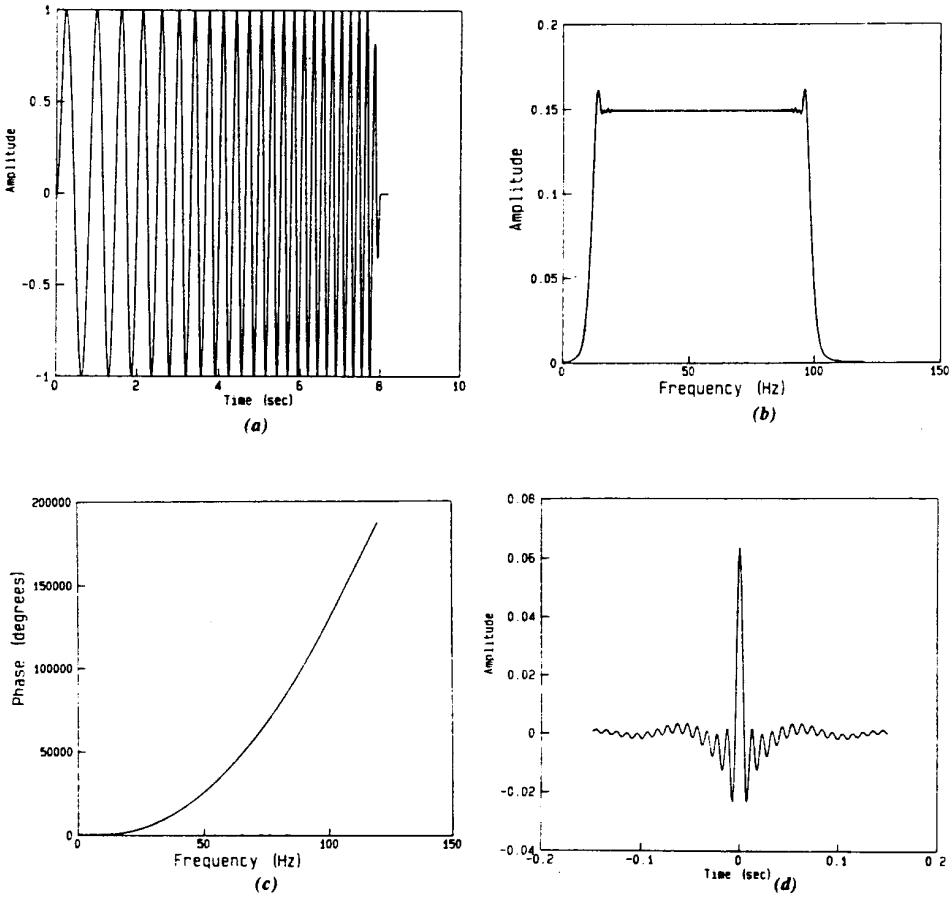

Figure 2.19: An 8 sec, 10-100 Hz upsweep with taper length of 250 msec. (a) Sweep in time domain; frequency range for this Figure is 1-5 Hz for display purposes, (b) amplitude spectrum of sweep, (c) phase spectrum of the sweep, in degrees, and (d) autocorrelation of sweep.

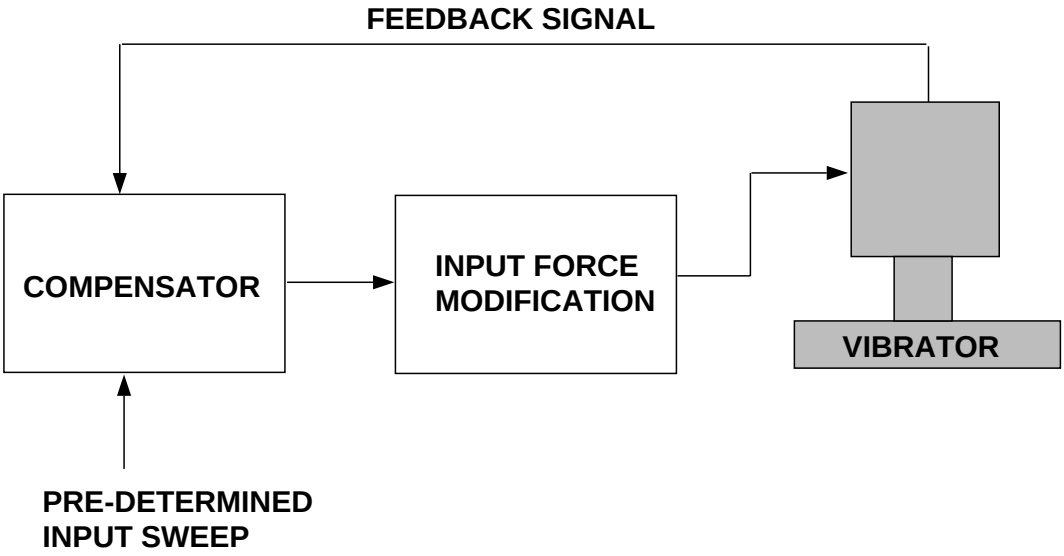

Figure 2.20: The feedback system of a seismic vibrator.

The pre-determined sweep input $q(t)$ (also called the pilot sweep) is compared with a feedback signal $f(t)$, which is a signal measured on the vibrator as explained in equation (2.23). In principle, any vibrator motion that can be measured can serve as a feedback signal. The main function of the feedback system is to produce a feedback signal which resembles the predetermined sweep as closely as possible. Amplitude and phase differences between these two signals are corrected for by a change in the time-varying input force. This correction for differences between the feedback signal and the pre-determined sweep is necessary because the vibrator electronics can, for the example of a hydraulic vibrator, only control the oil flow in the hydraulic piston, which in general is not equal to the feedback signal chosen on the vibrator.

In older days, the control system of the vibrator was designed to correct only for phase differences between the pre-determined sweep and the vibrator feedback signal. Since the early 1980's, amplitude control techniques have been in use which allow the vibrator to operate as close to the maximum holddown weight as possible without decoupling, i.e., jumping from the ground.

In order to appreciate the problem, we will look at the particle velocity created by a point source. Let us start with the solution of the wave equation for the pressure p, i.e.,:

$$P(\omega) = \frac{A}{r} \exp\left(-i\omega \frac{r}{c}\right) \tag{2.31}$$

in which A denotes some amplitude. On land, we put the ground in motion, so we then deal with particle velocity instead of pressure. We can determine from the pressure the particle velocity when we use the equation of motion (see also appendix B), i.e.,:

$$-\nabla p = \rho_0 \frac{\partial \vec{v}}{\partial t} \tag{2.32}$$

By transformation to the frequency domain the operator $\partial\vec{v}/\partial t$ becomes $i\omega\vec{v}$. In order to show the velocity in its simplest form, we assume spherical symmetry and use spherical coordinates; then the equation of motion in the frequency domain becomes:

$$-\frac{\partial P}{\partial r} = i\omega\rho_0 V_r \tag{2.33}$$

This means that we can determine the particle velocity from the pressure by differentiating the pressure with respect to r, and scale it with $-i\omega\rho_0$. We then obtain:

$$V_r = \frac{A}{i\omega\rho_0 r^2}\exp\left(-i\omega\frac{r}{c}\right) + \frac{A}{\rho_0 cr}\exp\left(-i\omega\frac{r}{c}\right) \tag{2.34}$$

The result comprises two terms, one term depending on $1/r^2$, while the other is depending on $1/r$. Since the first term is more important at small distances, this term is called the near-field term; the other term dominates at large distances, and is therefore called the far-field term. Another difference between these two terms is the factor $1/i\omega$ in the near-field term, showing a hyperbolic decrease of the spectrum with frequency. Therefore the near-field term mainly represents mainly lower frequencies; in time the $1/i\omega$ factor means integration.

The geophysical problem of the vibrator is the determination of the far field wavelet from measurements on the vibrator. For conventional geophysical applications, the wavelet $s(t)$ that appears in the convolutional model is of interest. In the convolutional model, it is assumed that the wavelet $s(t)$ does not change its shape while propagating, and is the same in all directions. The first condition, that $s(t)$ remains constant, implies that $s(t)$ is the far field wavelet; the second condition, the source being non-directional, implies that the source dimensions must be small compared with a wavelength. The latter condition is usually satisfied when a single vibrator is considered. It should be noted that the term "far field wavelet" usually refers to the far field particle velocity, since in normal land seismic applications geophones are used for signal detection.

It is theoretically possible to calculate the far field wavelet from measurements on the vibrator. This calculated wavelet is called $s^{\mathrm{vib}}(t)$. The band-limited impulse response of the earth is obtained by cross-correlating the received seismogram x(t) with this far-field vibrator signal $s^{\mathrm{vib}}(t)$. The frequency-domain expression for the seismogram after cross-correlation, $c(t)$, is thus given by:

$$C(\omega) = X(\omega)S^{\mathrm{vib}*}(\omega) = S(\omega)S^{\mathrm{vib}*}(\omega)G(\omega) \tag{2.35}$$

If $s(t)$ and $s^{\mathrm{vib}}(t)$ are the same, the desired zero-phase impulse response $g(t)$ is obtained.

In practice, the measured seismogram $x(t)$ is cross-correlated in real time with the pre-determined sweep $q(t)$. Only the resulting correlogram $c(t)$, in the frequency domain given by:

$$C(\omega) = X(\omega)Q^*(\omega). \tag{2.36}$$

It is thus assumed in practice that the feedback system of the vibrator ensures that the feedback signal $f(t)$, which is a measure of the actual vibrator motion, and the pre-determined sweep $q(t)$, which is the output of a sweep generator, are equal. The question which feedback signal should be used to predict the far field wavelet has been a controversial issue since it was first raised by Lerwill in 1981.

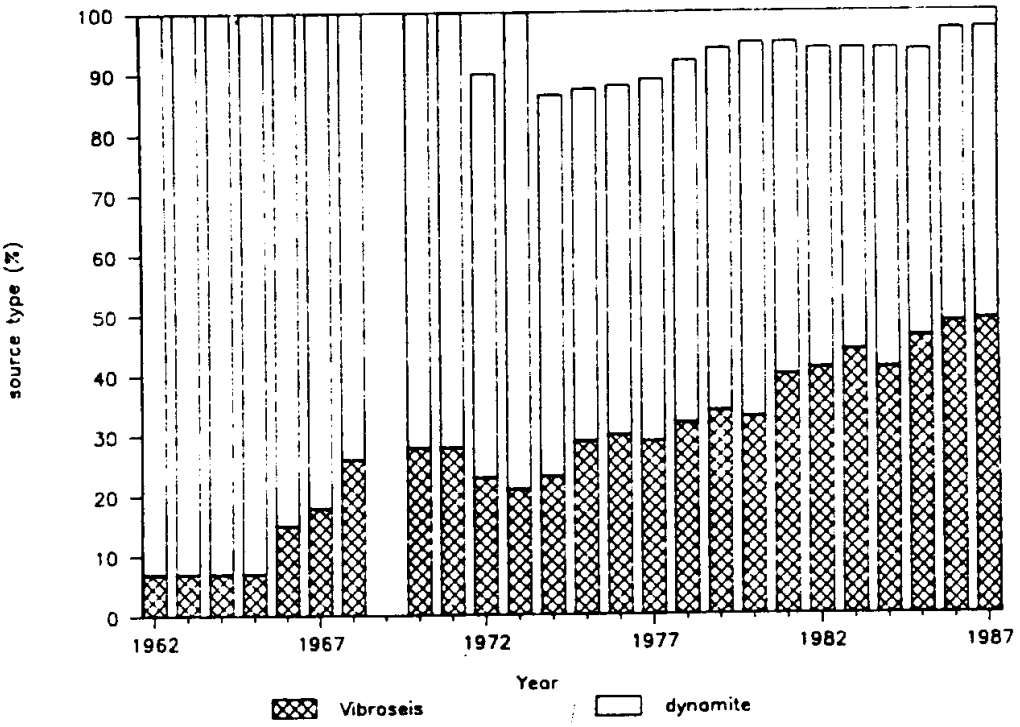

Figure 2.21: The contribution of Vibroseis and dynamite to the total number of crew months spent in land petroleum exploration, in %, for the years 1962-1987.

2.11 Comparison between Vibroseis and dynamite

One may wonder why it is not normal practice in seismic exploration to use an impulsive source, since, after all, it is the earth's impulse response we are after. As can be seen in Figure (2.21), the most well-known impulsive seismic source, dynamite, is indeed used very often in land seismic surveys. There are, however, some distinct disadvantages related to the use of an impulsive source like dynamite.

First of all, due to the high energy density of the dynamite explosion, severe harm can be done to the environment. In any case, the destructive nature of the dynamite source prohibits its use in densely populated areas. Second, a hole has to be drilled for every shotpoint in which the dynamite charge is placed; this means a lot of extra work. Third, the high energy-density of the explosion results in a non-linear zone surrounding the explosion. Although the ignition time of the dynamite itself is short compared with any time duration of interest in seismic exploration, this nonlinear zone results in a distorted wavelet. The high-frequency content of the signal decreases relatively to the low frequencies when the charge size is increased. This yields a trade-off between penetration and resolution: a large charge size has better penetration, but it is more difficult to use the high frequencies. Another disadvantage of the creation of a nonlinear zone around the dynamite explosion is that effectively a wavelet is transmitted into the earth that is not an impulse, and has a shape which is not accurately known and cannot be measured easily.

The Vibroseis source has some distinct advantages over the dynamite source. First, the emitted signal contains an amount of energy that is (roughly) comparable to the energy contained in a dynamite signal: Janak's (1982) results from a land seismic source study

Table 2.1: *Advantages and disadvantages of Vibroseis and dynamite.*

Source type	**Advantages**	**Disadvantages**
Vibroseis	1. Much less destructive than dynamite : can operate in urban areas 2. Not labour-intensive: cheap in operation 3. Some control over outgoing signal	1. Surface noise: many Rayleigh waves 2. Correlation not perfect: correlation noise 3. Can only operate in areas that can support 14 tons 4. One truck does not deliver enough energy: arrays, so directivity
Dynamite	1. Buried source: much less surface waves generated than with Vibroseis 2. Signal close to δ-pulse	1. Destructive: cannot operate in urban areas 2. Labour intensive for making shot-holes: expensive in operation

that a 2.5 kg dynamite charge buried at 5 m depth delivers an amount of energy of $9.5 \cdot 10^6$ Joules, whereas a single Litton model 311 P wave vibrator emitting a 10-79 Hz sweep (the drive level is not mentioned in the report) delivers $1.2 \cdot 10^6$ Joules. Because of the use of an expanded impulse, the energy density of the source wavelet in the Vibroseis technique is much less than the energy density of the dynamite wavelet. Therefore, destructive effects are much less severe. Secondly, Vibroseis provides us with a direct means to measure and control the outgoing wavelet. Thirdly, there is no need to drill holes when using Vibroseis.

There are, however, also some disadvantages connected with the use of Vibroseis as a source. Firstly, a single vibrator in general does not deliver a sufficient amount of energy required for seismic exploration purposes, so that arrays of vibrators have to be used. Typically, 4 vibrators vibrate at each vibration location simultaneously. Second, as vibrators are surface sources, large amounts of Rayleigh waves are generated. The generation of Rayleigh waves can be suppressed in a dynamite survey by placing the charge at or below the bottom of the weathered layer. In Vibroseis surveys, the Rayleigh waves have a very high amplitude and are an undesired feature on the seismogram. Thirdly, the Vibroseis method can be employed only in areas which are accessible to the seismic vibrator trucks, whose weight may exceed 20 tons. Fourth, correlation noise (i.e. the noise generated by the correlation process that converts the Vibroseis signal into a pulse) limits the ratio between the largest and smallest detectable reflections. In table (2.1) the advantages and the disadvantages of the Vibroseis and dynamite are given.

In spite of many disadvantages, the Vibroseis method is now a standard method in the seismic exploration for hydrocarbons. In 1987, Vibroseis was used more often in land seismics than dynamite (the contribution of Vibroseis to the total number of crew months spent in land seismic petroleum exploration was 49 %, whereas the contribution of dynamite was 48.3 %). The operational advantages of the Vibroseis method over the conventional dynamite survey result in an average cost per kilometre of Vibroseis which is only two-thirds of the cost per kilometre for a dynamite survey (figures for 1987). Also, the average number of kilometres that can be covered per crew month is 30 % higher for Vibroseis surveys than it is for dynamite surveys (figures for 1987). This cost-effectiveness and efficiency, together with the increasing importance of signal control in the search for higher resolution of seismic data and the non-destructive character of the method explains

the increasing popularity of Vibroseis.

2.12 References

Baeten, G.J.M. 1989. Theoretical and practical aspects of the Vibroseis method, Ph.D. thesis, T.U. Delft, ISBN 90-9002817-X.

Keller, J.B., and I.I. Kolodner, 1956. Damping of underwater expolsion bubble oscillations, Journal of Applied Physics 27, pp. 1152-1161.

Lerwill, W.E., 1981. The amplitude and phase response of a seismic vibrator. Geophysical Prospecting 29, pp. 503-528.

Parkes, G., A.M. Ziolkowski, L. Hatton and T. Haughland, 1982. The signature of an airgun array: Computation from near-field measurements including interactions - Practical considerations, Geophysics 48, pp.105-111.

Peet, W.E., 1960. A shock wave theory for the generation of the seismic signal around a spherical shot hole, Geophysical Prospecting 8, pp. 509-533.

Ziolkowski, A.M., 1987. The determination of the far-field signature of an interacting array of marine seismic sources from near-field measurements - results from the Delft Airgun Experiment, First Break 5, pp.15-29.

Ziolkowski, A.M., and K. Bokhorst, 1993. Determination of the signature of a dynamite source using the source scaling law, Geophysics 58, pp.1174-1194.

Ziolkowski, A.M., G. Parkes, L. Hatton and T. Haughland, 1982. The signature of an airgun array: Computation from near-field measurements including interactions, Geophysics 47, pp.1413-1421.

Chapter 3

Geophones and hydrophones

3.1 Introduction

The source generates a mechanical disturbance which propagates in the ground, is reflected, refracted or diffracted, and returns to the surface. When the disturbance propagates in a fluid such as water a temporary variation of pressure is created. Elastic deformation results in movements of the surface and at some point of the surface the acceleration, the velocity or the displacement of a point can be measured. In any case, whether a movement or a variation of pressure is observed, we have to represent it by some other physical quantity which can be easily stored and manipulated. Considering the development of electronic technology, a representation by an electrical voltage is evidently a good solution. The first field component of a seismic data acquisition system is the detector group. The detectors convert the seismic disturbance into a voltage of which the variations represent faithfully the variations of the mechanical disturbance detected, a voltage which is the analog of the seismic disturbance.

The detectors used for seismic exploration work are called geophones since they are used to "hear" echoes from the earth underneath. Sometimes, they are called seismometers but this term is more often applied to long period seismographs used for recording natural earthquakes. The term "detector" applies to all types of seismic-to-electrical transducers. From what has been said before, it will be clear that they can be classified into two main groups: motion-sensitive, mainly for land operations, and pressure-sensitive for operations in water (or fluids), be it for marine seismic work or in the mud column of a borehole, for well-shooting or a VSP. Pressure-sensitive detectors are also called hydrophones.

The types of detectors commonly used in practice, are electro-magnetic and piezo-electric transducers and we shall omit all others. Piezoelectric transducers which are pressure-sensitive are used as hydrophones and electro-magnetic transducers are used on land. In the moving coil geophone of the electro-magnetic type, a voltage is generated by the movement of a conductor in a strong permanent magnetic field. These types are used nowadays.

Geophones are the parts of the system which undergo the roughest treatment. They are planted and picked up many times, they are flung down, run over by the trucks, stamped into the ground by the line men. And yet, they are expected to generate an accurate, noise-free reproduction of the earth movements. They are built to withstand rough handling but a minimum of care on the part of the line men can help in obtaining

Figure 3.1: Schematic cross-section of a moving-coil geophone.

good quality data.

3.2 Electromagnetic geophones

A moving coil geophone (3.1) operates according to the principle of a microphone or a loudspeaker: the coil consisting of copper wire wound on a thin non-conducting cylinder ("former") moves in the ring-shaped gap of a magnet. Figure (3.1) is the cross section of a cylindrical structure. The annular magnet and polar pieces N and S in soft iron create a radial field in the gap. The only movement allowed for the coil, suspended from springs not shown in the picture, is a translation along the direction of the axis and in the gap. As the coil moves, its windings cut magnetic lines of force and an electromotive force is generated. The output voltage is proportional to the rate at which the coil cuts the lines of magnetic force, that is to say, proportional to the velocity at which it moves. Therefore this type of detector is known as "velocity geophone".

The main parts of the geophone are:

- the moving mass, made up by the coil and the "former" on which it is wound;
- the coil suspension, usually two flat springs, one at the top and one at the bottom, to avoid lateral displacement of the coil;
- the case, with the magnet and polar pieces inside a cylindrical container which protects the other elements against dust and humidity.

The case is placed on the ground and is supposed to follow the ground movement exactly (Figure 3.2). The output voltage is proportional to the velocity of the mass relative to the case and what we are interested in is this relative movement as a function of the movement of the case.

Figure 3.2: The geophone on the ground.

3.3 Theoretical evaluation of the geophone response

A complete description of geophones must take into account many phenomena beyond the scope of these lecture notes. The final design of a geophone is usually a compromise between conflicting requirements. For a geophysicist it is often sufficient to know the basic operating principle of the geophone in order to understand the behaviour of this component as part of the whole data acquisition network. Consequently, the considerations which follow are restricted to the response of an ideal geophone.

The geophone can be represented as in Figure (3.2) with a coil of mass M instead of a massive weight (Figure 3.3). Vertical movements are measured along axis OZ, with the positive values in the downward direction and with an origin O at the level of the coil when the geophone is at rest. The geophone case is assumed to be connected tightly to the ground and to follow exactly the movement of the ground. The movement of the coil lags behind that of the case and the voltage generated is a function of the relative movement. When the case is at level z, the coil is at level u and its relative displacement y is:

$$y = u - z \tag{3.1}$$

The forces acting on the coil are:

(a) its weight $+Mg$;

(b) The force F_1 exerted by the spring. This force is proportional to the increase of length of the spring with stiffness S,

$$F_1 = -Su = -S(y + z) = -(Sy + Mg) \tag{3.2}$$

where we see that Sz is the stretch under the weight of the coil, i.e., $Sz = Mg$.

(c) The friction and other mechanical damping forces opposing the displacement of the coil relative to the case. The resultant is a force F2 proportional to the velocity:

$$F_2 = -D\frac{dy}{dt} \tag{3.3}$$

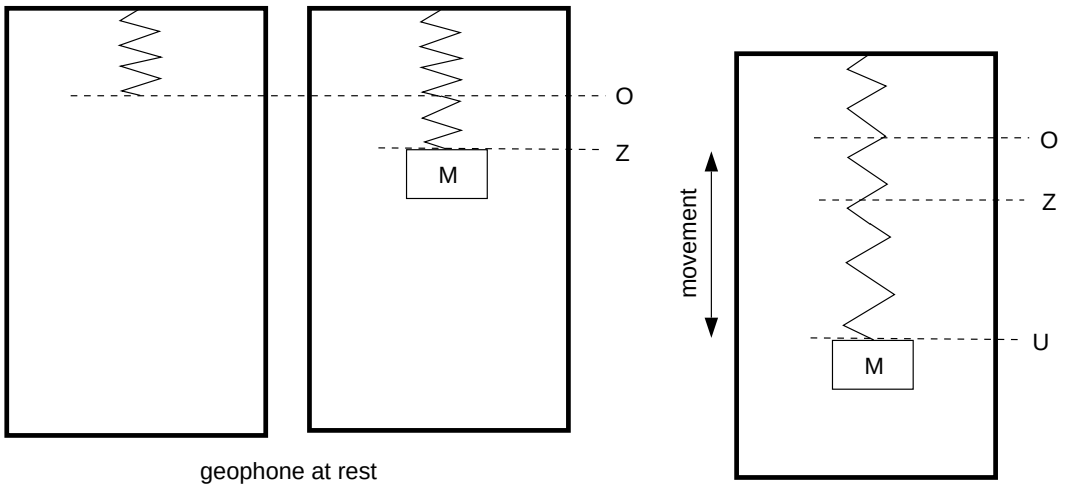

Figure 3.3: Displacement parameters, (a) rest position without weight, (b) rest position with weight, (c) in motion with weight.

where D is the mechanical damping factor.

(d) The electrical damping force F_3. This is the back electromotive force that opposes the motion. It is proportional to the length L of wire in the coil, to the magnetic induction B assumed to be constant, and to the current i flowing in the coil. Taking as positive the direction of the current generated when the relative displacement of the coil is negative, F_3 is expressed by:

$$F_3 = BLi \tag{3.4}$$

The voltage generated in the coil is proportional to the rate at which the coil cuts the magnetic flux. As the field is assumed to be radial and perpendicular to the wire everywhere,

$$E = -BL\frac{dy}{dt} \tag{3.5}$$

The geophone can be thought of as a generator (a voltage source with electro-motive force E) feeding the amplifier through a connecting line. For our simplified evaluation, the inductance of the coil is assumed to be negligible and all impedances are assumed to be pure resistances. The total circuit resistance is R_T and the resistance of the amplifier input is R_A, see also Figure (3.4). The current flowing in the circuit is given by

$$E = R_T i = -BL\frac{dy}{dt} \tag{3.6}$$

Figure 3.4: Circuit with geophone connected to amplifier input.

and the voltage at the amplifier input, the seismic signal is,

$$V = R_A i = -\frac{R_A}{R_T} BL \frac{dy}{dt} \tag{3.7}$$

The equation of the movement of the coil is obtained by equating the sum of the forces applied to the coil to the product of its mass and its acceleration:

$$Mg + F_1 + F_2 + F_3 = M\frac{d^2u}{dt^2} = M\frac{d^2(y+z)}{dt^2} \tag{3.8}$$

Replacing F_1, F_2 and F_3 by their values, the equation becomes

$$-Sy - D\frac{dy}{dt} + BLi = M\frac{d^2y}{dt^2} + M\frac{d^2z}{dt^2} \tag{3.9}$$

Differentiating this equation once and using the electrical relations, we get:

$$-S\frac{dy}{dt} - D\frac{d^2y}{dt^2} + BL\frac{di}{dt} = M\frac{d^3y}{dt^3} + M\frac{d^3z}{dt^3} \tag{3.10}$$

and we had, rewriting equation (3.7),

$$\frac{dy}{dt} = -\frac{R_T}{R_A}\frac{1}{BL}V \tag{3.11}$$

Combining these two, we obtain:

$$M\frac{d^2V}{dt^2} + \left(D + \frac{B^2L^2}{R_T}\right)\frac{dV}{dt} + SV = M\frac{R_A}{R_T}BL\frac{d^3z}{dt^3} \tag{3.12}$$

This is a differential equation with constant coefficients.

The frequency

$$f_0 = \frac{1}{2\pi}\left(\frac{S}{M}\right)^{1/2} \tag{3.13}$$

is the natural frequency of a spring. It is the frequency at which a mass M suspended on a spring of stiffness S oscillates in the absence of any other constraint.

Since $Mg = Sz$, we can write:

$$\omega_0 = \left(\frac{S}{M}\right)^{1/2} = \left(\frac{g}{z}\right)^{1/2} \tag{3.14}$$

The low frequency geophones are those in which the stretching OZ of the spring under the influence of the suspended weight is important. The natural frequency can be decreased by increasing the mass or by reducing the stiffness of the spring.

Writing

$$\frac{D}{M} + \frac{B^2L^2}{R_T M} = 2h\omega_0 \tag{3.15}$$

where we can recognize the first term as the damping due to mechanical effects, and the second term by the damping due to electromagnetic effects. Introducing the constant K as:

$$K = \frac{R_A}{R_T}BL \tag{3.16}$$

the differential equation becomes

$$\frac{d^2V}{dt^2} + 2h\omega_0\frac{dV}{dt} + \omega_0^2 V = K\frac{d^3z}{dt^3} \tag{3.17}$$

In this equation, ω_0 is the natural angular frequency, h is the total damping of the geophone, and K is the transduction constant, i.e., the conversion factor from particle velocity into voltage.

This equation relates the voltage at the input to the recording system to the vertical displacement z of the geophone case (assumed to be perfectly coupled to the ground) in the time domain. How does this geophone output vary with the frequency of the ground velocity? The vertical component of the velocity is:

$$v_z = \frac{dz}{dt} \tag{3.18}$$

We define the Fourier Transform $S(\omega)$ of $s(t)$ as:

$$S(\omega) = \int_{-\infty}^{+\infty} s(t)\exp(-i\omega t)\,dt \tag{3.19}$$

so that ds/dt transforms to $+i\omega S(\omega)$ and d^2s/dt^2 transforms to $(i\omega)^2 S(\omega) = -\omega^2 S(\omega)$. Our original equation therefore transforms to:

$$-\omega^2 V(\omega) + 2ih\omega\omega_0 V(\omega) + \omega_0^2 V(\omega) = -\omega_0^2 K v_z(\omega) \tag{3.20}$$

The ability of the geophone to convert particle velocity into volts, as a function of frequency is:

$$R(\omega) = \frac{V(\omega)}{v_z(\omega)} = \frac{\omega^2 K}{\omega^2 - 2ih\omega\omega_0 - \omega_0^2} \tag{3.21}$$

Consider now three situations:

$$\omega \to 0, \qquad R(\omega) \to -\frac{\omega^2}{\omega_0^2} K = \frac{\omega^2}{\omega_0^2} K \exp(\pi i)$$

$$\omega \to \omega_0, \qquad R(\omega) \to -\frac{K}{-2ih} = \frac{K}{2h} \exp(\pi i/2)$$

$$\omega \to \infty, \qquad R(\omega) \to K$$

These are depicted in Figures (3.5) and (3.6). The received voltage is proportional to the velocity of the ground only at frequencies well above the resonance frequency of the geophone. At these frequencies the constant K is the sensitivity of the geophone, with units of, for example, volts/mm/s.

3.4 Practical aspects of geophone behaviour

So far, we have worked out only the resonance frequency of the geophone since this was a problem which was useful to us and were able to solve. This characteristic is a feature at the lower end of the frequency range of interest when exploring for oil and gas. But there is also a limitation at the high-frequency end. The first problem we usually encounter at the high frequency end, is the so-called spurious frequency. This frequency is associated with resonance frequencies of the case. This is sometimes a not well understood problem because it is rather complicated. Usually this frequency is given with the product delivery.

For practical use the geophone is enclosed in a plastic case which serves two purposes: First, it protects the geophone and its terminals from leakage to the ground. It is made of some insulating material; second, it provides a mechanical protection against crushing.

Another important aspect of the geophone in practice, is the geophone-ground coupling, i.e., quality of the connection of the geophone with the ground. The coupling is, for instance, better in compacted soils than in loose formations, which is quite understandable. On paved areas, it is difficult to plant the geophones, and often tripods are used to keep the geophone vertical such that good coupling with the ground is maintained. In Figure (3.7) the effect is shown when the geophone is not planted properly, resonance frequencies may arise in the high-frequency range which, depending on the ground conditions, may become as low as 100 Hz. This can be troublesome for oil exploration, but for shallow seismics this can be disastrous. The consequence from this is that a party chief must take care that his geophones are planted properly!

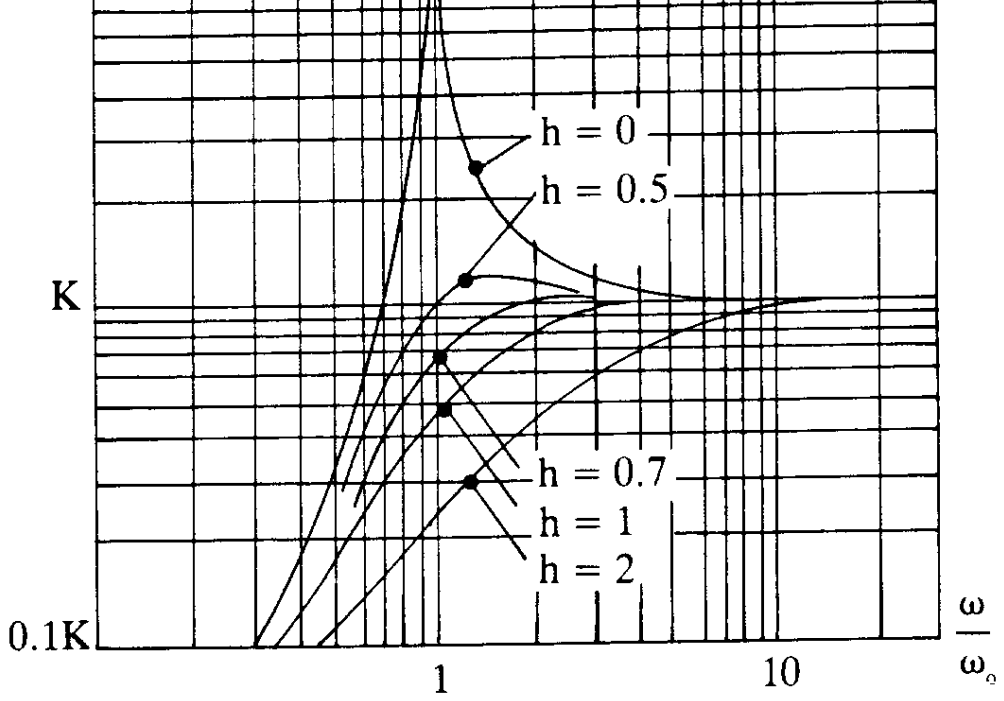

Figure 3.5: Amplitude response of geophone at constant velocity drive (From: Pieuchot, 1984)

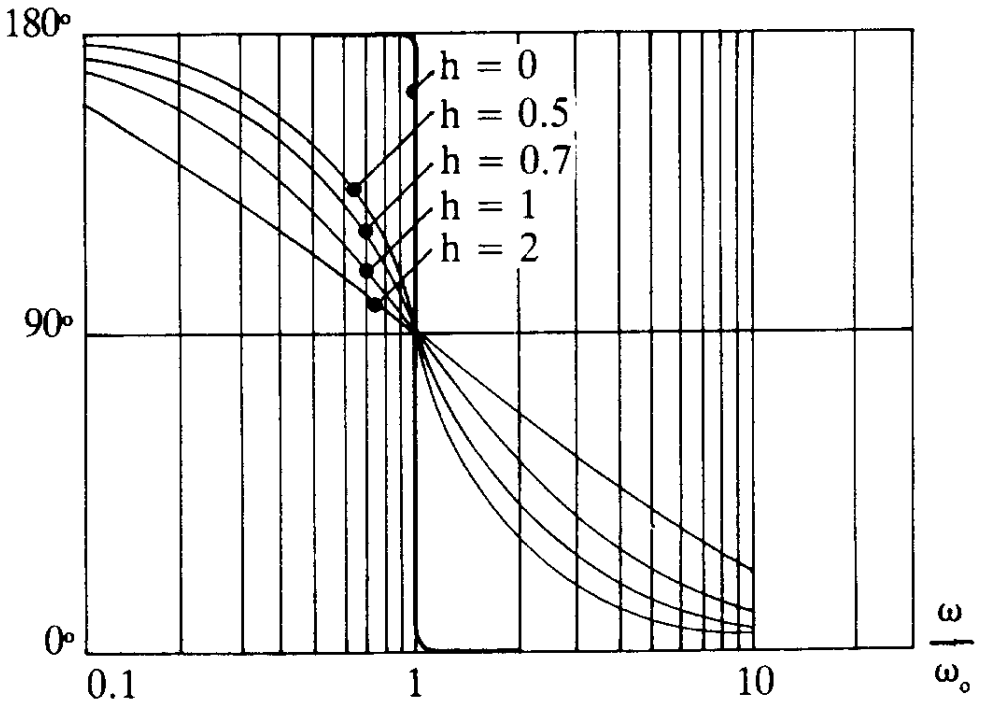

Figure 3.6: Phase response of geophone at constant velocity drive (From: Pieuchot, 1984)

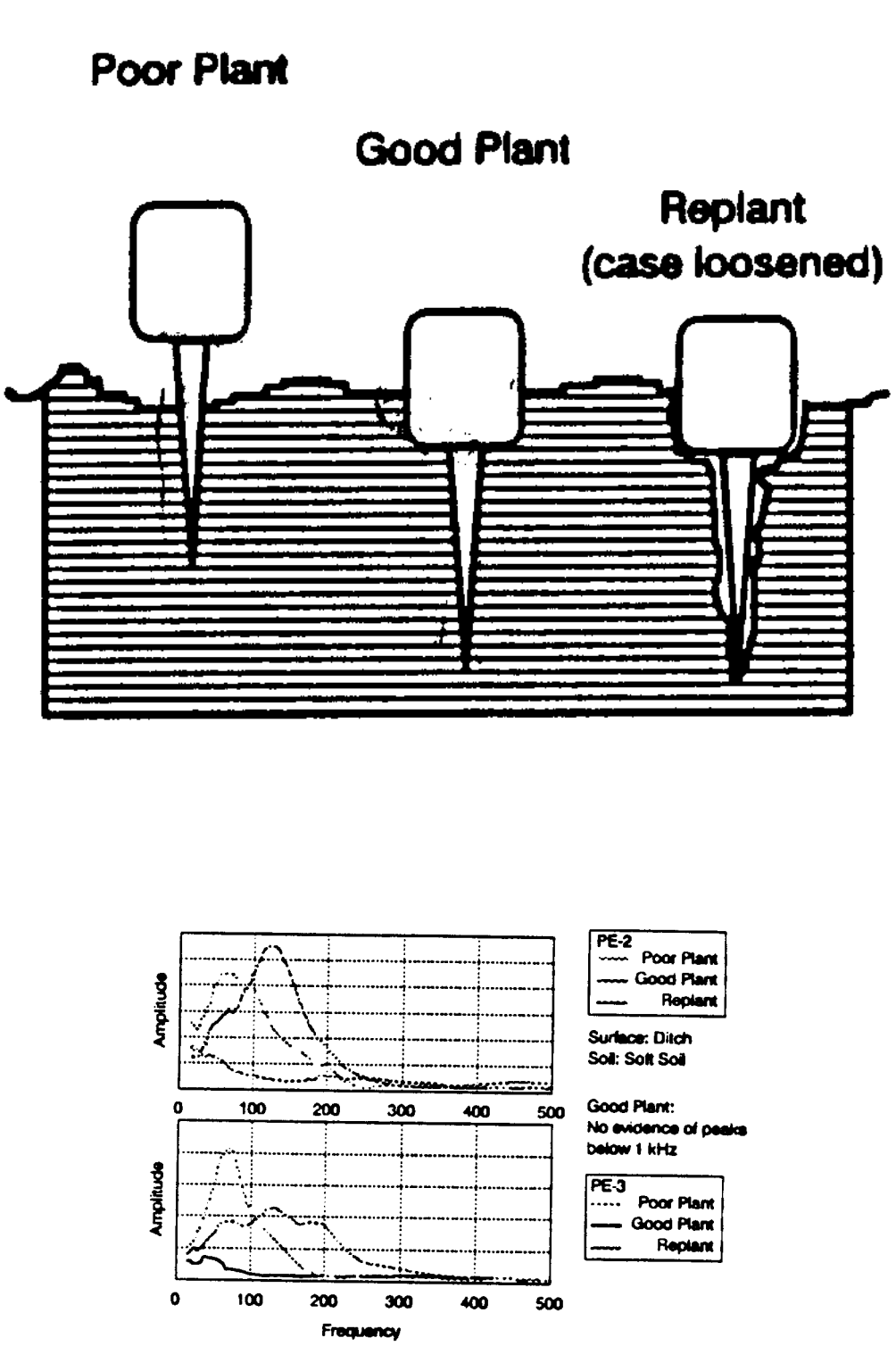

Figure 3.7: Effect of not properly planting geophones (from: Faber et al., 1994).

3.5 Arrays and directivity

The most important reason why arrays are used in the field, is data reduction. If we would sample the wavefield according to spatial Nyquist criteria, then the spacing would be of the order of meters. However, when we want to investigate depths up to 4 kilometers, we need also have geophones planted over at least such a distance in that direction. In 3D seismics, this would mean too many channels for any system. Therefore the data is reduced by using arrays of geophones which are hard-wire connected.

In the old days geophone arrays were used to suppress the ground roll but recording systems today can deal better with the loss of dynamic range caused by the large amplitudes of ground roll. Let us look more closely at the response of a pattern; for simplicity we take 4 detectors in a pattern. We sample points in space, delta functions d in space, so the spatial operator becomes:

$$A(x) = \delta(x - 3\Delta x/2) + \delta(x - \Delta x/2) + \delta(x + \Delta x/2) + \delta(x + 3\Delta x/2) \tag{3.22}$$

where we centered the points around zero. Let us first define the spatial Fourier transform as:

$$F(k_x) = \int_{-\infty}^{+\infty} f(x) \exp(2\pi i k_x x)\, dx \tag{3.23}$$

Applying this transformation to the above function:

$$A(k_x) = \exp(2\pi i k_x 3\Delta x/2) + \exp(2\pi i k_x \Delta x/2) + \exp(-2\pi i k_x \Delta x/2) + \exp(-2\pi i k_x 3\Delta x/2) \tag{3.24}$$

or

$$A(k_x) = \exp(3\pi i k_x \Delta x) + \exp(\pi i k_x \Delta x) + \exp(-\pi i k_x \Delta x) + \exp(-3\pi i k_x \Delta x) \tag{3.25}$$

We want to rewrite this equation into a different form. First, consider:

$$\sum_{m=0}^{3} Z^m = \left(1 + Z + Z^2 + Z^3\right) \tag{3.26}$$

$$Z \sum_{m=0}^{3} Z^m = Z\left(1 + Z + Z^2 + Z^3\right) \tag{3.27}$$

Substract these two and we obtain:

$$(1 - Z) \sum_{m=0}^{3} Z^m = 1 - Z^4 \tag{3.28}$$

or

$$\sum_{m=0}^{3} Z^m = \frac{1 - Z^4}{1 - Z} \tag{3.29}$$

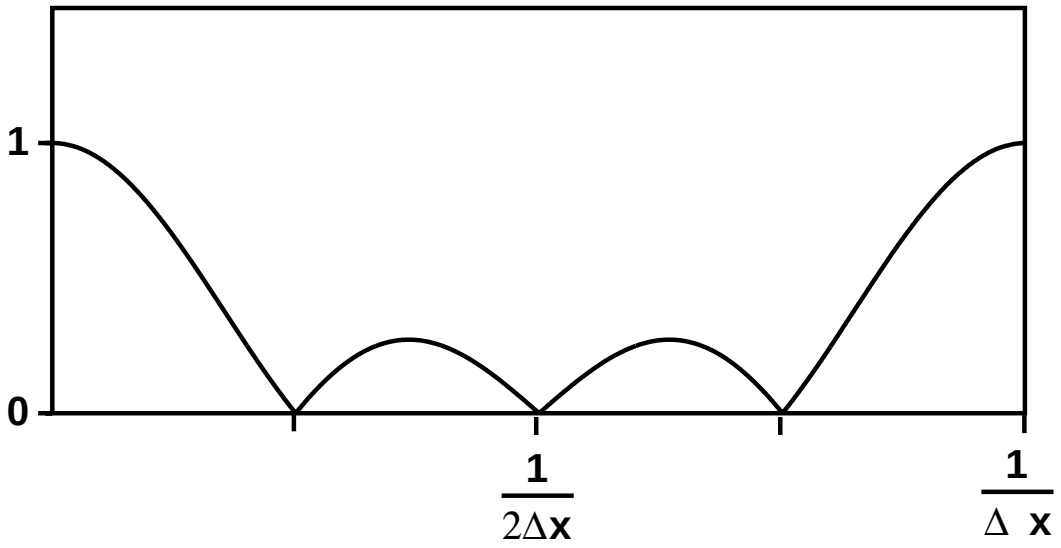

Figure 3.8: The array-effect in the wavenumber domain

Note that no approximation has been made. Inserting $Z = \exp(-2\pi i k_x \Delta x)$, this reads:

$$1+\exp(-2\pi i k_x \Delta x)+\exp(-4\pi i k_x \Delta x)+\exp(-6\pi i k_x \Delta x) = \frac{1-\exp(-8\pi i k_x \Delta x)}{1-\exp(-2\pi i k_x \Delta x)} \quad (3.30)$$

Let us return to our previous equation (3.25) and take $exp(3\pi i k_x \Delta x)$ out of brackets, and substitute the result from above:

$$\begin{aligned} A(k_x) &= \exp(3\pi i k_x \Delta x)\frac{1-\exp(-8\pi i k_x \Delta x)}{1-\exp(-2\pi i k_x \Delta x)} \\ &= \exp(3\pi i k_x \Delta x)\frac{\exp(-4\pi i k_x \Delta x)}{\exp(-\pi i k_x \Delta x)}\frac{[\exp(4\pi i k_x \Delta x)-\exp(-4\pi i k_x \Delta x)]}{[\exp(\pi i k_x \Delta x)-\exp(-\pi i k_x \Delta x)]} \\ &= \frac{\exp(4\pi i k_x \Delta x)-\exp(-4\pi i k_x \Delta x)}{\exp(\pi i k_x \Delta x)-\exp(-\pi i k_x \Delta x)} \\ &= \frac{\sin(4\pi k_x \Delta x)}{\sin(\pi k_x \Delta x)} \end{aligned} \quad (3.31)$$

The amplitude of this function is sketched in figure (3.8). We see that this filter is periodic, which is natural since if we discretise a continuous function (the wavefield) we get a periodic spectrum.

3.6 The Hydrophone

As has been shown in the foregoing sections, the geophone exhibits a flat pass-band characteristic from a few Hertz above the resonance frequency to the spurious frequency. In

that pass-band the output voltage V_{Geop} is proportional to (the vertical component of) the particle velocity v_z:

$$V_{\text{Geop}} \propto v_z \tag{3.32}$$

We will derive also in the next paragraph that in the pass band of the hydrophone, the output voltage V_{Hydr} is proportional to the acoustic pressure p, i.e.,:

$$V_{\text{Hydr}} \propto p \tag{3.33}$$

Hydrophones are thus pressure-sensitive detectors and they are used for operations in water-covered areas.

3.7 Piezoelectricity

At present often hydrophones with ceramic pressure-sensitive elements are used. They operate on the principle of piezoelectricity. A piezoelectric material is one which produces an electrical potential when it is submitted to a physical deformation. The phenomenon is observable in some crystalline structures such as quartz and tourmaline and is used in record player pick-ups. It can also be produced by in artificially-made poly-crystalline ceramics after they have been submitted to a high-intensity electric field (several tens of thousands volts per centimeter). The most commonly used material in seismic applications, is lead zirconate titanate (PZT).

Poly-crystalline materials are inert, and immune to moisture and other atmospheric conditions. The orientation of the DC poling field determines the orientation of the mechanical and electrical axes. The poling process permanently changes the dimension of a ceramic element. The dimension in the direction of the poling electrodes (x) increases, and the dimensions parallel to the electrodes (y) decrease. These effects are shown, greatly exaggerated, in Figure (3.9). The dimension between the poling electrodes is called the poling axis. After the poling process is complete, a voltage lower than the poling voltage changes the dimension of a ceramic element as long as the voltage is applied. A voltage with the same polarity as the poling voltage causes additional expansion along the poling axis (x) (Figure (3.10)) and contraction perpendicular to the poling axis (y). A voltage with the polarity opposite to the poling voltage has the opposite effect: contraction along the poling axis (x), and expansion perpendicular to the poling axis (y). The use of ceramic materials as a source for seismic (model) experiments is based on these principles. In both cases, the ceramic element returns to its poled dimensions when the voltage is removed from the electrodes. These effects are shown greatly exaggerated in Figure (3.10).

After the poling process is complete, compressive and tensile forces applied to the ceramic element generate a voltage. Refer to Figure (3.11). A voltage with the same polarity as the poling voltage results from a compressive force (a) applied parallel to the poling axis, or from a tensile force (b) applied perpendicular to the poling axis. A voltage with the opposite polarity results from a tensile force (c) applied parallel to the poling axis, or from a compressive force (d) applied perpendicular to the poling axis. The magnitude of piezoelectric forces, actions, and voltage is relatively small. For example, the maximum relative dimensional changes of a single element are in the order of 10^{-8}. Amplification is often required and accomplished by other components in the system, such as electronic circuits. In some cases, the design of the ceramic element itself provides the required

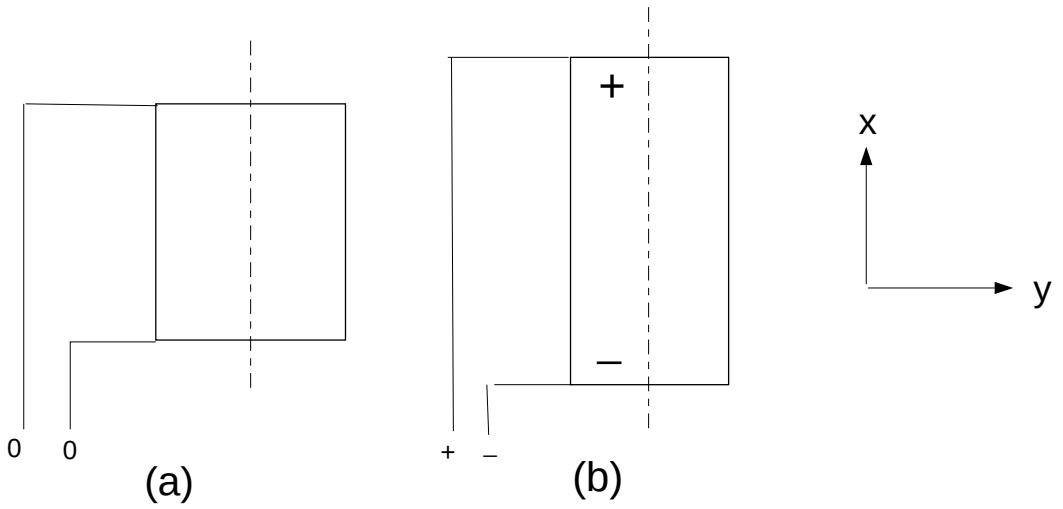

Figure 3.9: Effects of poling. (a) before poling; (b) after poling.

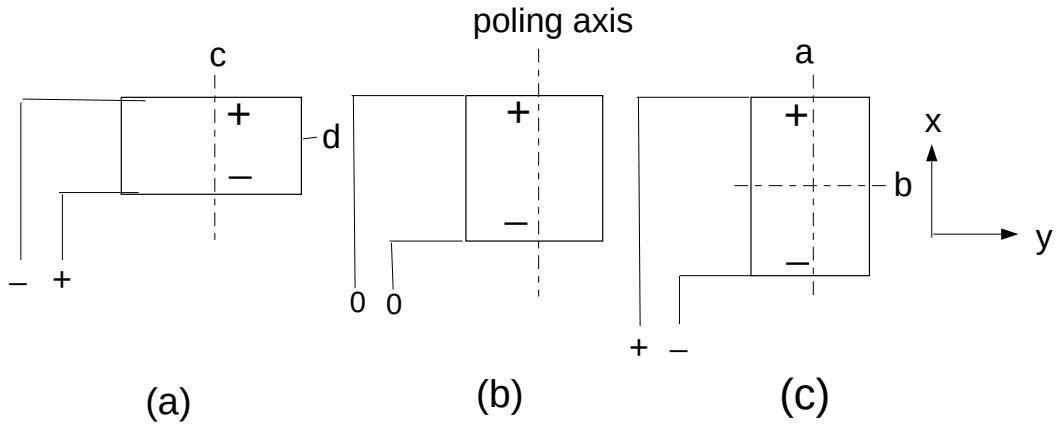

Figure 3.10: Piezoelectricity actions from applied voltages. (a) Applied voltage of opposite polarity as poled element; (b) no voltage on poled element; (c) applied voltage of same polarity as poled element.

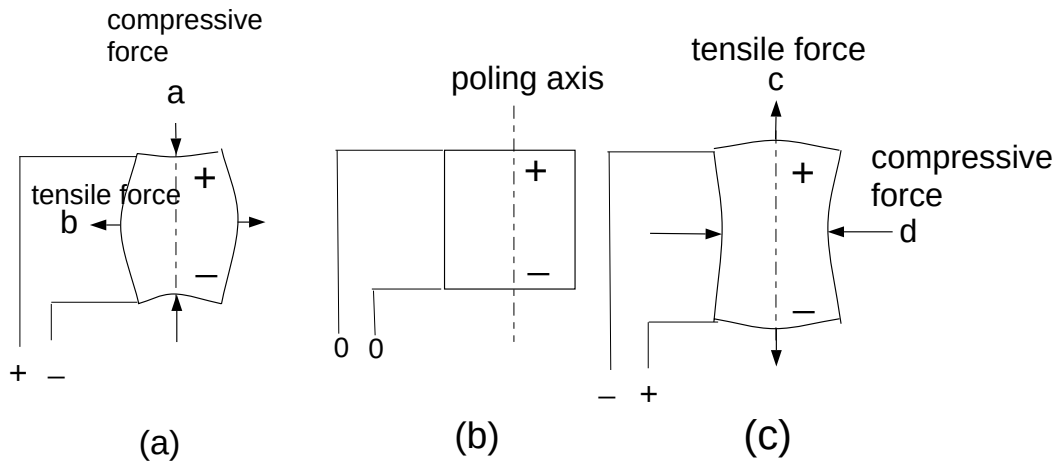

Figure 3.11: Piezoelectric voltages from applied force. (a) Outpur voltage of same polarity as poled element; (b) output voltage of opposite polarity as poled element.

mechanical amplification. The use of ceramic elements as seismic (pressure) detectors / hydrophones is based on these principles.

Most of the properties of piezoelectric ceramics change gradually with time. The changes tend to be logarithmic with time after poling. The aging rate of various properties depends on the ceramic composition and on the way the ceramic is processed during manufacture. Because of aging, exact values of various properties such as dielectric constant, coupling, and piezoelectric constant may only be specified for a standard time after poling. The longer the time period after poling, the more stable the material becomes.

The Curie point is the absolute maximum exposure temperature for any piezoelectric ceramic. Each ceramic composition has its own Curie point. When the ceramic element is heated above the Curie point, all piezoelectric properties are lost. In practice, the operating temperature must be substantially below the Curie point. At elevated temperatures, the aging process accelerates, electrical losses increase, efficiency decreases, and the maximum safe stress level is reduced.

3.8 The hydrophone response

Figure (3.12) represents the cross section of a typical piezo-electric hydrophone. It consists of a plate of the piezo-electric ceramic placed on an elastic electrode. The active element is deformed by pressure variations in the surrounding water and it produces a voltage collected between the electrode and a terminal bonded to the other face. The electrode rests on a metallic base which supports its ends and also limits the maximum deformation so as to avoid breaking the ceramic, even if the hydrophone is accidentally submitted to high pressures (when the streamer is broken and drops to the sea bottom, for instance).

With its mass, the active element produces a voltage not only under a variation of pressure but also when it is subjected to acceleration. In offshore operations, with the

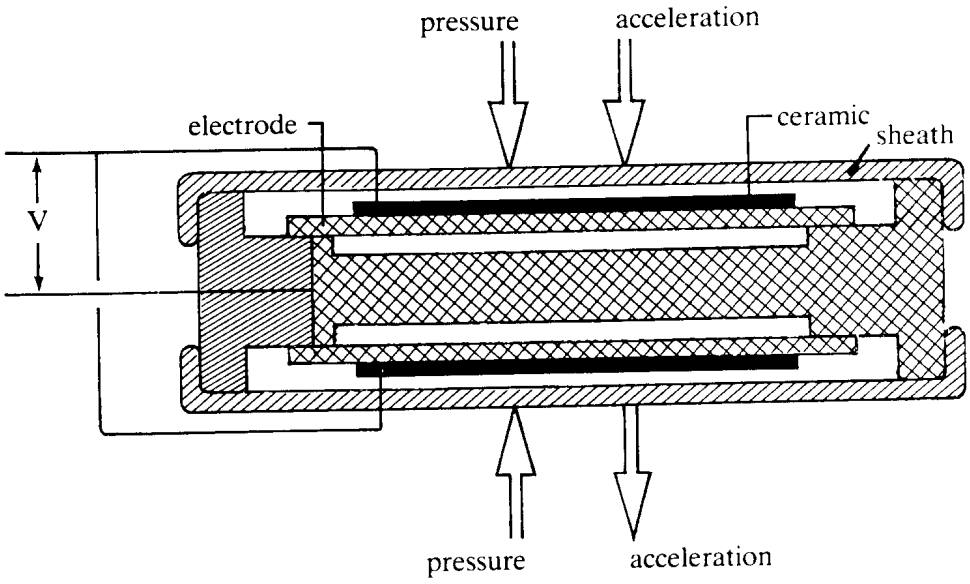

Figure 3.12: Schematic cross-section of a piezoelectric hydrophone (From: Pieuchot, 1984)

boat movements and the waves, the hydrophones are continually subjected to accelerations and this would create a high level of noise in the absence of any compensation. The protection against acceleration is obtained by assembling two elements as shown in the figure. The voltage produced by an acceleration cancel each other whereas those produced by a pressure wave add.

As with the geophones in land operations, the hydrophones are always assembled in multiple arrays at each position. They are often assembled so as to increase the capacitance (more hydrophones in parallel than in series) and decrease the low-frequency cut-off.

As in land operations, another purpose of replacing a single pick up by a directional array is the filtering effect obtained. In all cases, the group of hydrophones is equivalent to a single capacitance, exactly like a single hydrophone. In Figure (3.13), the group is replaced by a voltage generator E and a capacitance C in series.

V/E is the transfer function since E represents the variations of pressure in the water. From the circuit given in Figure (3.13), the transfer function can be derived:

$$\frac{V}{E} = \frac{R}{R + \frac{1}{i\omega C}} = \frac{i\omega CR}{1 + i\omega CR} \tag{3.34}$$

Consider now three situations:

$$\omega \to 0, \qquad \frac{V(\omega}{E} \to i\omega CR = \omega CR \exp(\pi i/2)$$

$$\omega \to 1/CR, \qquad \frac{V(\omega)}{E} = \frac{i}{i+1} = \frac{1}{2}\sqrt{2}\exp(\pi i/4)$$

$$\omega \to \infty, \qquad \frac{V(\omega)}{E} \to 1$$

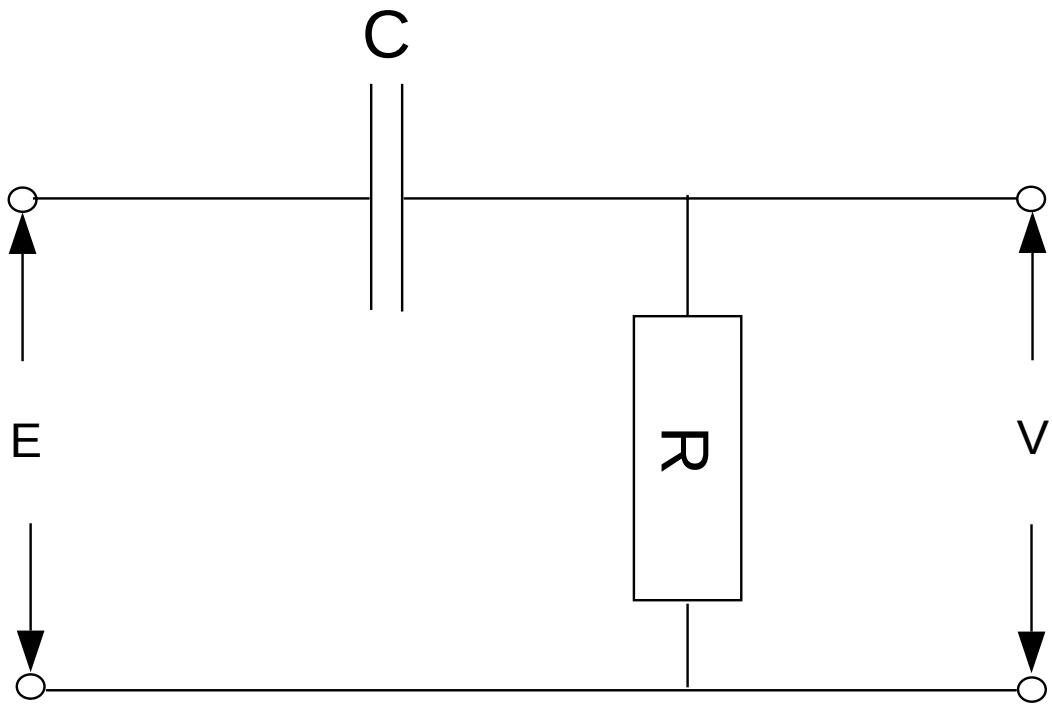

Figure 3.13: Simplified circuit for deriving the hydrophone response

The amplitude and phase response are given in Figure (3.14).

It is now interesting to compare this response to the one from the geophone. At low frequencies the responses are out of phase by $\pi/2$, decreasing to $\pi/4$ at higher frequencies and in phase at high frequencies. This can be important when comparing two seismic sections, one shot on land and the other one shot at sea.

The response so far, was the one for showing the general response of a hydrophone. In practice, we need a transformer at the hydrophone because the amplitudes are so low. Usually, the transformer needs a shunt resistor R_d; also, the line has a resistance R_L. The total circuit is then given in figure (3.15). Let us assume a current I_0, which splits into I_1 and I_2 through the resistances $(R_s + a^2(R_p + R_L + R_a))$ and R_d respectively. Then we obtain the following equations:

$$I_0 = I_1 + I_2 \tag{3.35}$$

$$E = \frac{1}{j\omega C} I_0 + R_d I_2 \tag{3.36}$$

$$\left(R_s + a^2 R_p + a^2 R_L + a^2 R_a\right) I_1 = R_d I_2 \tag{3.37}$$

We want to know the output voltage, i.e., W. Therefore we want to know the current I_1. Combining the above equations by substituting for I_0 and I_2, we obtain:

$$E = \left(\frac{1}{j\omega C} + \frac{1}{j\omega C} \frac{R_s + a^2 R_2}{R_d} + R_s + a^2 R_2 \right) I_1 \tag{3.38}$$

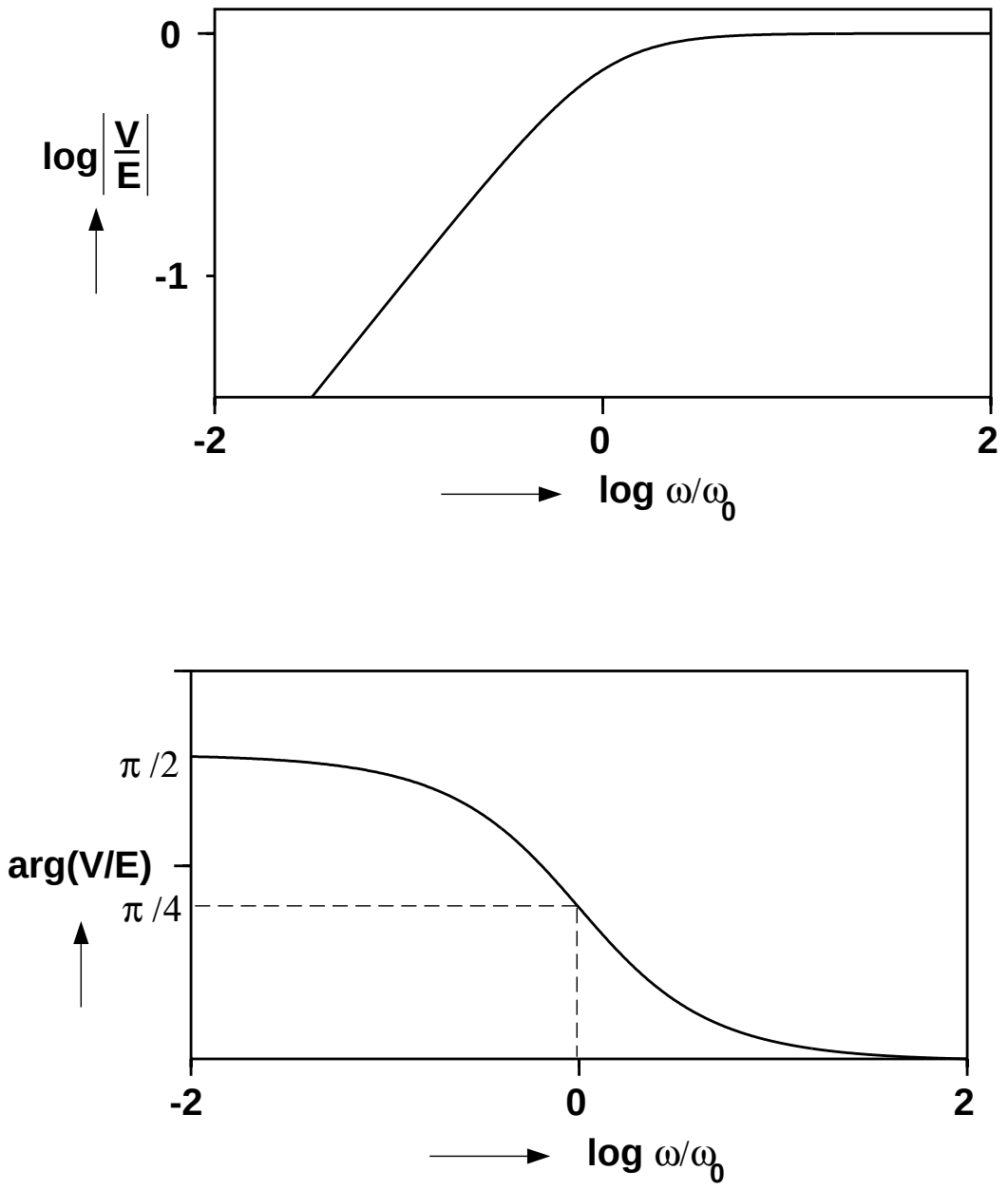

Figure 3.14: Amplitude and phase response of a hydrophone.

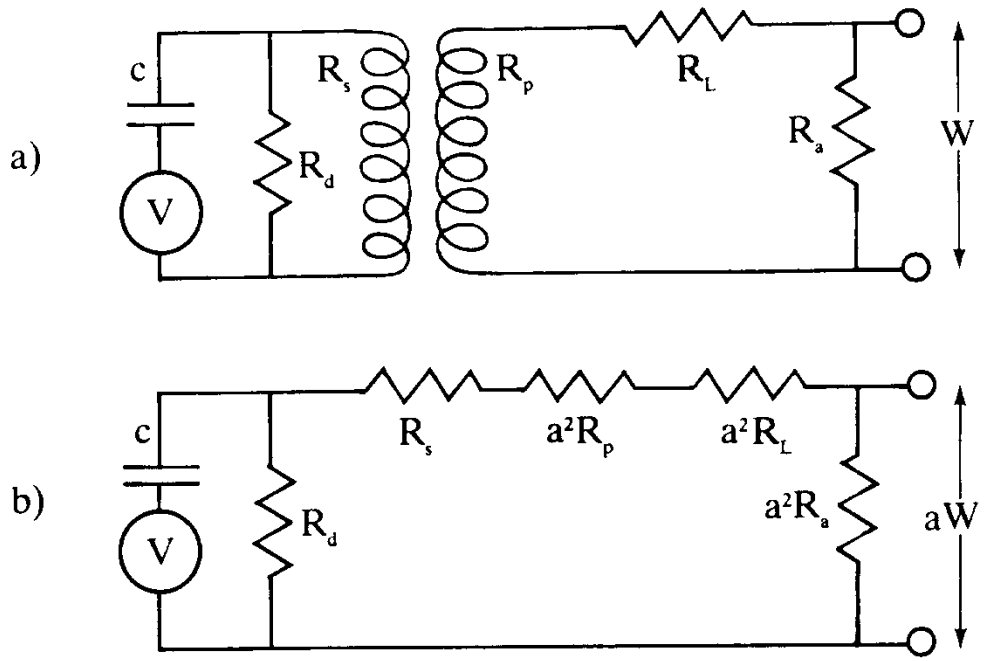

Figure 3.15: (a) Transformer coupled hydrophone circuit; (b) equivalent circuit (from: Pieuchot, 1984)

We have for aW:

$$aV = a^2 R_a I_1 \tag{3.39}$$

Thus we obtain for the ratio W/V:

$$\frac{V}{E} = \frac{aR_a}{\frac{1}{j\omega C}\left(1 + \frac{R_s + a^2 R_2}{R_d}\right) + R_s + a^2 R_2} \tag{3.40}$$

This equation has the same form as the simplified circuit as before.

3.9 References

Faber, K., P.W. Maxwell, H.A.K. Edelmann, 1994. Recording reliability in seismic exploration as influenced by geophone-ground coupling, 56th Meeting of the EAGE, Vienna, June.

Pieuchot, M., 1984. Seismic Instrumentation, In: Handbook of Geophysical Exploration, section I. Seismic Exploration (eds. K. Helbig & S. Treitel), vol. 2, Geophysical Press, London, 376 pp.

Chapter 4

Seismic recording systems

4.1 Introduction

The modern seismic data recording system is a compound of electric subsystems (amplifiers, filters, etc.). The (glasfibre) cable system may often be considered integral part of it. It has as input analog electrical signals from the seismic detectors (geophones and hydrophones, see Chapter 3) and puts digital data out on magnetic tape. Nearly all systems offer the facility of instant data verification through the creation of output on paper.

A recording system generally consists of the parts as depicted in figure (4.1). The first stage in the system is a pre-amplifier and a set of filters, as many as there are channels (each channel is receiving analog data from a geophone group). The next stage is the multiplexer which sequentially samples the analog input: it chops the analog input into little portions (short blockpulses) and outputs one long sequence of block pulses representing data of all channels arranged in a cyclical manner. Then, in order to sample the data, the A/D converter is used, together with the extra needed components; conventional A/D conversion with so-called sample-and hold, amplifier and A/D conversion is discussed, and then the converter using the so-called sigma-delta technology is used, with its modulator and decimator. The data will be ordered in a sequence such that we get it on tape as wished. Finally, in order to write the data onto tape, we have to amplify it again.

4.2 Pre-amplifier

The first stage in any data recording system is an amplification of the signal voltage before filtering in order to reduce the relative magnitude of the noise generated in the filters. Mostly, the amplification can be set in fixed steps by a switch on the system. As a use of a recording system, one often keeps this setting fixed.

4.3 Filters

What is more important, is the setting of the different filters. Some of these filters may be pre-determined but others must be left at the discretion of the user and must be

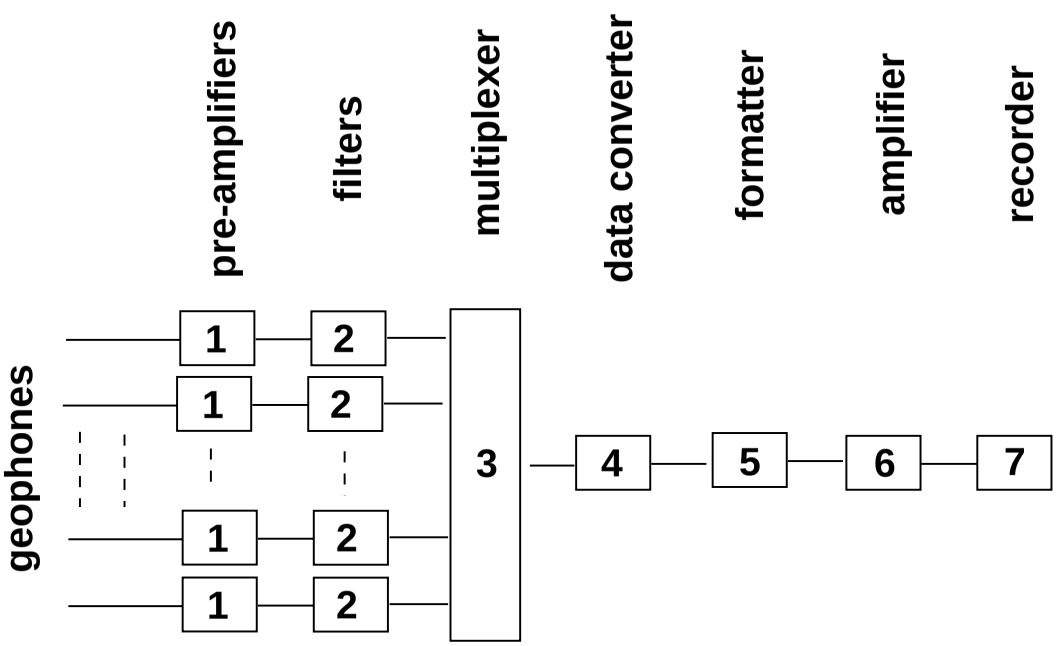

Figure 4.1: Synoptic diagram of a digital seismic data acquisition system: pre-amplifiers, analog filters, multiplexer, A/D converter with extra components, formatter, write amplifier and recorder.

adjustable in the field. Usually there are three types of filters available to the user in the field: low-pass (high-cut), notch and high-pass (low-cut) filters.

In the following the principles of so-called passive filters will be dealt with; a passive filter is built from electrical components: resistors, capacitors and coils. Let us look at a general scheme of a filter by considering figure (4.2). When a potential difference E is put over a series connection of two passive elements with impedances Y and Z, and when we measure the potential difference V over the Y component, the ratio of the two potentials is given by:

$$\frac{V}{E} = \frac{Y}{Z+Y} \tag{4.1}$$

For a resistance, the impedance is R, for an inductance $j\omega L$, and for a capacitance $1/j\omega C$ (see appendix A). So, when the component Y is an capacitance and Z a resistance, the measured potential difference is a "high-cut" (or "low-pass") version of the input voltage E. This can be seen by substituting the values in the above equation:

$$\frac{V}{E} = \frac{\frac{1}{j\omega C}}{\frac{1}{j\omega C}+R} = \frac{1}{1+j\omega CR} \tag{4.2}$$

which is a ratio, dependent on the frequency ω. When we write this in polar coordinates, we get:

$$\frac{V}{E} = \frac{1}{1+j\omega CR}\frac{1-j\omega CR}{1-j\omega CR} = \frac{1}{(1+\omega^2C^2R^2)^{1/2}}\exp(i\phi) \tag{4.3}$$

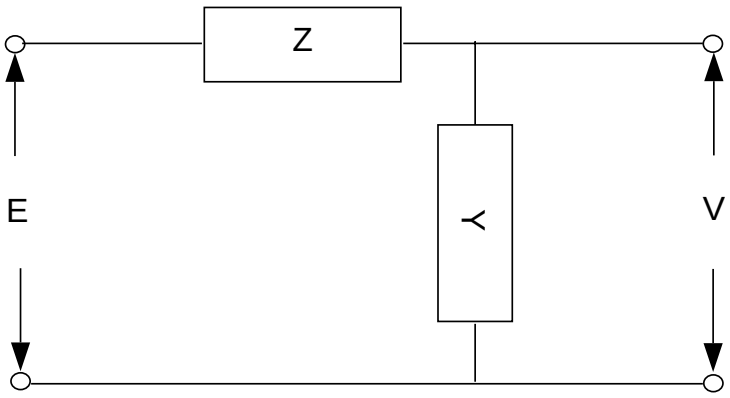

Figure 4.2: A passive filter.

where ϕ is the phase angle. When ω is large, then 1 can be neglected compared to ωCR in the amplitude factor and thus, V/E behaves like $1/\omega CR$: the amplitude becomes smaller when ω becomes larger. When ω is small, then ωCR can be neglected compared to 1, so V/E will approach 1.

In the same way we can derive that when Y is a inductance, the filter acts as a low-cut or high-pass filter. It is customary to specify a filter by its so-called corner frequency, i.e., the frequency where $\omega = 1/CR$. With a high-cut filter as above, the signal will be significantly damped above this frequency; with a low-cut filter the signal will be significantly damped below this frequency.

The foregoing filter was an example of a passive filter, i.e., a filter built-up of passive elements (R, L, C).

At present also so-called active filters are used, i.e., filters containing an active element, a high-gain amplifier. An example of an active filter is given in figure (4.3). We have introduced an amplifier G in the scheme. The transfer function for this filter is given by:

$$\frac{V}{E} = \frac{Y^2}{(Y+Z)^2} \tag{4.4}$$

Again, this function is frequency dependent. A high-cut or low-pass is obtained when Y is a capacitance and Z is a resistor. Inductances are rarely used, as is also the case for passive filters.

Why do we need these filters in our geophysical measurements? Let us discuss them separately, first the low-cut filter. As the name says, low-frequency waves can be suppressed with these filters. On land, filtering is sometimes applied to suppress the surface waves or ground roll, although there is a preference for keeping surface waves in the seismogram and remove them later during processing. At sea, a low-cut filter is needed to suppress the waves at the surface of the sea itself.

A most important filter is the anti-alias filter, needed for proper sampling in time of the seismic signal. Aliasing of the seismic signal should be avoided when we sample it in time. This means that the highest frequency in the signal should at least be sampled with 2 samples per full period. But we do not know the frequency content of our signal beforehand

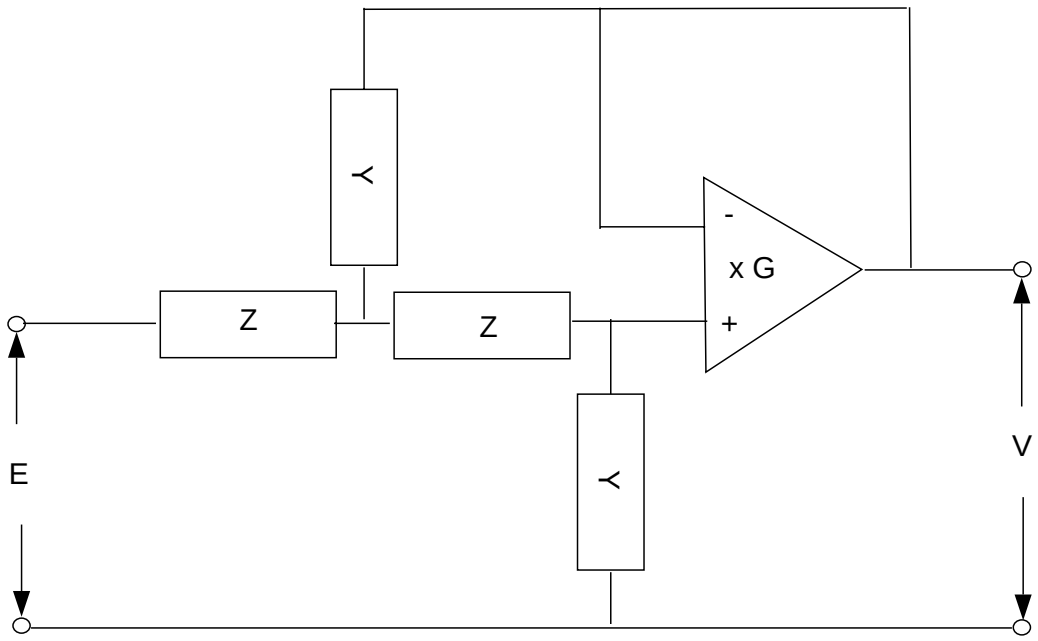

Figure 4.3: An active filter.

and therefore we make sure, using a high-cut filter, that above a certain frequency, the signal is suppressed below a certain level. The high-cut filter must reduce the signal above the Nyquist frequency below the noise level, otherwise aliasing can occur when digitising the signal. The Nyquist frequency is given by: $f_N = 1/2\Delta t$. The effect of aliasing in the time domain is illustrated in Figure (4.4). Once the frequency content of the signal is suppressed sufficiently above the Nyquist frequency, digitizing the data can be done with a minimum of signal distortion. Because of its action on the signal, this filter is also called an anti-alias filter or just alias filter. This filter must always be set according to the sampling rate.

Another type of filter which is usually present in a seismic recording system, is the notch filter. Once in a while, it can happen that 50 or 60 Hz interference from power cables is disturbing the seismic measurement (Europe 50 Hz, America 60 Hz). When input balancing circuits, cable screening fails to cure this problem, it is possible to use an active steep-flank so-called "notch filter" to cut the signal at these frequencies. It should be noted however that by cutting the signal before recording, we may also cut valuable information from our data and we may never be able to retrieve it later on.

4.4 The multiplexer

A multiplexer is an electronic device that connects several inputs to one output channel. This device is used to put the analog responses of all the channels in one long output trace. The device can be visualised as in Figure (4.5). A contact, turning at constant speed, connects inputs 1,2,3,etc... one after the other and in this order to the output. When the wheel has arrived at the last input channel, the first channel is connected again, and so on.

This device is necessary in order to be able to record all the data without waiting

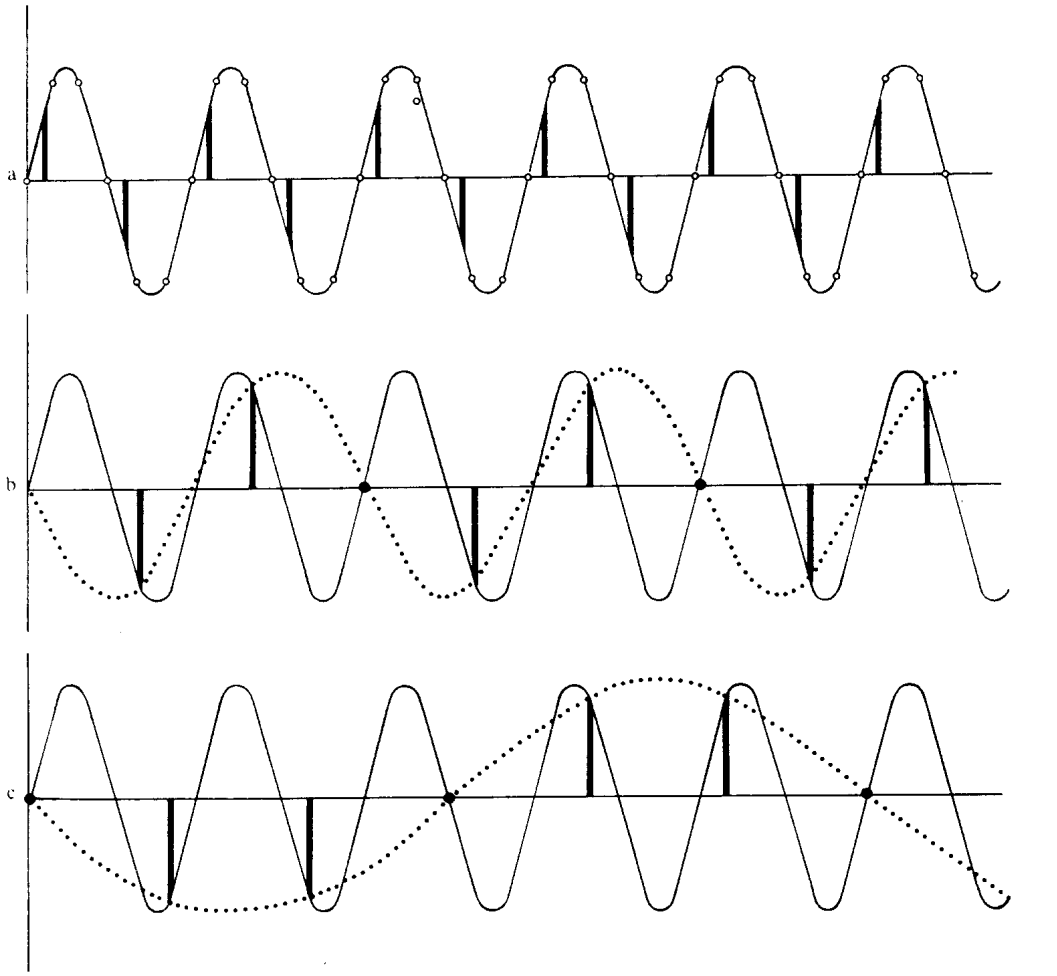

Figure 4.4: The time-domain aspect of aliasing.

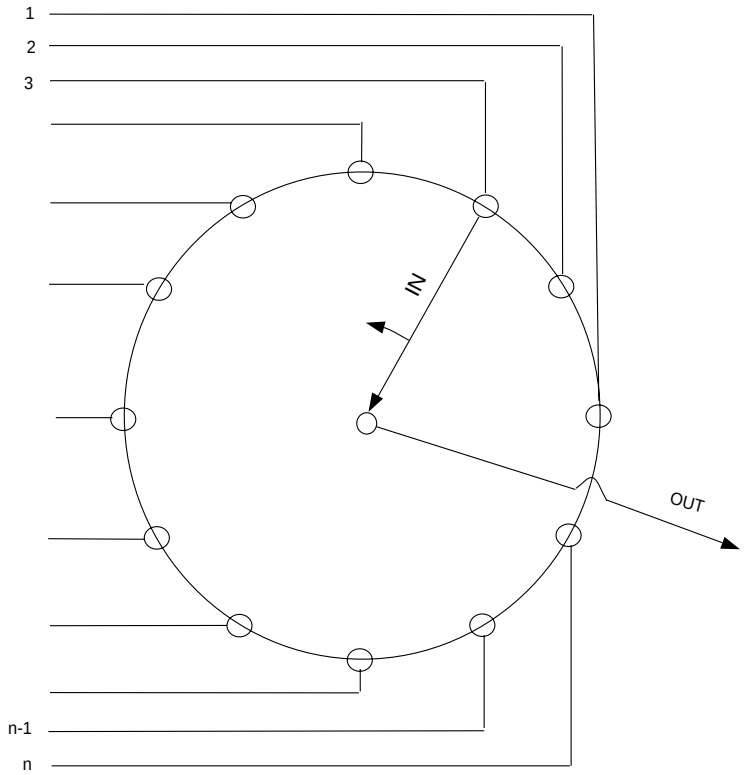

Figure 4.5: Mode of operation of the multiplexer.

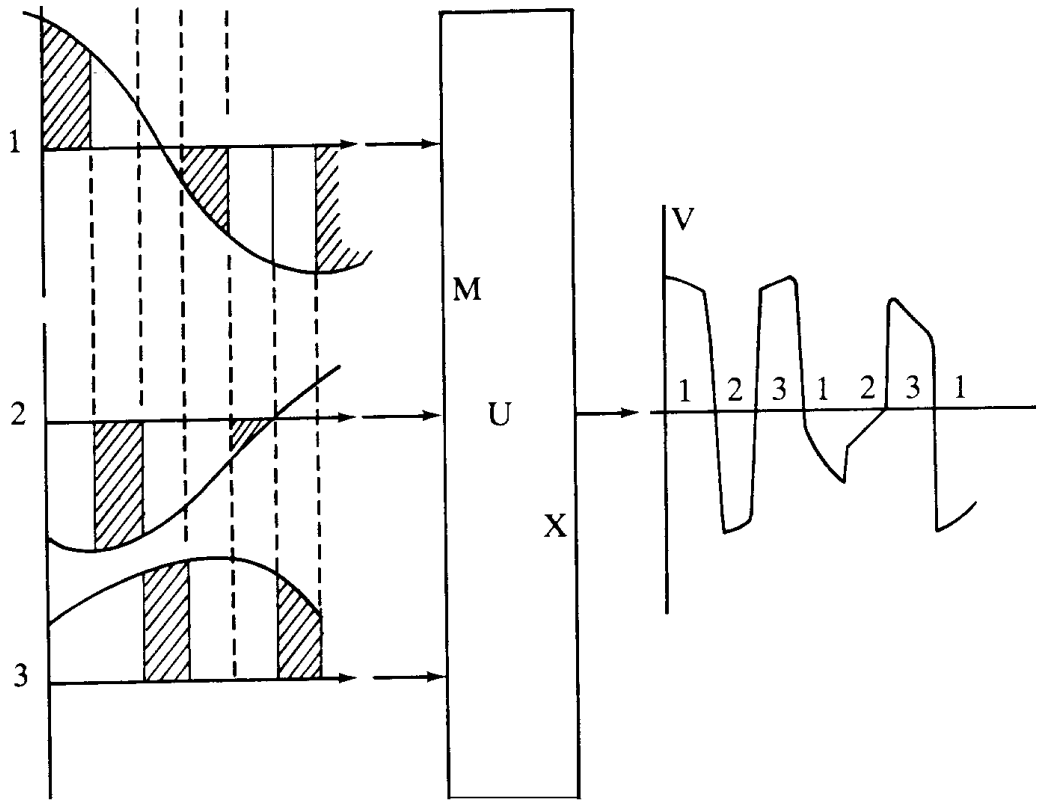

Figure 4.6: The data before and after multiplexing (from: Pieuchot, 1984)

for the time that the last sample (say 6 seconds) of the first trace has arrived. It would be nice to let through each trace separately, and then we would have to wait until the last sample of that trace has arrived before recording the next trace. In that case, we would have to buffer the data of the latter trace somewhere, and this is not very efficient data handling. The multiplexer allows us to record samples of all traces simultaneously within one sample record, by letting through the first sample of the first trace, the first sample of the second trace, the first sample of the third trace, etc.., and then the second sample of the first trace, the second sample of the second trace, etc... (see also Figure (4.6)). Once all the "multiplexed" data has arrived, it can afterwards be demultiplexed to trace-sequential format. With the increased speed of the computer, demultiplexing is often done in the field nowadays.

The next two sections are devoted to two types of data converters, namely one as conventionally used in industry, and one with the newest technology, namely sigma-delta ($\Sigma - \Delta$) conversion. In the conventional systems, the data conversion consists of the sequence of Sample-and-Hold, gain ranging amplifier and A/D conversion. In the sigma-delta technology, these steps consist of a sigma-delta modulator and a decimator. After the data conversion, the steps remain the same.

4.5 Conventional data converters

In this section, the conventional way of data conversion is discussed.

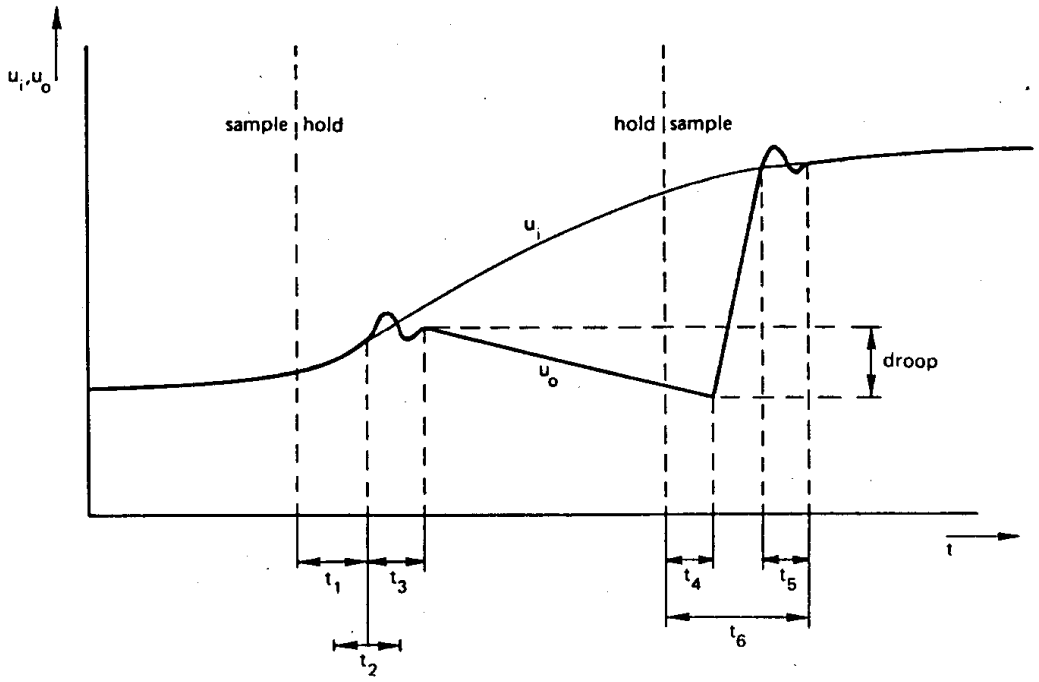

Figure 4.7: Operating principle of a sample-and-hold. (from: Regtien, 1993)

4.5.1 Sample-and-hold (S+H)

This device is necessary in order to make a good analog-to-digital (A/D) conversion possible. If we would do A/D conversion first, then we would lose accuracy. First of all, when we want to sample the signal, the signal must be rather stable. However, the time to load the signal voltage on a capacitor is the sampling time divided by the number of channels. This leaves very short time for the capacitor to load itself and therefore we need some extra time. Secondly, the losses in the capacitor must be small enough to prevent variation of voltage larger than the allowed error. Thirdly, we must have time enough to determine the value of the sample in order to reach required accuracy. These three aspects make it necessary to retain the sample for a small portion of time. This is visualised in Figure (4.7).

4.5.2 Gain-ranging amplifier

The next part in a seismic recording system is the amplification of the signal, necessary to raise the input voltage to a level allowing to record it with a maximum accuracy. One can imagine that the level of the signals early in the seismogram coming from the shallow subsurface is high, while the level of signals at late times (say 6 s) coming from the deeper subsurface will be small. The amplifier must be able to handle both these signals. In the early days, fixed-gain amplifiers were used, and today they are used again, but then with a much higher dynamic range. There are still many seismographs around that use so-called Instantaneous-Floating-Point (IFP) amplifiers; they can deal with different levels of signal, not requiring any fine tuning of the operator.

Let us first look at a simple example of how much the amplitudes can differ in a seismic reflection survey. Say, we have a reflector at 6000m deep; the reflection coefficient of the reflector is 0.1; the losses due to absorption can be valued at 0.1 dB per wavelength of 120m. In this description we use the dB, which is defined as:

$$\text{dB} = 20\ {}^{10}\log(A/A_0)$$

The factor A_0 is some reference value, while the factor 20 has been chosen since the dB is actually defined in terms of energies. Since the energy of a signal is proportional to the amplitudes squared, we can take the power of 2 in front of the log. Another often used unit is the bit, the unit for digital data. One bit can also be expressed in dB's since an extra bit means a factor of 2, so then:

$$1\ \text{bit} = 20\ {}^{10}\log\ 2 = 6$$

Let us return to our problem. The value A_0 is set at the value with the strongest signal at 25m. The damping due to geometrical spreading along the 12000m path is ($A \propto 1/R$):

$20\ {}^{10}\log(25/12000) = -54$ dB

The reflection coefficient has a loss of:

$20\ {}^{10}\log(0.1) = -20$ dB

Absorption for 120m wavelength signal along travelled path (100 wavelengths) : –10dB

This gives us already 84 dB necessary to cope with. But, then we still want to record data with a certain accuracy, say 60 dB's (10 bits). Then we totally need a dynamic range of 144 dB.

4.5.3 The Analog-to-Digital (A/D) converter

The analog-to-digital conversion takes place in this step. The input is a continuous signal voltage, while the output is a sequence of bits. There are several ways of converting an analog signal to a digital one; we shall only discuss the one called the converter by successive approximations. This type of converter starts to compare the voltage from the side where the signal is largest so which will result in the first bit being the "most-significant" bit. Let us consider Figure (4.8).

First the voltage is compared to a reference voltage E, divided by 2. If the voltage is larger, then the first bit will be set to 1, otherwise to zero. In the second stage, an amount of $E/4$ is added to or subtracted from the earlier amount of $E/2$, and again the comparison is made with the signal. If the signal is again larger, a bit value of one will added to the earlier one, otherwise a zero. And so we go on with adding or subtracting E/8, and so on, and so on, until we have reached the maximum amount of bits. An A/D converter is usually given by the amount of bits, e.g. a 16-bits converter. Here it may become even clearer why we need a gain-ranging amplifier: the output of the amplifier should be such that the signal can still be digitised. We can see that we make an error when we digitise the data; the error will be half the so-called least-significant bit (LSB).

Often in the terminology, people talk about 16 bits with a range of 90 dB's; this seems funny since one bit corresponds to 6 dB and so 16 bits corresponds to 96 dB's. The reason why is that in the above example we assumed the input signal to vary between 0 and a maximum, but we have to account for negative values as well. Then, the first bit determines whether the value is positive or negative, and therefore this is then called the sign bit.

The amount of bits resulting from a seismic survey is usually enormous, especially in

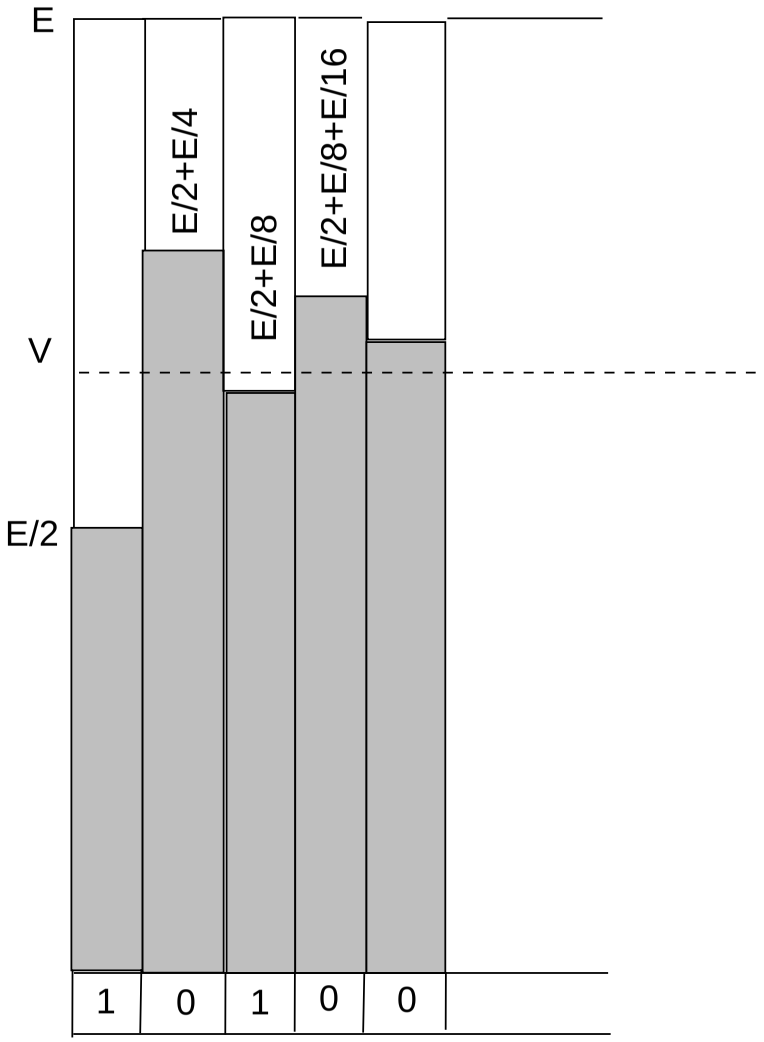

Figure 4.8: Conversion by successive approximations.

3-D seismics. A simple example: assume we have 1000 channels, and we record data for 6 seconds with a sampling rate of 2 ms (500 samples per second); the value of the sample is given by 16 bits. Then the total amount of samples per shot would be: 1000 x 6 x 500 x 16 = 48 . 10^6 bits = 6 Megabits per record (shot). This is an incredible amount of data.

These days, the amplification, anti-alias filtering, sample-and-hold and A/D conversion takes place in the field, in boxes, before it is transmitted digitally to the recording truck. Especially with 3-D seismics this prevents to have to transmit the signals from all the channels to the recording truck; it saves having to transmit all the different geophone outputs separately through the cable (1000 channels is 2000 wires!), while the digital signal can be transmitted through the cable as one large stream of bits. With optical cables, the afore-mentioned amounts can easily be handled. These systems where A/D conversion takes place in the field, are called telemetry-systems.

4.6 Sigma-delta ($\Sigma\Delta$) data converters

A recent development in low-frequency electronics, is the so-called $\Sigma\Delta$ technology. Most newly developed systems for seismic applications are in fact based on this technology. A $\Sigma\Delta$ system required a completely new design of acquisition systems, since the components are entirely different from the conventional systems. $\Sigma\Delta$ systems are based on oversampling the data and a subsequent reduction in the digital stage to the desired Nyquist distance by digital filtering. Use of oversampling overcomes the analog accuracy problem by trading digital complexity and speed for the desired insensitivity to analog non-idealities. In a $\Sigma\Delta$ system, a precision sample-and-hold circuitry is not required any more, and the performance requirements on the analog anti-alias filter that precedes the sampling operation, can be relaxed.

The development of $\Sigma\Delta$ systems already dates back to the 1950's, where feedback systems were used for improving the effective resolution of a coarse quantizer. It has only recently become a viable technique because of the far-developed field of digital filtering, together with the recent developments in semiconductor technology. An extra boost was given by the need of society of higher levels of integration, lower cost and lower voltage. This technology is mainly used in the frequency ranges where the signal can be well oversampled, and thus the signals must be slowly varying compared to the speed of the A/D converter. In the $\Sigma\Delta$ systems, the oversampling is traded for resolution in digital filtering stage. The main field of application for $\Sigma\Delta$ systems are thus the low-frequency bands (< 100 kHz) with high resolution (> 12 bits). These are the ranges where the audio industry has much interest in, and the main applications lie there at this moment.

Much of the following material is derived from the book by Norsworthy (1996), which is completely devoted to $\Sigma\Delta$ data convertors. It would go too far to discuss all items associated with this technology, and for further details, the reader is referred to this book. In our discussion, we limit ourselves to the concepts.

The total seismic data acquisition system, based on $\Sigma\Delta$ technology, is still as depicted in Figure (4.1), only the sample-and-hold, gain ranging amplifier and A/D converter is now the $\Sigma\Delta$-modulator and decimator. Another difference with the previously discussed circuitry is that the analog anti-alias filter at the front end of the $\Sigma\Delta$ modulator does not need to be a high-performance filter. The modulator digitizes the analog signal to a well oversampled signal, and still includes the modulation noise. The decimator is the stage in which a oversampled digital signal is filtered from the modulation noise, and reduced to the desired sampling interval. Let us first look in more detail at the $\Sigma\Delta$ modulator.

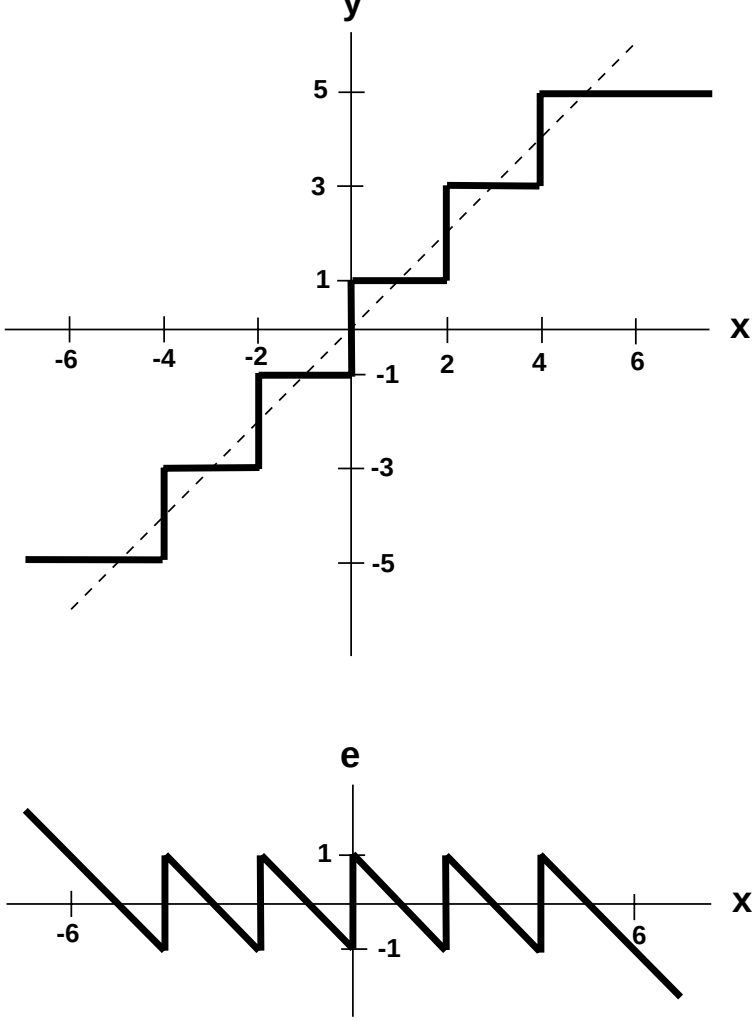

Figure 4.9: Uniform multilevel quantization characteristics. (Redrawn from Norsworthy (1996).

4.6.1 The sigma-delta ($\Sigma\Delta$) modulator

A modulation is a signal processing technique in which the shape of the signal is changed, in principle such that no information loss occurs. Often, modulation is applied in order that the signal is less sensitive to disturbances. Modulation is a process in which use is made of an extra signal of which one parameter is changed in the rhythm of the input signal. In case of the $\Sigma\Delta$ modulator, the aim is to digitize the signal such that no information loss occurs, i.e., the signal will be sampled sufficiently.

At the heart of all digital modulators is the quantization of amplitude and sampling in time. Quantization introduces distortion, and the objective in designing modulators is to limit this distortion. Let us discuss some basic properties of quantization that will be useful for specifying noise from modulators. Figure (4.9) shows a uniform quantization that rounds off a continuous amplitude signal x to odd integers in the range ± 5. The spacing Δ between the quantized levels is 2. The quantized signal can be represented by a linear function x with an error e, i.e,

$$y = x + e \tag{4.5}$$

It can be seen that the error e, in case the quantizer does not saturate (i.e. when $-6 < x < 6$) the error is bounded by $\pm\Delta/2$. The error is completely defined by the input. However, if the input would change randomly between samples without causing saturation, then the error is largely uncorrelated from sample to sample and has equal probability of lying anywhere in the range between $-\Delta/2$ and $+\Delta/2$. Then, the mean square error of the quantization is given by:

$$e_{\text{rms}}^2 = \frac{1}{\Delta}\int_{-\Delta/2}^{\Delta/2} e^2\, de = \frac{\Delta^2}{12} \tag{4.6}$$

Let us, from now on, assume that all the power of the noise is in the range of the positive frequencies. When a digital signal is sampled at frequency $f_s = 1/\Delta t_s$, all of its power folds into the frequency band $0 < f < f_s/2$. If the quantization is then assumed to be white (amplitude spectrum constant, phase spectrum random), the spectral density of the sampled noise is given by

$$E(f) = e_{\text{rms}}\sqrt{\frac{2}{f_s}} = e_{\text{rms}}\sqrt{2\Delta t_s} \tag{4.7}$$

This discussion quantizes the error of a simple quantizer. Let us now turn to the $\Sigma\Delta$ quantizer. The simplest $\Sigma\Delta$ quantizer is shown in figure (4.10). The input to the circuit feeds to the quantizer via an integrator, and the quantized output is fed back to the input and is subtracted from the input. The feedback forces the average value of the quantized signal to track the average input. In order to show this, let us analyze the modulator by means of the equivalent circuit also shown in figure (4.10). Again, e represents the quantization error. Since the equivalent circuit is a sampled-data circuit, the integration becomes accumulation (summation). The output of the quantizer is the output of the integrator with the error of the quantization, i.e.,

$$y_i = w_i + e_i \tag{4.8}$$

while the output of the integrator is:

$$w_i = w_{i-1} + x_{i-1} - y_{i-1} \tag{4.9}$$

where we used the error as defined by equation (4.5). Now the total output of the quantizer, by substituting equation (4.9) into equation (4.8), using $w_{i-1} - y_{i-1} = -e_{i-1}$:

$$y_i = x_{i-1} + (e_i - e_{i-1}) \tag{4.10}$$

Thus the circuit has as output x so leaves the signal unchanged, except for a delay, and it differentiates the quantization error via a first difference.

From this system it can be seen why the modulator is called a $\Sigma\Delta$ modulator. First the signal is integrated (Σ), and then the quantized signal is subtracted from the input, and thus gives a difference (Δ). In the electrotechnical literature, the name of delta-sigma ($\Delta\Sigma$) is also often adopted, since it was first introduced as such.

In order to determine the resolution of the $\Sigma\Delta$ modulator, it is assumed that the input signal is sufficiently busy that the error e behaves a white noise that is uncorrelated with the signal. The modulation noise is given by

$$n_i = e_i - e_{i-1} \tag{4.11}$$

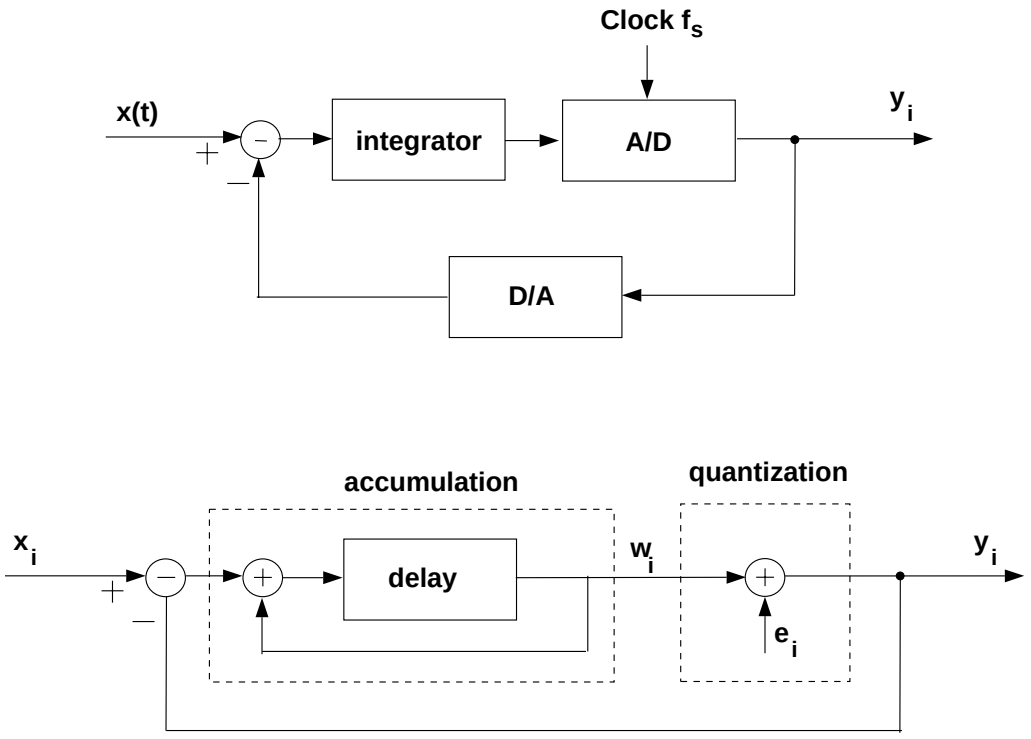

Figure 4.10: Block diagram of a $\Sigma\Delta$ quantizer (above) and its sampled-data equivalent (below). (Redrawn from Norsworthy (1996)).

so that its spectrum is given by;

$$N(f) = E(f)|1 - e^{-j\omega\Delta t_s}| = 2e_{\text{rms}}\sqrt{2\Delta t_s}\sin(\omega\Delta t_s/2) \tag{4.12}$$

where $\omega = 2\pi f$. In figure (4.11), this spectrum is compared to that of the quantization noise as derived earlier (eq.(4.7)). What can be seen is that at low frequencies the noise is reduced.

Now the idea of oversampling is introduced. Say, the signal band is given by $0 < f < f_0$, while the sampling frequency is f_s. The ratio of these two frequencies is often expressed in the so-called oversampling ratio (OSR):

$$\text{OSR} = \frac{f_s}{2f_0} = \frac{1}{2f_0\Delta t_s} \tag{4.13}$$

Assuming now the oversampling ratio is large, i.e., $f_s >> f_0$, the total noise power in the signal band (low frequencies) can be determined by approximating $\sin(\omega\Delta t_s/2)$ by $(\omega\Delta t_s/2)$:

$$n_0^2 = \int_0^{f_0} |N(f)|^2\, df \approx e_{\text{rms}}^2\frac{\pi^2}{3}(2f_0\Delta t_s)^3 \tag{4.14}$$

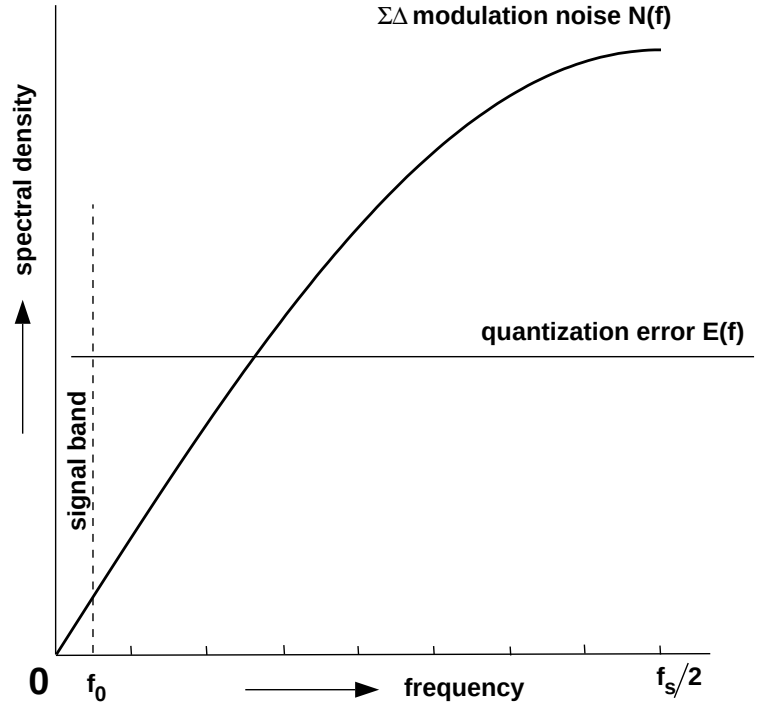

Figure 4.11: Spectral density of ordinary quantization error $E(f)$ and of $\Sigma\Delta$ modulation noise $N(f)$. (Redrawn from Norsworthy (1996))

or its rms-value:

$$n_0 = e_{\rm rms}\frac{\pi}{\sqrt{3}}(2f_0\Delta t_s)^{3/2} = e_{\rm rms}\frac{\pi}{\sqrt{3}}({\rm OSR})^{-3/2} \tag{4.15}$$

Thus we have the result that oversampling reduces the in-band noise (0 to f_0) from sigma-delta quantization by the (3/2) power of the oversampling ratio. This thus provides 9 dB or 1.5 bits of extra resolution for each doubling of the oversampling ratio. This is the main feature of oversampling : resolution in time is traded for resolution in amplitude.

Let us illustrate this by a numerical example. But before that, we need to say something about the A/D converter first. The A/D converter which is integrated in the $\Sigma\Delta$ circuitry, is a different one than the one used in conventional systems: the A/D converter only needs to be a very simple one, often only a 1-bit converter. What will be shown here by a numerical example, is that the 1-bit resolution is increased to higher resolution making use of oversampling. For the illustration, we take the A/D converter to be nothing else than one simple comparator where the signal is either above or below zero. If the signal is above zero, a 1 is stored and after the D/A converter the signal is decreased by a reference current $I_{\rm ref}$; if the signal is below zero, a 0 is stored and after the D/A converter the signal is left unchanged.

Let us assume we have an input signal of, say, 0.3 $I_{\rm ref}$ at time 0 Δt_s. In general, the sampling will be very fast compared to the changes in the signal so the signal can be assumed to be constant over a small amount of samples. The comparator sees a number larger than zero, so a 1 is sent to the bit-output [total bit-output: 1]. The signal at the next time without feedback, time 1 Δt_s, would have been 0.6 $I_{\rm ref}$ (because of the

Table 4.1: *Numerical example digitization of number 0.3.*

time (Δt_s)	0	1	2	3	4	5	6	7	8	9	10	11	12
signal value	0.3	–0.4	–0.1	0.2	–0.5	–0.2	0.1	–0.6	–0.3	0.0	0.3	–0.4	–0.1
bit	1	0	0	1	0	0	1	0	0	0	1	0	0

integrator) but then the comparator has fed back a signal of $-I_{\text{ref}}$, so the signal at the next time 1 becomes –0.4 I_{ref}. It comes into the comparator again, and the comparator sees a number of less than zero: a 0 is sent to the bit-output [total bit-output: 10]. At the next time 2 Δt_s, the signal is left unchanged, so no feedback occurs, only integration; the signal becomes –0.1 I_{ref}. The comparator sees a number smaller than zero again, so it sends a 0 to the bit-output[total bit-output: 100]. At the next time step the signal becomes larger than zero again an the comparator sees a 1 [total bit-output: 1001]. And so on. For the first 12 times, the total bit-output is given in table (4.1). Because of our chosen number 0.3, the signal becomes identical after time 9 Δt_s again: we have 10 bits to represent 0.3: we have three 1's out of 10 bits. This is exactly right.

What we can see from the example is that the number of 1's divided by the total number of bits represent the signal value. If we would have chosen a stranger number in the example, say 0.354675 I_{ref}, then we would have needed a very long bitstream to represent it exactly, but it can be shown that with a lesser number of bits, the number of 1's divided by the total number of bits in the bitstream approximates the number 0.354675 to the resolution of the number of bits.

4.6.2 Decimation filter for sigma-delta modulated signals

The output from the sigma-delta modulator is a well oversampled digital signal. The decimator is a digital filter that serves to attenuate all energy outside the signal band above f_0 so that the signal may be resampled at the Nyquist rate without incurring any noise because of aliasing.

The out-of-band that needs to be attenuated by the decimation filter, consist of two types: the modulation noise, and the out-of-band components of the input signal. The first one is generally easy to filter since its spectrum rises slowly. However, removal of out-of-band components of the signal is harder to achieve and requires abrupt low-pass filters; such filters are expensive to build at the high sampling rates of the modulator. Therefore, in practice, the decimation is nearly always done in two stages where the first stage is mainly designed to remove the modulation noise whereas the second is designed to remove out-of-band components of the signal.

Let us focus first on the first-stage decimation. We define an intermediate decimation frequency f_D, and call the ratio f_s/f_D the decimation ratio N. In figure (4.12) an example is given for a filter which is used before the signal is resampled at f_D. What is important to realize, if the modulated signal is resampled at f_D, is that the bands above f_D fold back into the basis band, the important band being the signal band. In order to attenuate the bands which fold into the signal band, it is sensible to place the zeros of the filter at f_D and its harmonics. We do not need to bother too much about the bands between f_0 and f_D since the noise folds on itself without entering the signal band.

The simplest form of such a decimator is a k-point moving average from the f_s-sampled input. If the input samples are x_i, sampled at f_s, and the output samples y_i, sampled at

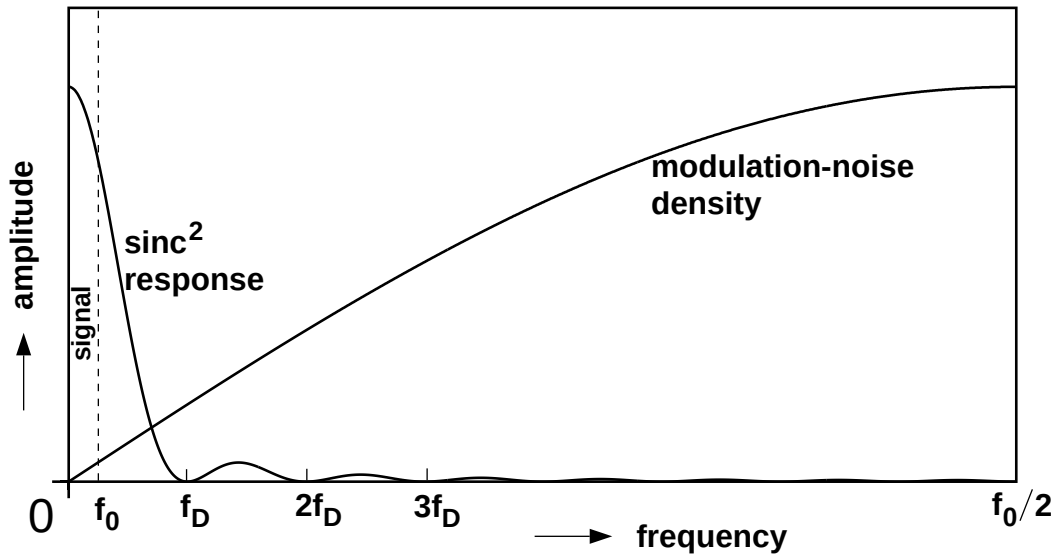

Figure 4.12: Spectra of modulation noise and (digital) sinc2-filter. f_0 =maximum frequency of signal band, f_D = intermediate sampling frequency, f_s = oversampling frequency. (redrawn from Norsworthy (1996)).

f_D, then

$$y_k = \frac{1}{N} \sum_{i=(k-1)N}^{kN-1} x_i \tag{4.16}$$

The transfer function of the filter is

$$H(z) = \frac{Y(z)}{X(z)} = \frac{1}{N} \sum_{i=0}^{N-1} z^{-i} = \frac{1}{N} \frac{1 - z^{-N}}{1 - z^{-1}} \tag{4.17}$$

and its frequency response is given by ($z = \exp(j\omega \Delta t_s)$):

$$H(f) = \frac{\mathrm{sinc}(\pi f N \Delta t_s)}{\mathrm{sinc}(\pi f \Delta t_s)} \tag{4.18}$$

This function has zeros at f_D and all of its harmonics.

This filter is an example of how to design a filter which has zeros at f_D and its harmonics. In practice much better performance can be obtained by using filters that are products of sinc functions. For the sigma-delta modulation analyzed so far, a sinc^2 function is close to being optimal.

The choice of f_D is important in the design of the total modulator. If f_D is too high, we still do not make optimally use of the slowly varying spectrum of the modulation noise and

we put too much effort in the second-stage filter to have an abrupt low-pass characteristic to filter the out-of-band components of the signal. If f_D is too low, the sinc-filter does not have enough anti-alias capabilities to remove the out-of-band components of the signal, and thus we obtain extra noise. Often, a factor 4 is chosen for the first-stage decimation ratio.

The last decimator to go from the intermediate frequency to the final signal-band Nyquist frequency f_0 consists again of a filter with a resampler. As mentioned before, the filter must have good anti-alias characteristics in order to remove the out-of-band components of the signal. Because we are now at a much lower sampling rate, such a design can be done very efficiently.

4.6.3 Some aspects of sigma-delta modulators

In the discussion, it was assumed that the error of the quantizer is white and uncorrelated noise. Of course, this is never truly the case but often the assumption is sufficient for practice, and sometimes does not need to be assumed for the analysis to be valid. However, there are signals in which the modulator has difficulties, and that is a DC (constant) input. In figure (4.13) the input is given as $3/7\ \Delta$, and the quantized output is given. The input is $3\Delta/7$ away from a level and this results in a pattern that repeats every seven periods. In general, the modulation noise depends on the DC input level. It could happen that this repetition frequency lies in the signal band, and then the modulation becomes noisy. This type of noise can be observed as pattern noise.

Another type of noise from sigma-delta modulators can be dead zones. In figure (4.13) the output of the integrator is shown. As can be seen, is that the waveform may be raised as much as $\Delta/7$, with respect to the quantizer threshold level, without changing the sequence of decisions. A change of level at the output, corresponds to an impulse at the input. Therefore, small fast changes in the input may be ignored by the modulator; this can happen under certain conditions. In general, pattern noise is more noticeable than dead zones.

As mentioned in the introduction of the $\Sigma\Delta$ technology, the performance of the analog anti-alias filter can be relaxed. Often, a simple (one-pole) RC-circuit is sufficient to prevent aliasing since only at the very low frequency end of the oversampled signal, the original signal must be kept unchanged. Above this frequency (f_0), the signal will be filtered during the decimation stage.

In the discussion so far, we assumed the simplest form of a sigma-delta modulator, where there is only one feedback loop. It is possible to include a second feedback loop in the system, as shown in figure (4.14). It can be shown that the output of this modulator is given by:

$$y_{i-1} = x_{i-1} + (e_i - 2e_{i-1} + e_{i-2}) \tag{4.19}$$

The modulation noise is now the second difference of the quantization error. This type of modulation is called second-order sigma-delta modulation.

The spectral density of the noise is:

$$N(f) = E(f)\left(1 - e^{-j\omega\Delta t_s}\right)^2 \tag{4.20}$$

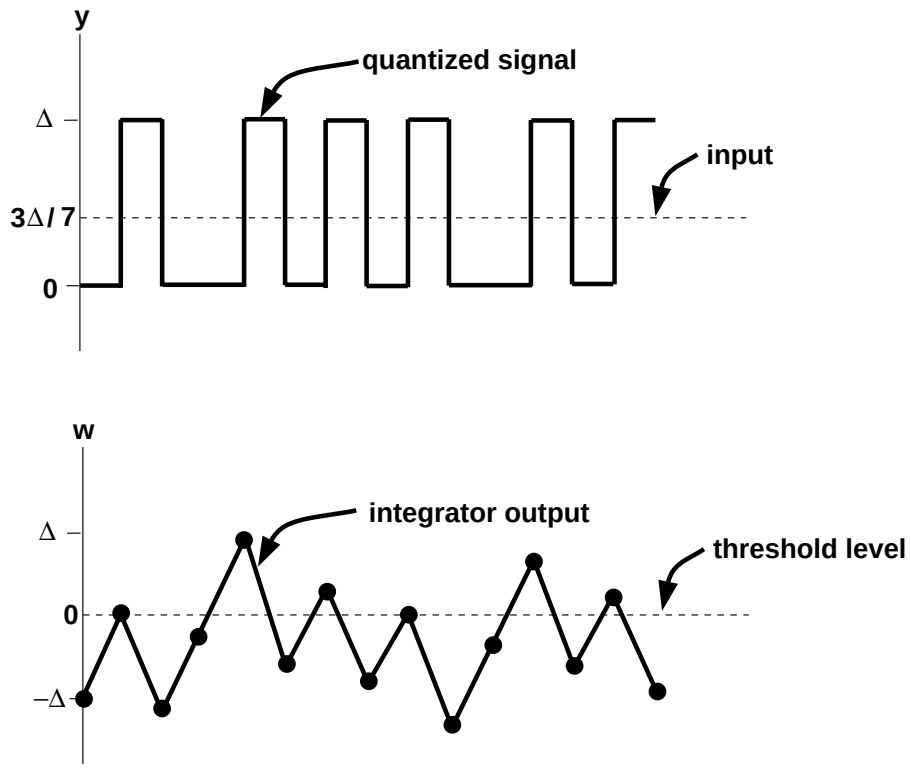

Figure 4.13: DC input and its output from quantizer and integrator. (redrawn from Norsworthy (1996)).

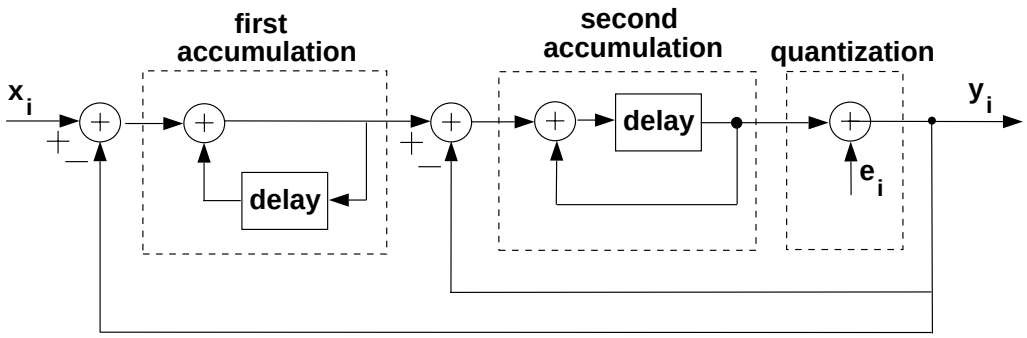

Figure 4.14: Second-order ΣΔ quantizer. (Redrawn from Norsworthy (1996))

for which the modulus is given by:

$$|N(f)| = 4e_{\text{rms}}\sqrt{2\Delta t_s}\sin^2(\omega\Delta t_s/2) \tag{4.21}$$

Assuming we have a large oversampling ratio, i.e., $f_s >> f_0$, the rms noise in the signal band is given by:

$$n_0 \approx e_{\text{rms}}\frac{\pi^2}{\sqrt{5}}(2f_0\Delta t_s)^{5/2} = e_{\text{rms}}\frac{\pi^2}{\sqrt{5}}(\text{OSR})^{-5/2} \tag{4.22}$$

It can be seen that the noise is now inversely proportional to power 5/2 of the oversampling ratio. This means that extra loops can be used to provide extra resolution. Even higher-order loops can be designed, but certain instabilities arise which need to be solved. In practice, second-order modulation is often used.

The performance of a modulator can be improved by taking a measure of its noise, digitizing that measure in a second modulator, and combining the output of the two modulators in a way that cancels the noise of the first modulator. Such modulators are called cascaded modulators. The advantage of cascaded modulators is that first-order modulation can be used to obtain the same performance as second-order modulation. This technique has been widely applied to sigma-delta modulators. More on these modulators can be found in Norsworthy (1996).

4.7 Formatter

Once we have obtained a stream of bits, we want to convert this stream to a certain format, (like words,) a certain type of grouping the bits as bytes or words such that they can later be fed into a computer. Also, we want to define records, end-of-file marks etc. Common formats in the industry are SEG-D, SEG-Y and SEG-2, where SEG stands for the Society of Exploration Geophysicists. The standardisation committee from this society has defined certain formats which have, fortunately, been adopted by the industry. SEG-D is a packed format such that the wordlength can be decreased, e.g. 2 1/2 bytes, such that we can write faster onto tape. Usually, in the computer, one word is made up of 4 bytes. The conversion from lower-length bytes to 4 bytes takes place in the processing centre, where another format is adopted: SEG-Y. On floppy's for a PC(/DOS)-environment, there is a format SEG-2.

4.8 (Write-amplifier and) Recorder

The last step of the seismic data recording process is recording the digital seismic data on magnetic tape (or disc). A write amplifier in the recorder system amplifies the signal to create a sufficiently strong magnetic field in the write heads of the recorder to magnetize the tape (or disc). Until recently seismic surveys have been recorded on 9-track 1/2-inch tapes. At present more processing centres use 3480 IBM cartridges, which can store the same amount of data but are much smaller in size. Developments are continuing : many systems use now small Exabyte tape cartridges, especially portable field systems. These days, this is still changing because of the developments in the computer world.

4.9 References

Norsworthy, S.R., R. Schreier and G.C. Temes (eds), 1997. Delta-Sigma Data Converters, Theory Design, and Simulation, IEEE Press, New York.

Pieuchot, M., 1984. Seismic Instrumentation, In: Handbook of Geophysical Exploration, section I. Seismic Exploration (eds. K. Helbig & S. Treitel), vol. 2, Geophysical Press, London, 376 pp.

Regtien, P.P.L., 1993. Instrumentele Electronica, Delftse Uitgevers Maatschappij, pp. 448.

4.10 Acknowledgements

The author greatfully acknowledges the discussion with Dr. Frank Riedijk on $\Sigma\Delta$ technology; without the discussions with him, the written piece would not have been so complete.

Chapter 5

Seismic survey design

5.1 Introduction

When we are going to survey an area with the seismic reflection technique, then the question arises: How do we set the parameters in the field? And, what determines these parameters? We have already discussed some of these aspects in the previous chapters, however not all. In this chapter we will discuss the most important considerations leading to a choice of parameters. As is obvious from the previous chapters, we have parameters related to the source, the detectors and the recorder. They will be discussed in this order. Sometimes, no data is available for a certain area in which one wants to carry out a survey. Then it is advisable to shoot a so-called noise spread there, allowing us to evaluate the parameter settings in relation to the seismic wave phenomena observed, reason why we will discuss the noise spread as well. As is common practice in exploration for gas and oil, we need to stack data in order to reach a certain signal-to-noise ratio, and the field technique used in order to achieve this multiple coverage is the CMP technique. Then, finally, one has to take account of the global areal coverage aspects of the survey, i.e. one has to continue the seismic recording quite a distance beyond the subsurface target itself (with a wider "aperture"), in order to be able to carry out certain processes, such as migration, reliably, later in the processing centre.

5.2 The source parameters

(a) The first thing is to decide on the source type. On land, we have a choice for dynamite or Vibroseis. The choice for this type depends on the practical circumstances as discussed in the section on the Vibroseis in chapter 4. If none of these points put restrictions on the use of any of these two sources, then Vibroseis has the preference because the costs are lower. At sea, there is hardly a choice since the airgun has proved to be the best source in that environment. For shallow seismics, the situation is quite different, but the most popular one seems to be the Betsy which can be seen as a gun shooting vertically into the ground.

(b) The next parameter is the source depth, which is a parameter for the dynamite source on land and the airgun source at sea. We have already demonstrated the effect of a free surface on the total outgoing signal when discussing the airgun, and very briefly for

the dynamite source. We had in both cases a quarter wavelength (, although some people prefer to put the dynamite straight at the interface of the consolidated and unconsolidated layer). It is usually the case that the first few metres of ground is unconsolidated. Dynamite exploded in such material does not usually generate powerful bodywaves. Mostly, large amplitude surface waves are generated. In order to generate the bodywaves which are needed for reflections, it is necessary to put the dynamite in consolidated material. When we put the dynamite below the interface, then we have a slightly different problem then at sea, since on land we do not know the velocity on beforehand. A possibility is shooting a small refraction profile. Extra information can be obtained from the drilling; one will notice when one is beyond the blurry substance from the surface layer.

(c) Next, we have to decide on the source power. This is a parameter for all sources, although at sea we pretty well know how to create enough energy. On land, this is different since we sometimes can loose energy in the near surface layer, e.g., peat is known to be a nasty high-absorbent material; with this material Vibroseis could be very well in problems.

(d) A last parameter is the source pattern. This is particularly important for the Vibroseis source where we work with several trucks simultaneously. The same arguments can be applied as for a geophone array, which will be discussed in the next section.

5.3 Detector parameters

The parameters related with the signal detection have effect on the temporal as well as the spatial character of the measurement. The spatial character is a consequence of the fact that (in the field) we sample a wavefield, and therefore this wavefield sampling puts constraints on the spatial dimensions as well.

(a) The first choice is obviously on the detector type. This can be a vertical (one-component) geophone, a hydrophone or a 3-component geophone. The response of the detector at low frequencies is important. Geophones have a resonance frequency and below resonance the response decays at about 12 dB/octave, while above resonance the response is essentially flat. (see the relevant figures in chapter 3). We can therefore attack the groundroll if we use high frequency geophones, e.g. 50-Hz phones. This would mean filtering already in the field and we try to avoid this: we like to keep as many frequencies in the records as possible. High-frequency phones are used in shallow seismics in order to boost the high frequencies. With hydrophones we also have damping at low frequencies so therefore we have some choice in the type of hydrophone as well.

(b) The next parameter is the detector spacing. This parameter is determined by the spatial-aliasing concept. What is spatial aliasing? Spatial aliasing is the effect when we do not take 2 but less samples per highest spatial frequency in the x-direction. The visual aspect of spatial aliasing is shown in figure (5.1). In words, we can say that: spatial aliasing occurs when the distance travelled by the wave to get from one detector to the next is larger than half the smallest wavelength. There are some parameters in this description: the angle with which the wave impinges on the surface; the smallest wavelength, which depends on the highest frequency and the velocity. Before we perform an experiment, we know the highest frequency since this is determined by the sampling rate Δt, but we cannot determine the angle of incidence and the velocity accurately: we must make a good guess either originating from earlier surveys in that area, or from areas with the same circumstances. So the receiver spacing is determined by the maximum wavenumber $k_{\max}$ in the data, i.e.:

$$k_{\max} = f_{\max}/c_{\min} \tag{5.1}$$

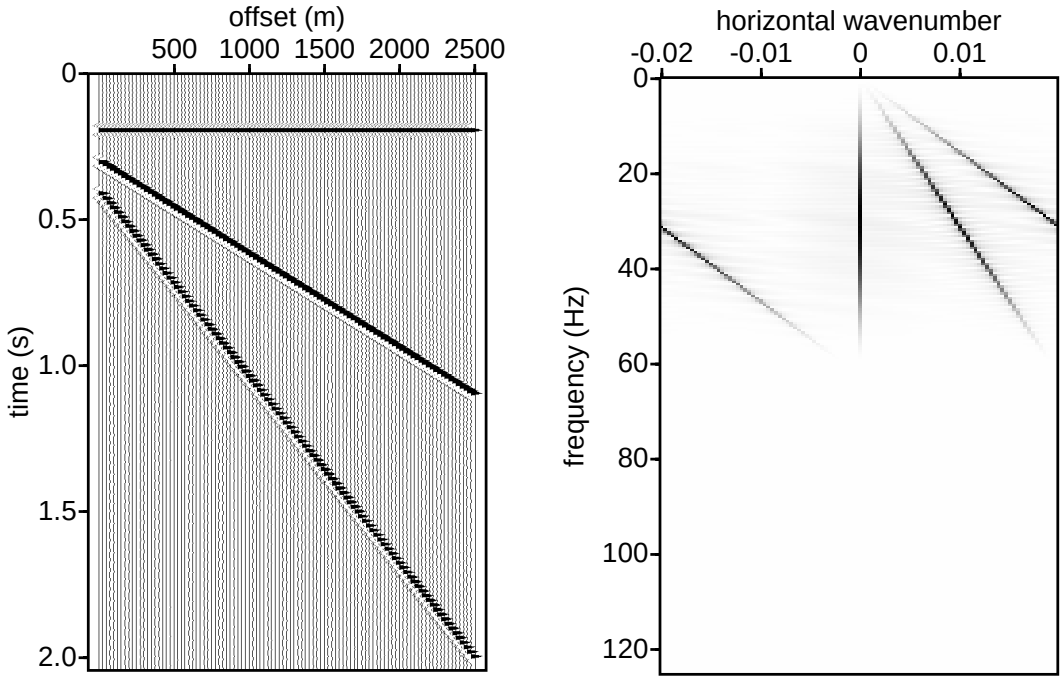

Figure 5.1: The effect of spatial aliasing in t-x and f-k

where $f_{\max}$ is the maximum frequency of an event and $c_{\min}$ is the minimum velocity of an event. In this criterion, we take account of several events in order to keep Δx at reasonable levels. If we would take $f_{\max}$ as the Nyquist frequency and $c_{\min}$ the minimum velocity in the data, then Δx would become very small. So we take that event for which $k_{\max}$ is such that we do not have any spatial aliasing for that event, i.e.,

$$\Delta x \leq \frac{1}{2k_N} = \frac{c_{\min}}{2f_{\max}} \tag{5.2}$$

We call this value of Δx_r the basic sampling interval. Take for instance the ground roll, which is usually the most demanding event. Ground roll can have frequencies up to 50 Hz and say that the minimum velocity is 200 m/s. Then Δx_r is 200/(2x50) = 2 m. In practice we cannot sample the wavefield that frequently, it would be a too heavy burden on the field logistics and make the field work uneconomic (slow and costly). As long as seismic data acquisition is not carried out using the basic sampling interval, patterns (arrays) of seismic detectors can be used to circumvent some of the sampling problems, reason why detectors patterns are discussed in the following.

(c) In the old days geophone pattern were used to suppress the ground roll but recording systems today can deal better with the loss of dynamic range caused by the large amplitudes of ground roll. These days with better recording systems, geophone (and source) patterns are not aimed so much to suppress noise, but more to act as a spatial anti-alias filter and as a resampling operator. In the chapter on detectors we derived the

wavenumber-domain response of a 4-geophone array, which we repeat here:

$$A(k_x) = \frac{\sin(4\pi k_x \Delta x)}{\sin(\pi k_x \Delta x)} \tag{5.3}$$

The amplitude of this function is sketched in figure (5.2) (c). This filter is periodic one, as explained earlier. As an anti-alias filter it does not do a very good job, since it is not flat at all in the passband, and has some moderate values above the Nyquist wavenumber. There are ways to improve the response of the pattern by using more complex geometries, but in practice static corrections and differences in ground coupling and sensitivities do not make it worthwhile using complex patterns.

Let us now look at Figure (5.3) for the choice of the group distance. In that figure, we show the array response by a drawn line, while the array response from the next period is shown by a dotted line. Remember that discetisation with distance d in the spatial domain has a periodic wavenumber spectrum with period $(1/d)$. As we can see from the upper figure from Figure (5.3), we could choose to have the first zero crossings of the two periods to coincide. In that case we have:

$$d = 2\Delta x, \tag{5.4}$$

so the group length is two geophone spacings, while the group has 4 geophones. This type of array is called a fully overlapping pattern or 100 percent overlapping pattern.

Another way of choosing the zero crossings is to let the first zero crossings of the next period fall exactly on $k = 0$, as shown in the lower figure of Figure (5.3). Equivalently, the first zero crossing of the group response coincides with the peak of the response of the next period. In that case we have:

$$d = 4\Delta x, \tag{5.5}$$

so the group spacing is as long as the array itself. This type of array is called the stack array. This name is chosen because stacking is nothing else then adding the responses on the $(k = 0)$–axis. This can be seen by taking $k = 0$ in the forward spatial Fourier transform:

$$F(k_x = 0) = \int_{-\infty}^{+\infty} f(x)\, dx \tag{5.6}$$

(d) The final parameters to determine are the minimum and maximum offsets. In the professional practice the minimum offset is zero because it is best to shoot split-spread, which is common practice on land. At sea this is different because we cannot push the kilometers-long streamers in front of the boat. Choosing the maximum offset is an important parameter for both. We must have enough offset to do later a proper velocity analysis (see figure (5.4)). A rule of thumb is that the maximum offset is equal to the depth of the target; if the detectors are further from the shot than this, they will see refractions before they see reflections. The minimum offset is important at sea. There it could be said that the smallest distance possible would be the best, and so it purely depends on how near the streamer(s) can be put at the back of the boat without pulling too much. This pulling is usually damped by a stretch section before the hydrophones, and it is this part which will determine the minimum offset.

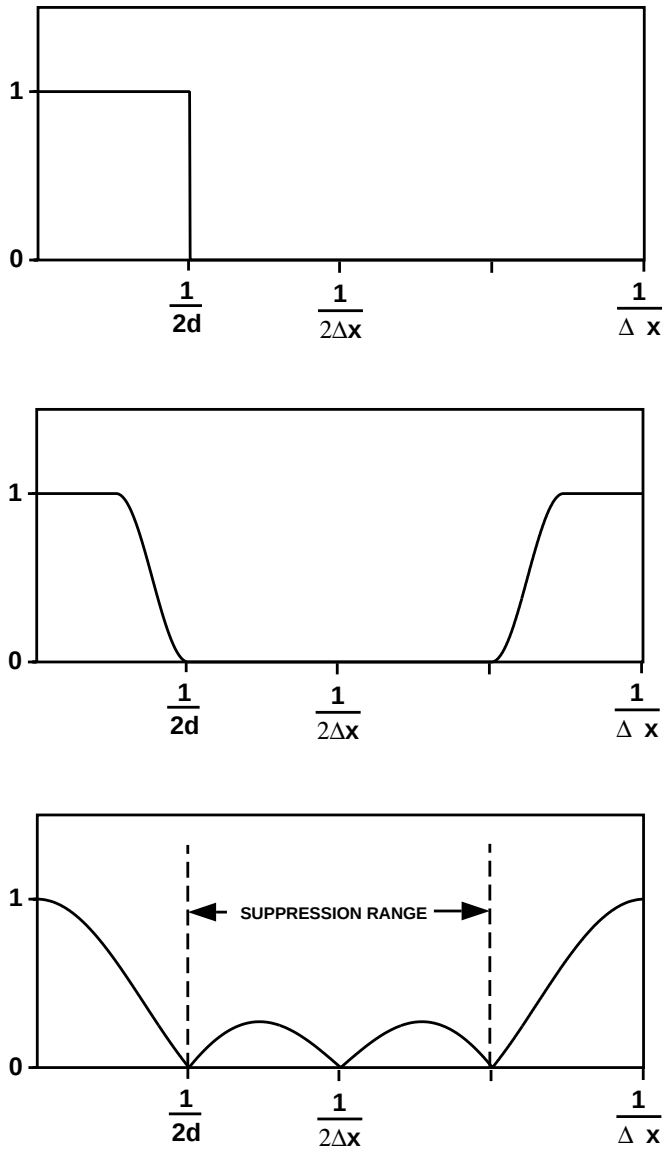

Figure 5.2: Pattern as digital anti-alias filter. Δ_x = distance between pattern elements, d = new sampling interval. In this example $d = 2\Delta x$. (a) Desired response, (b) Normal digital anti-alias filter response, (c) Pattern response with equal filter coefficients.

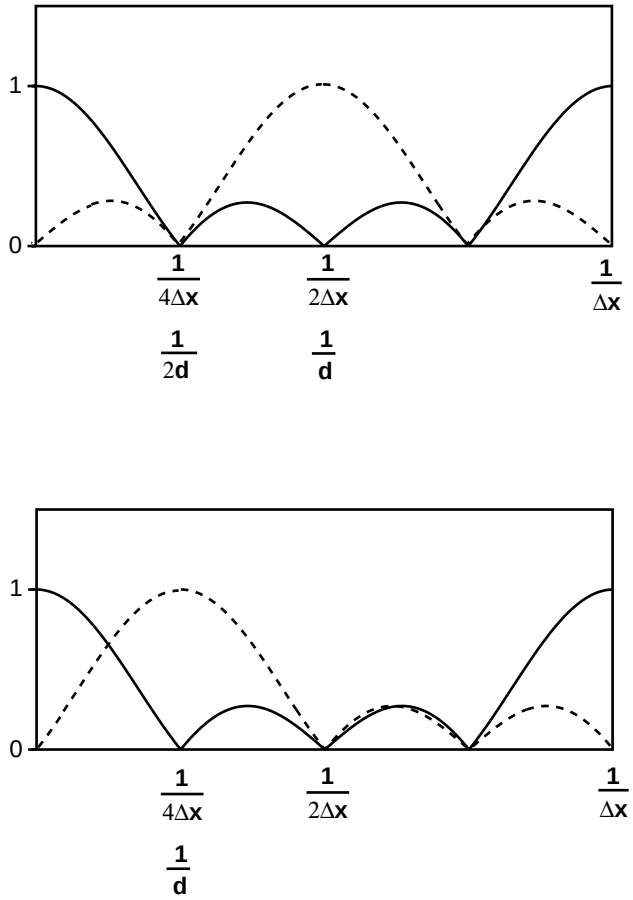

Figure 5.3: Choice of group spacing depending on choice of Nyquist wavenumber: fully overlapping pattern (upper figure), and the stack array (lower figure).

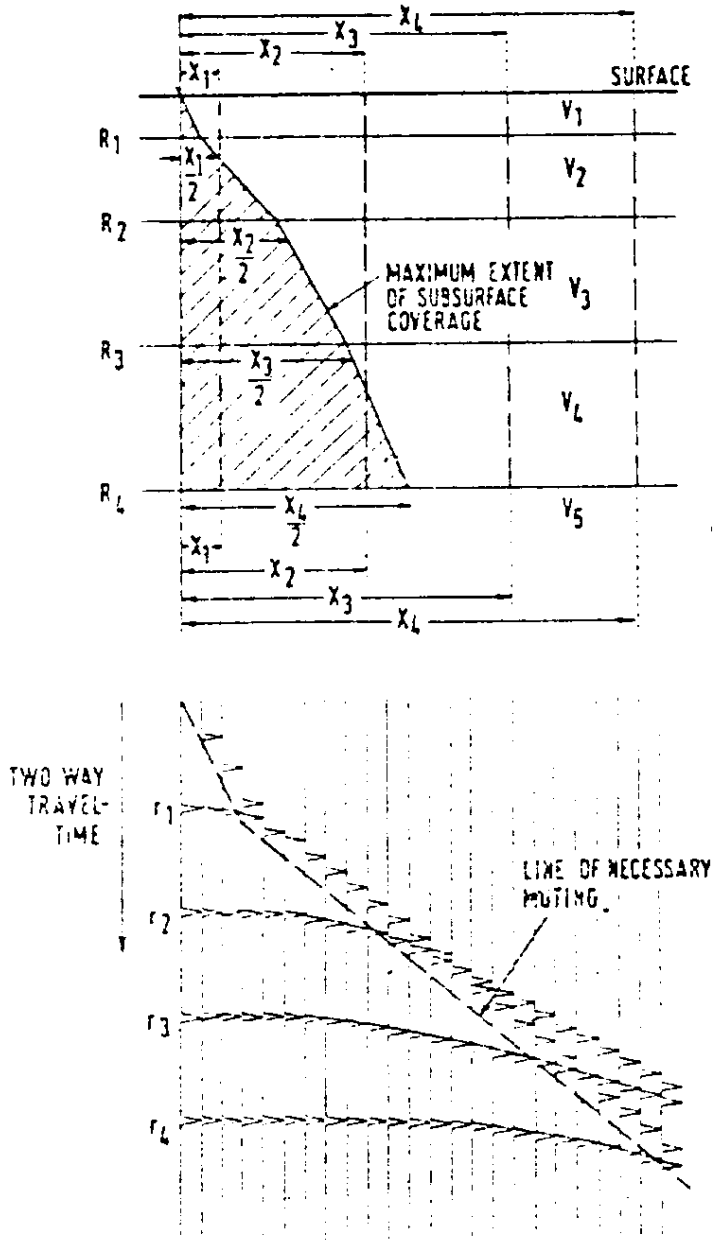

Figure 5.4: Relationship between maximum subsurface coverage and depth of target. Reflections on record r_1, r_2, r_3 and r_4 correspond to interfaces R_1, R_2, R_3 and R_4 respectively. Line of muting defines maximum shot-geophone distance for these reflectors as X_1, X_2, X_3 and X_4, respectively.

5.4 The recording parameters

In chapter 4 we dealt with the hardware aspects of seismic data acquisition systems. Here we will only discuss the aspects / parameter settings the practicing geophysicist has to deal with from a user point of view. Usually, these parameters are related to the temporal character of the data. The user has to decide on:

(a) Time sampling and time length. These are obvious: the time sampling is determined by the Nyquist frequency $\Delta t = 1/(2f_N)$ in order to avoid aliasing. The rule of thumb is: from previous studies it is known at which frequency the desired data (reflections) have its maximum amplitude. We choose the Nyquist frequency at least four times this amount. This then determines the sampling rate in time. Often, reflection data for the oil industry peaks at 60 Hz, so the Nyquist frequency is at least 240 Hz. So choosing the sampling rate 2 ms, this criterion is satisfied. The choice of time length is rather obvious. when we want to "look into" the subsurface, the seismic recording times should be long enough to "see" our target, of course with some safety margin. A simple rule can be that we have a velocity of 2000 m/s, so if we record 6 seconds of data we will look 6 km deep, taking account of the fact that the wave has to travel downwards and upwards.

(b) Filter settings. We have three kind of filters: low-cut, high-cut and notch filters. On land, low-cut filters are sometimes used to filter out the ground-roll. However, the recording systems today can handle the amplitude variations as shown by the ground roll. Although it may be a powerful method to suppress the low frequencies, we should keep in mind that what is not recorded, can never retrieved in the processing centre. Filtering can always be done at a later stage in the computer and it is advisable to do this if the amplitude of the groudroll is not too high, that is: such that the amplitudes of the reflections are not accurate any more. At sea, it is always necessary to use some low-cut filter because we are always hindered by noise of the sea surface.

The second filter, the high-cut filter is of course needed to prevent (temporal) aliasing. We must make sure we have enough suppression of the signal at the Nyquist frequency. This topic was already discussed in chapter 2.

The third filter is the notch filter which is not frequently used. When there is 50-Hz noise from power cables, it may be useful to use this filter. Using this filter should only be done as a last resort. Note that reflection data for oil exploration has large spectral amplitudes around 60 Hz, so filtering nearby these values will have a great influence on data quality.

5.5 Noise spread (/ Microspread / Walk-away spread)

In the past the noise spread was used to measure the wavelengths of the (unwanted) ground-roll in order to be able to suppress this "noise" as much as possible. This was necessary to prevent clipping of the amplitudes due to the type of amplifiers used at that time. There are still recording instruments around which show this feature and then it is important to look at the effect of ground roll. Options are then using smaller and deeper charges, use a low-cut filter on the recorder, use high-frequency geophones and use source- and/or receiver patterns around the dominant wavelength of the ground roll.

Today we do not have to be so much concerned about the ground roll anymore since the data acquisition systems have enough dynamic range. The aim of the noise spread is then different. The most important aim is the spatial aliasing concept. The best way to deal with both effects of ground roll and spatial sampling, is to use the basic sampling

interval between the elements of the geophone string and use so many geophones in one string that it covers exactly one wavelength of the dominant frequency of the ground roll. This is ideal, but this would make the amount of geophones in a string variable and so rather impractical in the field.

For one spread we can lay down the geophones such that we do not have any spatial aliasing. We can make an (f, k)–domain plot to see which wavenumbers are in the data and use that information in order to see whether the geophone (or source) pattern does a good job. If it does not do a good job it can be several things. First, there can be point to point variations of the statics. If statics vary rapidly over the length of the pattern, then the pattern could cause severe distortions. Second, there could be variations in geophone sensitivities and ground coupling. These things can all be investigated with the noise spread.

What is also still important is the power of the source, that means with dynamite the charge size, and the charge depth. We discussed this in the previous section. We must make sure we get enough energy in the desired frequency range in order to get good reflections from our target. An example of a composite shot record is shown in figure (5.5). The (f, k)-domain representation of this data is given in figure (5.6). When we would use a pattern, we would get the result as shown in figure (5.7).

5.6 CMP data acquisition

One of the most powerful tools that is applied in seismic data acquisition is the so-called Common MidPoint (CMP) technique, introduced as the Common Depth Point technique by Mayne, published in 1962. The CMP technique provides the means to achieve multiple subsurface coverage. As a consequence, redundancy in the data is achieved, so that the signal-to-noise (S/N) ratio can be improved.

Let us only recall that the multiplicity for any configuration can be obtained from the relation:

Multiplicity = (no. of receivers per shot) / (2 * no. of receiver spacings per shot spacing)

When we record data using the CMP technique, we should reconsider spatial aliasing again. During processing we regroup traces in the so-called CMP gathers. When we do this, we can get aliased again because the trace distance in a CMP gather are twice as large as in a shotgather. Therefore the basic sampling interval as defined earlier in section 5.3 should be halved.

5.7 Fringe determination

The last point to discuss is the fringe determination. When we want to survey an area, it can be felt intuitively that we do not stop exactly where our target stops. During processing we need some data beyond those areas, such as for reaching full fold coverage at the end of the structure. We shall discuss the most important features in order to determine the fringe of the survey. The distance beyond which we need to obtain still data is determined by the maximum of these calculations. The effects are illustrated in figure (5.8).

The first consideration is the migration aperture. This is illustrated in figure (5.9).

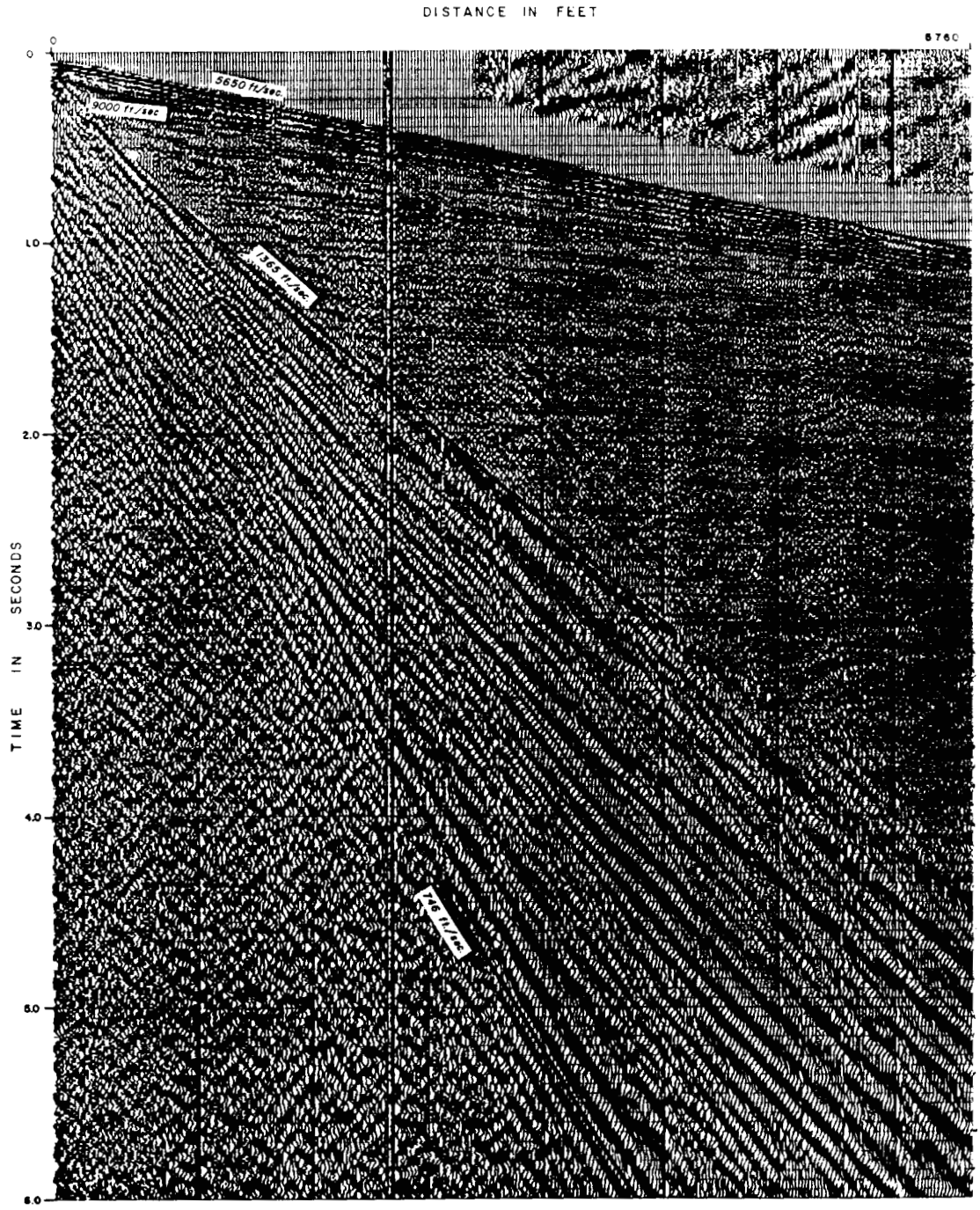

Figure 5.5: Composite shot record.

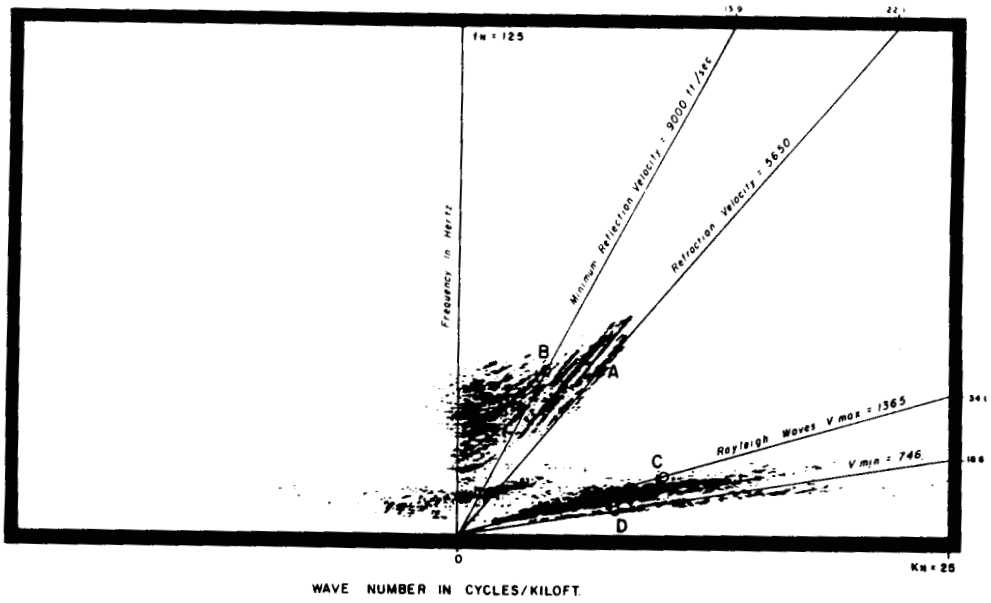

Figure 5.6: f-k domain representation of data given in Figure 5-5.

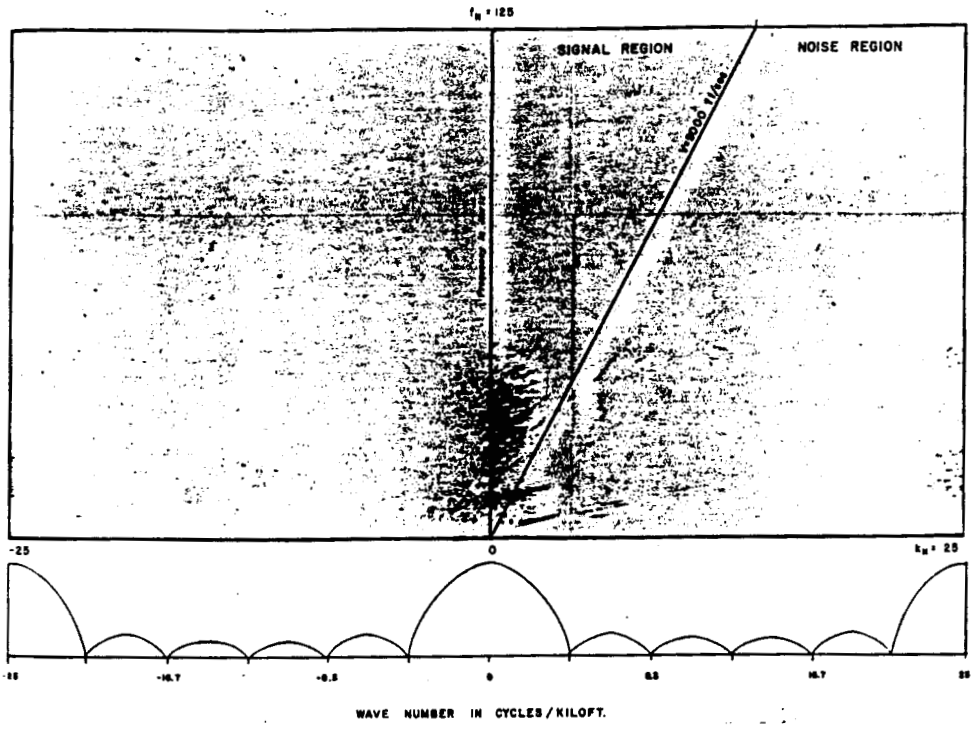

Figure 5.7: f-k domain representation of data after filtering with six-element uniform pattern.

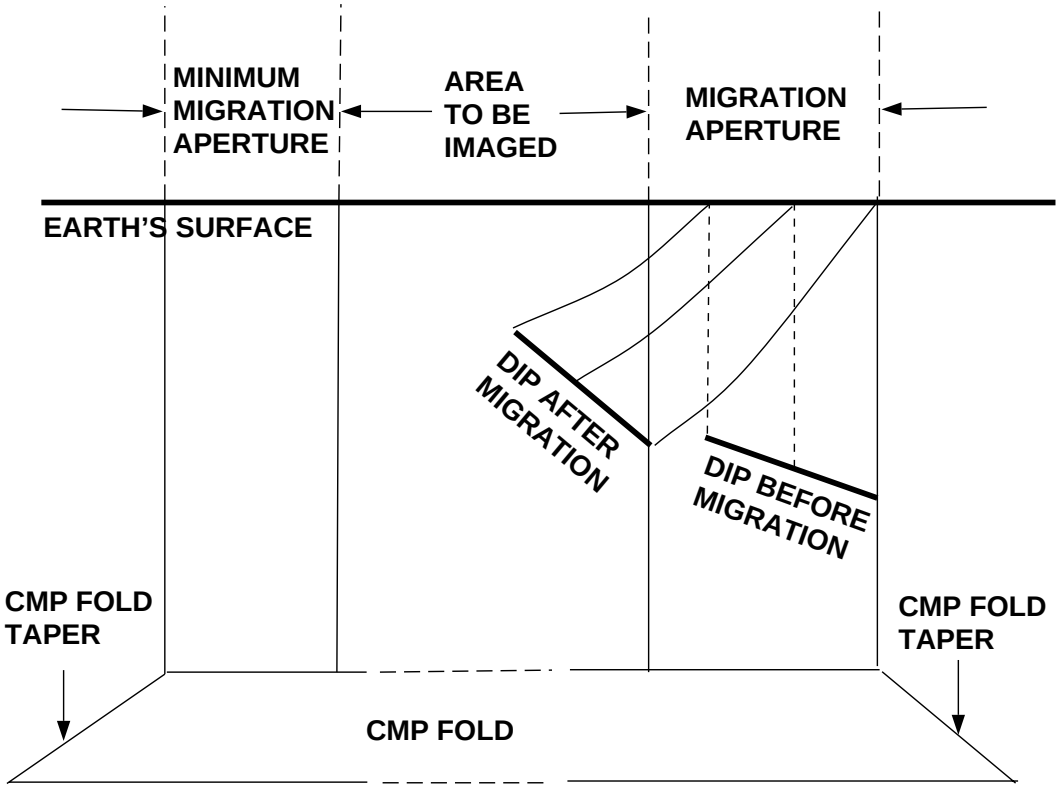

Figure 5.8: Extra fringes beyond survey area.

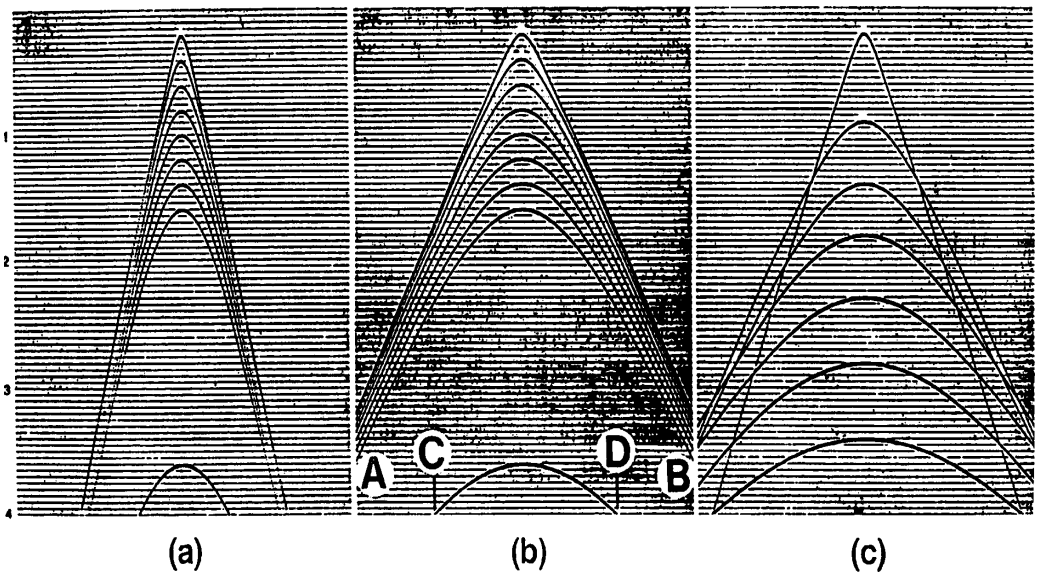

Figure 5.9: The effect of migration aperture on the determination of the fringe (from Yilmaz, 1987).

When we migrate data, we stack along hyperbola's, where the hyperbola's are determined by the velocity. When we are at the end of a structure we also want to have the "leg" of the hyperbola which is out of the area of interest. In this figure the effect of the velocity on the migration aperture is illustrated. Remember that we do not know the velocity on beforehand so a good guess must be made on the basis of other data, either previously shot seismic data, or other data, such as well data or geological data. In practice, we do not need to have the complete "leg" until the bottom of the section; 2 seconds for a 4–ms, 6–s section is sufficient. At the end of the leg the velocity must be estimated very accurately in order to have also the bottom energy, and since we usually do not know the velocity that accurately (before migration) we will not include that energy anyway.

The next consideration is the effect of dip. If a dipping interface is situated in the subsurface, then the migration process will move the dipping reflector laterally. If the dip is inward, i.e. in the direction of the structure, then those traces will contribute that lie more inwards of the area to be imaged. But when the dip is outwardly oriented, then we need traces that are lying more outwards than the area to be imaged. This is also illustrated in figure (5.8).

Finally, an important factor in the determination of the fringe, is the Fresnel zone. The Fresnel zone expresses whether two observations reveal different information about, say, a reflector. It is then obvious that lower frequencies have a larger Fresnel zone than higher frequencies. Two observations reveal information if the difference is more than a quarter wavelength. Consider for this figure (5.10), then the radius of the Fresnel zone is

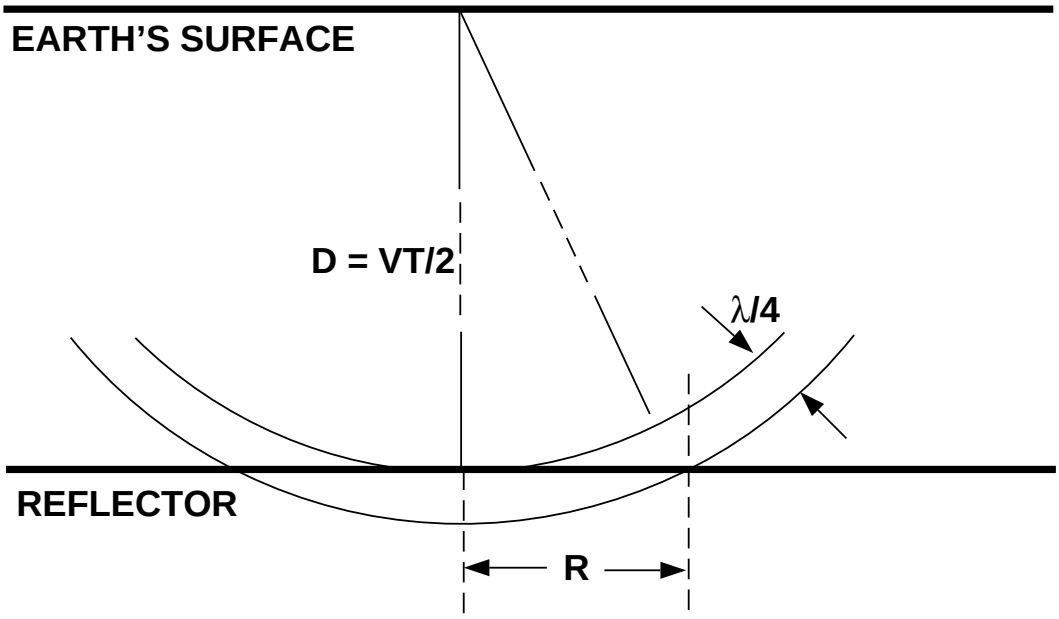

Figure 5.10: The effect of Fresnel zones on determination of fringe.

given by:

$$R = \left[\left(D + \frac{\lambda}{4}\right)^2 - D^2\right]^{1/2} = \left[\frac{D\lambda}{2} + \frac{\lambda^2}{16}\right]^{1/2} \approx \left[\frac{D\lambda}{2}\right]^{1/2} \tag{5.7}$$

Noticing that $D = cT/2$ and $\lambda = c/f$, we can write for the maximum distance $R_{\max}$:

$$R_{\max} = \frac{c}{2}\left[\frac{T}{f_{\min}}\right]^{1/2} \tag{5.8}$$

5.8 References

Kearey and Brooks, 1984. An introduction to geophysical exploration, Blackwell Scientific Publications, 296pp.

Yilmaz, O., 1987. Seismic Data Processing, Society of exploration Geophysicists (SEG), Tulsa, USA.

Vermeer, G.J.O.,1990. Seismic Wavefield Sampling, Society of Exploration Geophysicists, Tulsa, Oklahoma, ISBN-0-931830-47-8.

Chapter 6

Acquisition aspects in 3-D

6.1 Introduction

When seismics was started to be used as a tool for exploring for gas and oil, sections were put next to each other in order to look for structures. With the introduction of the CMP gather in 1962 and, of course, the computer, seismic images of the subsurface were much improved. Much effort was put into improving in processing techniques in the subsequent period. Then, at a certain stage, it was realized that seismic surveys were done along lines and that this sometimes made some characteristics of the subsurface unresolved. There is not a clear point where people started to use 3-D seismics but it is sure that 3-D seismics became popular in the 1980's. Especially SHELL has done pioneering work in this direction. This direction had consequences along the whole range of the seismic technique: data acquisition, processing and interpretation. Many principles remained the same as for 2-D, only we had to make the logical extensions of these principles to 3-D. With data acquisition, we had to spread out geophones along several lines for one shot, instead of geophones along one line. Also, 3-D required much more channels in the recording instrument, making them much more expensive. On the processing side, there were also consequences for the fact that we had to increase computer memory drastically and the same is valid for the power of the computer. Then on the interpretation side, we had to deal with much more data at the same time also requiring large computers. In spite of all these considerations, it was still worthwhile doing such a 3-D survey, and it is now standard in exploring for oil and gas, especially since large oil fields are harder to find these days, and we need 3-D to evaluate the geology in a better way. We shall go into some more detail of the aspects specific for a 3-D seismic survey in this chapter. The ones we will consider are

- Instrumentation aspects
- Binning, offset-azimuth distributions
- Survey design aspects

6.2 Instrumentation aspects

In the previous chapters we already dealt with the aspects of instrumentation for 2-D seismics. Already before full 3-D surveys were performed, the amount of traces for one shot were already going up to many traces, like 120 channels. In order to deal with this amount, already quite some organisation had to take place. With 3-D seismics this became even more important. What is minimally necessary these days in 3-D seismics, is to have telemetry systems. This means that the amplification and A/D con- version takes place locally in the field and it is the digital signal that will be sent across the line. The electronic aspects of the seismic data acquisition systems are further the same as for 2-D seismics.

With respect to the geophones and hydrophones, it can be said that just more detectors are employed, and they are usually employed in parallel lines where the shot position is somewhere in between and follows a certain pattern. We will come to that later on when discussing binning.

With respect to the seismic source, it can be said that just many more positions need to be sampled with all the organisational aspects of it. At sea, it is possible to use several airgun arrays in order to sample all the necessary shot positions.

6.3 Binning

In 2-D seismics a bin is defined as the strip in which a certain CMP position lies. If all is regular, each shot-receiver pair in successive shots will be at exactly the same midpoint position. Because of practical reasons that the midpositions never lie exactly on the same position for a CMP gather, the bin is introduced. It is necessary to have enough shot/receiver pairs in one bin, otherwise the CMP gather will contain very few traces and the stack will not be very good, that means the signal-to-noise ratio will not be increased very much by the stacking procedure. In 3-D the extension of the bin is pretty obvious; it is a (usually) rectangular-shaped region in which midpoint positions must lie. This is illustrated in figure (6.1).

In 2-D the positioning of source and receivers must be known pretty accurately but with 3-D the demands on the positioning systems become even greater. In an actual sense the quality data depends on the quality of the positioning. Also the positioning has improved greatly these days because of the advent of satellites and computer technology. These systems make it possible that we can do a 3-D seismic survey at all.

We have spoken so far of the bin and that we want to have enough traces in the bin in order to get enough fold-coverage of the subsurface. But in 3-D there are also other considerations which one does not need to bother about in 2-D. Those are the azimuth and offset distributions. That we have to deal with these is a consequence of the fact that in 3-D we do not shoot with a complete block of receivers, but with a few lines. Let us consider figure (6.2); filled circles mean shots, and open circles mean geophone positions. In figure (6.2) we have placed the shot positions perpendicular to the receivers. The subsurface coverage is given by the hashed area. We can now define a bin with half the receiver distance and half the source distance. Then, for this configuration, there will be one shot-receiver pair in each bin. But also in each bin, the source-receiver pair has a certain offset, and will have a certain angle with the receiver line. This is depicted in the figures (6.3) and (6.4). These figures show very well the principles of the offset and azimuth distributions.

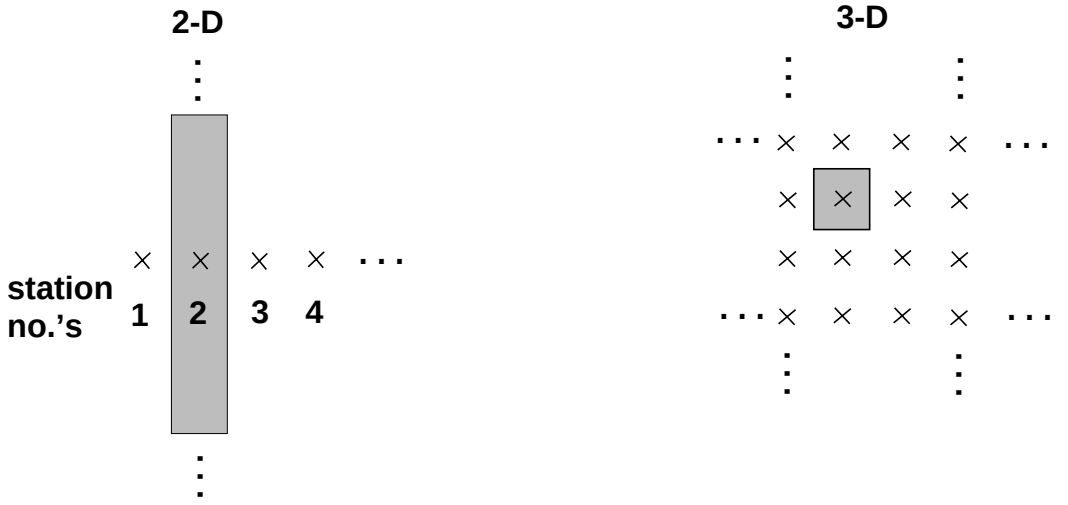

Figure 6.1: The bin in 2-D and 3-D seismics. (crosses are stations).

Many configurations have been proposed, sometimes depending on the circumstances in the field. Worthwhile mentioning is the so-called zig-zag configuration which is shown in figure (6.5). This figure shows the actual configuration in the field for the simplest "cell", in the same figure the fold coverage is shown, and figures (6.6) and (6.7) give the offset and azimuth distributions, respectively. We see here that the offset distribution is very good, while the azimuth distribution is not. This latter is deliberate, and because of the similarity with 2-D, i.e., along a line in one direction, and because of the simple source configuration, this configuration is mostly used in the field.

It is worthwhile mentioning one other technique which even has a better offset distribution. the layout is given in given in figure (6.8). The source positions look rather strange but when we look at the offset distribution in figure (6.9), it looks very evenly spaced, better than for the zig-zag configuration. For completeness, the azimuth distribution for this configuration is given in figure (6.10).

Worthwhile mentioning is also one layout which has a good azimuth distribution, and these are shown in figures (6.11) to (6.13).

6.4 Survey-design aspects

The next consideration in the field, is the question in which direction to put the receivers. Here there is a spatial aliasing consideration. Now in 3-D spatial aliasing can occur in two directions. It is easier to put the geophones in one line near to each other than making the distance between geophone lines small. Therefore we choose the direction of our lines in that direction where we should have the smallest spatial sampling, and that means in the direction of maximum dip in the subsurface, assuming the velocity of the ground-roll is the same in both directions. Still, the distance between the geophone lines is often chosen too large when we look only at this criterion. It is sufficient to say that people then use "smart" interpolators in order to suppress aliased energy.

Figure 6.2: Plan of one line of source positions and one line of receiver positions.

Figure 6.3: Offset distributions for single line of source and receiver positions for each bin.

Figure 6.4: Azimuth distributions for single line of source and receiver positions for each bin.

Figure 6.5: Layout of zig-zag configuration with fold of multiplicity.

Figure 6.6: Offset distributions for zig-zag configuration for each bin.

Figure 6.7: Azimuth distributions for zig-zag configuration for each bin.

Figure 6.8: Layout of configuration with good offset distribution with fold of multiplicity.

Figure 6.9: Offset distributions of configuration with good offset distribution for each bin.

Figure 6.10: Azimuth distrubutions of configuration with good offset distribution for each bin.

Figure 6.11: Layout of configuration with good azimuth distribution with fold of multiplicity.

Figure 6.12: Offset distributions of configuration with good azimuth distribution for each bin.

Figure 6.13: Azimuth distributions of configuration with good azimuth distribution for each bin.

Appendix A

Network outline

Time t, angular frequency $\omega = 2\pi f$, voltage u, current i,
resistance R, impedance Z, capacitance C, inductance L.

Table A.1: *Impedances for resistors, coils and capacitors*

Impedance type	**time**	**frequency**	**impedance**
Resistor	$u(t) = Ri(t)$	$U = RI$	$Z_R = \frac{U}{I} = R$
Coil	$u(t) = L\frac{di(t)}{dt}$	$U = Lj\omega I$	$Z_L = \frac{U}{I} = j\omega L$
Capacitor	$i(t) = C\frac{du(t)}{dt}$	$I = Cj\omega U$	$Z_C = \frac{U}{I} = \frac{1}{j\omega C}$

Table A.2: *Resistances and impedances in series and parallel*

Configuration	**Resistances**	**Impedance**
in parallel	$\frac{1}{R_{\mathrm{TOT}}} = \frac{1}{R_1} + \frac{1}{R_2}$	$\frac{1}{Z_{\mathrm{TOT}}} = \frac{1}{Z_1} + \frac{1}{Z_2}$
in series	$R_{\mathrm{TOT}} = R_1 + R_2$	$Z_{\mathrm{TOT}} = Z_1 + Z_2$

Appendix B

Derivation of the wave equation

In this appendix we will derive the wave equation for homogeneous media, using the conservation of momentum (Newton's second law) and the conservation of mass. In this derivation, we will follow Berkhout (1984) (appendix C), where we consider a single cube of mass when it is subdued to a seismic disturbance (see figure (B.1)). Such a cube has a volume ΔV with sides $\Delta x, \Delta y$ and Δz.

Conservation of mass gives us:

$$\Delta m(t_0) = \Delta m(t_0 + dt) \tag{B.1}$$

where Δm is the mass of the volume ΔV, and t denotes time. Using the density ρ, the conservation of mass can be written as:

$$\rho(t_0)\Delta V(t_0) = \rho(t_0 + dt)\Delta V(t_0 + dt) \tag{B.2}$$

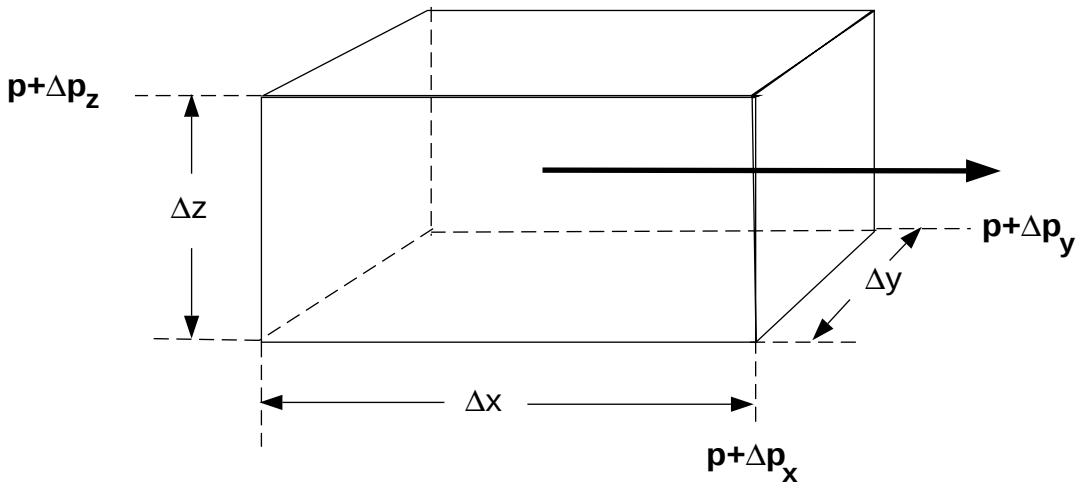

Figure B.1: A cube of mass, used for derivation of the wave equation.

Making this explicit:

$$\begin{aligned} \rho_0 \Delta V &= (\rho_0 + d\rho)(\Delta V + dV) \\ &= \rho_0 \Delta V + \rho_0 dV + \Delta V d\rho + d\rho dV \end{aligned} \tag{B.3}$$

Ignoring lower-order terms, i.e., $d\rho dV$, it follows that

$$\frac{d\rho}{\rho_0} = -\frac{dV}{\Delta V} \tag{B.4}$$

We want to derive an equation with the pressure in it so we assume there is a linear relation between the pressure p and the density:

$$dp = \frac{K}{\rho_0} d\rho \tag{B.5}$$

where K is called the bulk modulus. Then, we can rewrite the above equation as:

$$dp = -K \frac{dV}{\Delta V} \tag{B.6}$$

which formulates Hooke's law. It shows that for a constant mass the pressure is linearly related to the relative volume change. Now we can also derive that:

$$\begin{aligned} \frac{dV}{\Delta V} &= \frac{(\Delta x + dx)(\Delta y + dy)(\Delta z + dz)}{\Delta x \Delta y \Delta z} - \frac{\Delta x \Delta y \Delta z}{\Delta x \Delta y \Delta z} \\ &\simeq \frac{dx}{\Delta x} + \frac{dy}{\Delta y} + \frac{dz}{\Delta z} + O(dxdy) + O(dxdz) + O(dydz) \end{aligned} \tag{B.7}$$

For dx we can write:

$$\begin{aligned} dx &= (v_x dt)_{x+\Delta x} - (v_x dt) \\ &= \frac{\partial (v_x dt)}{\partial x} \Delta x \end{aligned} \tag{B.8}$$

where v_x denotes the particle velocity in the x–direction. We can do the same for the y and z–component and obtain:

$$\begin{aligned} \frac{dV}{\Delta V} &\simeq \left[\frac{\partial v_x}{\partial x} + \frac{\partial v_y}{\partial y} + \frac{\partial v_z}{\partial z} \right] dt \\ &= (\nabla \cdot \mathbf{v}) dt \end{aligned} \tag{B.9}$$

Substitute this in Hooke's law (equation B.6):

$$dp = -K(\nabla \cdot \mathbf{v}) dt \tag{B.10}$$

or

$$\frac{1}{K}\frac{dp}{dt} = -\nabla \cdot \mathbf{v} \tag{B.11}$$

The term on the left-hand side can be written as :

$$\frac{1}{K}\frac{dp}{dt} = \frac{1}{K}\left[\frac{\partial p}{\partial t} + \mathbf{v} \cdot \nabla p\right] \tag{B.12}$$

Ignoring the second term in brackets (low-velocity approximation), we obtain for equation (B.11):

$$\frac{1}{K}\frac{\partial p}{\partial t} = -\nabla \cdot \mathbf{v} \tag{B.13}$$

This is one basic relation needed for the derivation of the wave equation.

The other relation is obtained via Newton's law applied to the volume ΔV :

$$\Delta \mathbf{F} = \Delta m \frac{d\mathbf{v}}{dt} \tag{B.14}$$

where $\mathbf{F}$ is the (vectorial) force working on the element ΔV. Consider the force in the x–direction:

$$\begin{aligned} \Delta F_x &= -\Delta p_x \Delta S_x \\ &= -\left(\frac{\partial p}{\partial x}\Delta x + \frac{\partial p}{\partial t}\Delta t\right)\Delta S_x \\ &\simeq -\frac{\partial p}{\partial x}\Delta V \end{aligned} \tag{B.15}$$

ignoring the term with Δt, and ΔS_x is the surface in the x–direction, thus $\Delta y \Delta z$. So we can write:

$$\begin{aligned} \Delta \mathbf{F} &= -\left(\frac{\partial p}{\partial x}, \frac{\partial p}{\partial y}, \frac{\partial p}{\partial z}\right)^T \Delta V \\ &= -\Delta V(\nabla p) \end{aligned} \tag{B.16}$$

Substituting in Newton's law (equation B.14), we obtain:

$$\begin{aligned} -\Delta V(\nabla p) &= \Delta m \frac{d\mathbf{v}}{dt} \\ &= \rho \Delta V \frac{d\mathbf{v}}{dt} \end{aligned} \tag{B.17}$$

We can write $d\mathbf{v}/dt$ as $\partial\mathbf{v}/\partial t$; for this we have used a low-velocity approximation:

$$\frac{d\mathbf{v}}{dt} = \frac{\partial \mathbf{v}}{\partial t} + (\mathbf{v}\cdot\nabla)\mathbf{v} \approx \frac{\partial \mathbf{v}}{\partial t} \tag{B.18}$$

We divide by ΔV to give:

$$-\nabla p = \rho_0 \frac{\partial \mathbf{v}}{\partial t} \tag{B.19}$$

This equation is called the equation of motion.

We are now going to combine the conservation of mass and the equation of motion. Therefore we let the operator $(\nabla\cdot)$ work on the equation of motion:

$$\begin{aligned} -\nabla\cdot(\nabla p) &= \nabla\cdot\left(\rho\frac{\partial \mathbf{v}}{\partial t}\right) \\ &= \rho\frac{\partial}{\partial t}(\nabla\cdot\mathbf{v}) \end{aligned} \tag{B.20}$$

for constant ρ. Substituting the result of the conservation of mass gives:

$$-\nabla^2 p = \rho_0 \frac{\partial}{\partial t}\left(-\frac{1}{K}\frac{\partial p}{\partial t}\right) \tag{B.21}$$

Rewriting gives us the wave equation:

$$\nabla^2 p - \frac{\rho_0}{K}\frac{\partial^2 p}{\partial t^2} = 0 \tag{B.22}$$

or

$$\nabla^2 p - \frac{1}{c^2}\frac{\partial^2 p}{\partial t^2} = 0 \tag{B.23}$$

in which c can be seen as the velocity of sound, for which we have: $c = \sqrt{K/\rho}$.

Appendix C

Minimum-phase

In this appendix we will explain what a minimum-phase wavelet is, making use of the Z-transform. The Fourier transform of a function x_k, which is specified at fixed distances Δt, is given by:

$$X(f) = \sum_{k=-\infty}^{+\infty} x_k \exp(-2\pi i f k \Delta t) \tag{C.1}$$

in which $X(f)$ is Fourier transformed function of x_k, f denotes the frequency. We left out the scaling factor Δt in front of the summation for convenience. We introduce the Z-transform by taking $Z = \exp(-2\pi i f \Delta t)$; then the Fourier transform above can be written as

$$X(Z) = \sum_{k=-\infty}^{+\infty} x_k Z^k \tag{C.2}$$

where $X(Z)$ is now the Z-transformed function of x_k.

We will now introduce the inverse of a wavelet. This can be expressed in two ways, in the time domain or in the Z (or frequency) domain. The simplest way at the moment is in the Z domain. When we wish to find the inverse of a spectrum $A(Z)$, we are looking for a signal $B(Z)$ such that:

$$A(Z)B(Z) = 1 \tag{C.3}$$

It is simple to see that $B(Z)$ is $1/A(Z)$. Of course, this expression has an equivalent in the time domain, namely:

$$a_k * b_k = \delta_k \tag{C.4}$$

in which the asterisk $*$ denotes convolution and dk denotes the Dirac delta function, i.e.,

$$\delta_k = \ldots, 0, 0, 1, 0, 0, \ldots \tag{C.5}$$

where the 1 occurs for $k = 0$. Let us consider the two-sample series a_k,

$$a_k = \ldots, 0, 0, a_0, a_1, 0, 0, \ldots \tag{C.6}$$

with the Z-transform:

$$A(Z) = a_0 + a_1 Z \tag{C.7}$$

We substitute this in the expression for the Z-transformed wavelet $B(Z)$:

$$B(Z) = \frac{1}{a_0 + a_1 Z} \tag{C.8}$$

Because of the form of $B(Z)$ we cannot recognize the time-domain series from this expression, since we do not have a series in powers of Z. To that extent we must expand the denominator:

$$B(Z) = \frac{1}{a_0\left(1 + \frac{a_1}{a_0}Z\right)} \approx \frac{1}{a_0}\left[1 - \frac{a_1}{a_0}Z + \left(\frac{a_1}{a_0}\right)^2 Z^2 - \left(\frac{a_1}{a_0}\right)^3 Z^3 + \ldots\right] \tag{C.9}$$

where we made use of the standard Taylor expansion of the function $1/(1+x)$. The Taylor expansion is only valid for values of $|x|$ which are less than 1, so in our case $|(a_1/a_0)Z|$ must be less than 1. This condition can be reduced by looking more carefully at Z. For real frequencies f, Z has the length:

$$|Z| = |\exp(-2\pi i f \Delta t)| = |cos(2\pi f \Delta t) - i\sin(2\pi f \Delta t)| = 1 \tag{C.10}$$

so the condition $|(a_1/a_0)Z|$ reduces to $|a_1/a_0|$. In $B(Z)$, this means that $|a_1/a_0|$ must be smaller than 1 in order to make the Taylor expansion valid, so the second sample must be smaller than the first. What happens if a_1 is larger than a_0? Then we must write equation (C.9) differently, i.e., by taking $a_1 Z$ out of brackets instead of a_0 :

$$B(Z) = \frac{1}{a_1 Z\left(1 + \frac{a_0}{a_1}Z^{-1}\right)} \approx \frac{1}{a_1 Z}\left[1 - \frac{a_0}{a_1}Z^{-1} + \left(\frac{a_0}{a_1}\right)^2 Z^{-2} - \left(\frac{a_0}{a_1}\right)^3 Z^{-3} + \ldots\right] \tag{C.11}$$

since now $|a_0/a_1|$ is smaller than 1. When we look at the two wavelets depending on the value of the ratio $|a_1/a_0|$ whether it be smaller or larger than 1, we get positive powers and negative powers of Z, respectively. In the time domain, this means that in the first case ($|a_1/a_0| < 1$) we obtain a causal time series so only non-zero values for times larger than or equal to zero. In the other case, i.e. $|a_1/a_0| > 1$, we obtain only negative powers of Z for b_k so only non-zero values for times smaller than 0, which is not causal.

Obviously, there is some fundamental difference between the two wavelets $B(Z)$ above and we must differentiate between the two. Therefore we define the minimum-phase wavelet as:

A minimum-phase wavelet is a causal wavelet that has a causal inverse.

In this definition we have included the fact that a wavelet is a signal that has a finite amount of energy so at infinity the values must certainly be going to zero. In mathematical

terms this means that the series expansion of the denominator in $B(Z)$ must be a valid one.

So far, we have specified $B(Z)$ in terms of a_0 and a_1 and the times series b_k could be obtained via the ratio a_0/a_1. There is also another way of looking at it, namely looking at the value Z_{root} corresponding to these values for a_0 and a_1. When we are looking for the inverse of the wavelet $A(Z)$, we want to find Z_{root} such that:

$$a_0 + a_1 Z_{\text{root}} = 0 \tag{C.12}$$

so that $Z_{\text{root}} = -a_0/a_1$. When a_0 is larger than a_1, then Z_{root} is larger than 1; when a_1 is larger than a_0, then Z_{root} is smaller than 1. For the minimum-phase wavelet, a_0 is larger than a_1, so Z_{root} is larger than 1. In general terms, with complex Z_{root}'s, we can say that for a wavelet a_k to be minimum-phase, its roots must lie outside the unit circle.

The arguments used above may now easily be applied to wavelets with more than two samples. Consider the $n+1$ length wavelet $(a_0, a_1, ..., a_n)$ with Z-transform

$$A(Z) = a_0 + a_1 Z + ... + a_n Z^n \tag{C.13}$$

which may be written as

$$A(Z) = a_n \prod_{k=1}^{n} (Z - Z_k) \tag{C.14}$$

The inverse of the wavelet has the following Z-transform

$$\frac{1}{A(Z)} = \frac{1}{a_n} \prod_{k=1}^{n} \frac{1}{(Z - Z_k)} \tag{C.15}$$

If $|Z_k| > 1$, the quotient $1/(Z - Z_k)$ can be expanded as a series in increasing powers of Z with converging coefficients; that is, it can be expressed as a causal time series with finite energy. This corresponds to the case of the minimum-phase two-point wavelet discussed above. If any one of the roots Z_k lies inside the unit circle, the coefficients of the expansion do not decrease with increasing powers of Z. Therefore the inverse can be causal but does not have finite energy. In order to ensure that the energy of the inverse is bounded, it is necessary to expand the quotient in decreasing powers of Z, thus making the inverse non-causal. It follows that the inverse of a_k can only be causal with finite energy if all the roots Z_k lie outside the unit circle. This is the condition that a_k is minimum phase.

The evaluation of the Z-transform on the unit circle in the complex Z plane corresponds to computation of the discrete Fourier transform, in which the frequency f is real. If f is allowed to be complex, this corresponds to the zones inside and outside the unit circle. This can be seen as follows. Let f be complex, i.e., $f = f' + if"$. Then the complex Z-plane is related to the complex frequency plane via the relation:

$$Z = \exp[-2\pi i f \Delta t] = \exp[-2\pi i (f' + if")\Delta t] = \exp[2\pi f" \Delta t] \exp[-2\pi i f' \Delta t] \tag{C.16}$$

From this the following relation holds: the area outside the unit circle in the Z-plane ($|Z| > 1$) corresponds to the upper half plane in the complex frequency plane ($f" > 0$);

the unit circle in the complex Z-plane corresponds to the real axis in the complex frequency plane ($f" = 0$); and the area inside the unit circle in the Z-plane ($|Z| < 1$) corresponds to the lower half plane ($f" < 0$) in the complex frequency plane. So in terms of frequencies, it follows that a minimum-phase wavelet has no poles or zeroes in the lower half of the complex frequency plane.

The previous discussion gives us insight in the specific characteristic of a minimum-phase wavelet. Does the previous discussion means that if we want to know whether a wavelet is minimum-phase, we must determine all the roots of a wavelet? No. There is a simple way to see whether a wavelet is minimum-phase, and that is by looking at the phase spectrum of the wavelet. The phase of the wavelet should, at the Nyquist frequency, return to zero. If it is not minimum-phase, then the phase will be a multiple of 2π at the Nyquist frequency. This is very simple to observe when plotting the phase spectrum.

With the recognition of a wavelet being minimum-phase we made use of a frequency-domain description. Of course, this has a time-domain equivalent. In the time-domain, out of a sequence wavelets sharing the same amplitude spectrum, the minimum-phase wavelet is that wavelet which has the fastest energy build-up. This means that the energy of the wavelet is closest to the beginning as possible.